

Tracking Offshore Occurrence of Common Terns, Endangered Roseate Terns, and Threatened Piping Plovers with VHF Arrays



Tracking Offshore Occurrence of Common Terns, Endangered Roseate Terns, and Threatened Piping Plovers with VHF Arrays

April 2019

Authors:

Pamela H. Loring, US Fish and Wildlife Service (USFWS), Division of Migratory Birds
Peter W.C. Paton, Department of Natural Resources Science, University of Rhode Island
James D. McLaren, Environment and Climate Change Canada, Science and Technology Branch
Hua Bai, University of Massachusetts Amherst, Department of Electrical and Computer Engineering
Ramakrishna Janaswamy, University of Massachusetts Amherst, Department of Electrical and Computer Engineering
Holly F. Goyert, University of Massachusetts Amherst, Department of Environmental Conservation
Curtice R. Griffin, University of Massachusetts Amherst, Department of Environmental Conservation
Paul R. Sievert, University of Massachusetts Amherst, Department of Environmental Conservation

Prepared under BOEM Intra-Agency Agreement No. M13PG00012

By
US Department of Interior
US Fish and Wildlife Service
Division of Migratory Birds
300 Westgate Center Dr.
Hadley, MA 01035



**US Department of the Interior
Bureau of Ocean Energy Management
Office of Renewable Energy Programs**

BOEM
Bureau of Ocean Energy
Management

DISCLAIMER

This study was funded, in part, by the US Department of the Interior, Bureau of Ocean Energy Management (BOEM), Environmental Studies Program, Washington, DC, through Intra-Agency Agreement Number M13PG00012 with the US Department of Interior, US Fish and Wildlife Service, Division of Migratory Birds, Hadley, MA. This report has been technically reviewed by BOEM, and it has been approved for publication. The views and conclusions contained in this document are those of the authors and should not be interpreted as representing the opinions or policies of the US Government, nor does mention of trade names or commercial products constitute endorsement or recommendation for use.

REPORT AVAILABILITY

To download a PDF file of this report, go to the US Department of the Interior, Bureau of Ocean Energy Management Data and Information Systems webpage (<http://www.boem.gov/Environmental-Studies-EnvData/>), click on the link for the Environmental Studies Program Information System (ESPIS), and search on 2019-017. The report is also available at the National Technical Reports Library at <https://ntrl.ntis.gov/NTRL/>.

CITATION

Loring PH, Paton PWC, McLaren JD, Bai H, Janaswamy R, Goyert HF, Griffin CR, Sievert PR. 2019. Tracking Offshore Occurrence of Common Terns, Endangered Roseate Terns, and Threatened Piping Plovers with VHF Arrays. Sterling (VA): US Department of the Interior, Bureau of Ocean Energy Management. OCS Study BOEM 2019-017. 140 p.

ABOUT THE COVER

Cover photos by Peter Paton, University of Rhode Island.

ACKNOWLEDGMENTS

For study administration, guidance, and oversight, we thank the following individuals from the Bureau of Ocean Energy Management: David Bigger, Mary Boatman, Tim White, Jim Woehr (retired) and Paula Barksdale, as well as Scott Johnston, Caleb Spiegel, and Pamela Toschik from the US Fish and Wildlife Service (USFWS). We thank Annelee Motta, Laurie Racine, and Laurie McDermott (USFWS) and Deb Wright (MA Cooperative Fish and Wildlife Unit) administrative support.

We thank staff from the Rhode Island National Wildlife Refuge Complex, Ryan Kleinert, John Veale, Jennifer White, and Charlie Vandemoer, for providing key field support for tagging and monitoring Piping Plovers in Rhode Island, as well as extensive logistical support for the tracking tower array. We thank Suzanne Paton of the USFWS Southern New England-New York Bight Coastal Program for providing staff and logistical support for bird tagging and tracking towers. We also thank our Rhode Island cooperators who provided landowner permission for tagging and field support, including Janice Sassi and staff from Napatree Point Conservation Area. We thank Susi vonOettingen and Anne Hecht from USFWS Endangered Species for providing expertise on Roseate Terns and Piping Plovers.

For field support with capturing and tagging Piping Plovers and Common Terns in Massachusetts, we thank Monomoy National Wildlife Refuge staff for equipment and logistical support, and especially Kate Iaquinto and Stephanie Koch for helping to lead the effort. We also thank our Massachusetts cooperators who provided landowner permission for tagging and field support, including the Town of Chatham, Massachusetts and Massachusetts Audubon Society Coastal Waterbird Program. We thank Dan Catlin and the Virginia Tech Shorebird Program for coordinating leg flag combinations and resights of Piping Plovers, and Jeffery Spendelow from USGS Patuxent Wildlife Research Center for coordinating auxiliary markers on Roseate Terns. For tern capture, tagging, and monitoring in Buzzards Bay, Massachusetts, we thank Carolyn Mostello and staff with the Massachusetts Division of Fisheries & Wildlife. For tern capture, tagging, and monitoring on Great Gull Island, New York we thank Helen Hays, Grace Cormons, Joe Dicostanzo, and Catherine Neal of the Great Gull Island Project, as well as the many volunteers and staff on Great Gull Island.

We thank the following members of our field crew during the five-year study for their assistance with building and maintaining tracking towers, tagging and monitoring birds, and data management: Brett Still, Kevin Rogers, Michael Abemayor, Christine Fallon, Steve Ecrement, Calvin Ritter, Derek Trunfio, Kaiti Titherington, Josh Siebel, Matthias Malin, Dallas Jordan, Adam Ellis, Jennifer Malpass, Alex Cook, Gillian Baird, Emma Paton, Stephen Fox, Georgia Meale, and Brian Lang.

For field and logistical support with automated radio telemetry towers operated for this study, we thank our many cooperators from following entities: UMass Amherst-USGS Cooperative Fish and Wildlife Unit, USFWS Southern New England-New York Bight Coastal Program, USFWS Division of Migratory Birds, University of Rhode Island, Cape Cod National Seashore, Eastern MA National Wildlife Refuge (NWR) Complex, Waquoit Bay National Estuarine Research Reserve, US Army Corps of Engineers/Cape Cod Canal Field Office, Rhode Island NWR Complex, Shearwater Excursions, Nantucket Islands Land Bank, Nantucket Conservation Foundation, Napatree Point Conservation Area, CT Department of Energy & Environmental Protection, American Museum of Natural History/Great Gull Island Project, Plum Island Animal Disease Center, Block Island Southeast Lighthouse Foundation, Camp Hero State Park, Fire Island National Seashore, Gateway National Recreation Area, Wildlife Conservation Society/New York Aquarium, Rutgers University Marine Field Station, Conserve Wildlife Foundation of New Jersey, New Jersey Division of Fish and Wildlife, Avalon Fishing Club, DE Department of Natural Resources/Cape Henlopen State Park, The Nature Conservancy Virginia Coast Reserve, Chincoteague NWR, Eastern Shore of VA NWR, Back Bay NWR, NOAA R/V Henry Bigelow, and Shearwater Excursions. We also thank the many partners operating automated radio telemetry stations throughout the Western Hemisphere as part of the Motus Wildlife Tracking System. We thank Jim Wortham (USFWS Migratory Bird Program) for piloting the aerial telemetry surveys and Blair Perkins (Shearwater Excursions) for captaining the boat surveys. For technical support and assistance with data management and analysis, we thank Stu Mackenzie and Zoe Crysler (Motus Wildlife Tracking System, Bird Studies Canada); Phil Taylor and John Brzustowski (Acadia University); Paul Smith (Environment and Climate Change Canada); and Mike Vandentillart (Lotek Wireless).

This study was funded in part by the US Department of the Interior, Bureau of Ocean Energy Management, Environmental Studies Program, Washington DC, through Intra-Agency Agreement Number M13PG00012 with the Department of Interior, Fish and Wildlife Service. This study was also supported through the NSF-sponsored IGERT: Offshore Wind Energy Engineering, Environmental Science, and Policy (Grant Number 1068864) at the University of Massachusetts Amherst.

Summary

The Bureau of Ocean Energy Management (BOEM) is responsible for managing renewable energy development on the Outer Continental Shelf (OCS) of the United States. The OCS extends from the boundary of each state's jurisdictional waters (generally 3 nautical miles offshore) to the outer boundary of the US Exclusive Economic Zone (approximately 200 nautical miles offshore). In the Atlantic OCS, over 5,492 km² is presently under lease agreement for development of commercial-scale offshore wind energy facilities and an additional 12,976 km² is in the planning stages for potential lease (BOEM 2018). Development in the United States to date (February 2019) is limited to a 30-MW, five turbine demonstration-scale facility in state waters off the coast of Block Island, RI. Herein, BOEM Lease Areas and BOEM Planning Areas are broadly referred to as Wind Energy Areas (WEAs).

With large areas of the Atlantic OCS under consideration for development of offshore wind energy facilities, information on offshore movements and flight altitudes of high-priority bird species is needed for estimating exposure of birds to collision risks in WEAs and for developing strategies to manage adverse effects (BOEM 2017). Adverse effects of offshore wind turbines to birds vary by species, and include direct mortality from collisions with infrastructure, and indirect effects of disturbance and habitat loss (Fox et al. 2006). Understanding the species-specific, cumulative adverse effects to bird populations resulting from exposure to multiple, commercial-scale wind energy facilities throughout their migratory ranges will be increasingly important as offshore wind energy development advances in US waters (Goodale and Milman 2016).

This study provides new information on the offshore movements and flight altitudes of Common Terns (*Sterna hirundo*), Federally-Endangered Roseate Terns (*Sterna dougallii*), and Federally-Threatened Piping Plovers (*Charadrius melodus*) within the Atlantic OCS. Common and Roseate Terns are colonial seabirds with nesting populations in the northeastern portion of the US Atlantic coast. Both species use migratory staging sites along the US Atlantic coast and migrate to South America for the non-breeding period. Piping Plovers are migratory shorebirds with nesting populations that breed along the US Atlantic coast and winter in the southeastern US and Caribbean. Species-specific information on the routes, timing, and environmental conditions associated with flights over the Atlantic OCS is needed to refine assessments of exposure to offshore WEAs and to improve estimates of collision risk with offshore wind turbines (Burger et al. 2011). Information on flight altitudes is also needed to assess exposure to the Rotor Swept Zone (RSZ), generally 25 to 250 m above sea level (asl).

In this study, adult Roseate Terns (n=150), Common Terns (n=266), and Piping Plovers (n=150) were fitted with digital VHF transmitters at select nesting areas on the US Atlantic coast from 2014 to 2017. Tagged individuals were tracked using an array of automated VHF telemetry stations within a Study Area encompassing a portion of the US Atlantic OCS, extending from Cape Cod, MA to southern VA. We developed novel movement modeling techniques to assess the frequency and extent of offshore movements over Federal waters and WEAs within the Study Area. Our specific objectives were to: (1) develop spatially-explicit, 3-dimensional models to estimate movements of Common Terns, Roseate Terns and Piping Plovers in the Atlantic OCS Study Area during breeding and post-breeding periods; (2) estimate the exposure of Common Terns, endangered Roseate Terns and threatened Piping Plovers to

Federal Waters and to each BOEM Lease Area and BOEM Planning Area in the Atlantic OCS Study Area during breeding and post-breeding periods; and (3) quantify effects of meteorological conditions (e.g., wind speed, wind direction, barometric pressure, temperature, visibility, precipitation), temporal variation (time of day, date), and demographic variation (breeding population, sex, reproductive success) on occurrence of Common Terns, Roseate Terns and Piping Plovers within Federal waters and WEAs within the Atlantic OCS Study Area.

Common and Roseate terns were exposed to Federal waters and WEAs during the breeding period through post-breeding dispersal. The highest probability of exposure occurred during post-breeding dispersal (mid-July through late September), as terns from multiple colonies made extensive movements throughout the eastern Long Island Sound to the southeastern region of Massachusetts. Exposure to WEAs was highest among Common Terns dispersing from Great Gull Island across Rhode Island Sound to staging areas in southeastern Massachusetts. Peak exposure of Common and Roseate Terns to Federal waters primarily occurred in mid-July and August during morning hours and fair weather conditions (high atmospheric pressure). Offshore flight altitudes of terns were generally below the RSZ of offshore wind turbines (25 to 250 m asl).

Peak exposure of Piping Plovers to Federal waters occurred in early August. Piping Plovers departing from their breeding grounds in Massachusetts and Rhode Island primarily used offshore routes to stopover areas in the mid-Atlantic. Individual Piping Plovers were exposed to up to four WEAs on offshore flights across the mid-Atlantic Bight. Flights in Federal waters and WEAs were strongly associated with southwest wind conditions providing positive wind support. Offshore flight altitudes of Piping Plovers generally occurred above the RSZ.

In this study, digital VHF telemetry was an effective method for assessing broad-scale exposure of terns and plovers to Federal waters and WEAs in the Atlantic OCS. However, maximizing the detection or resolution of movement patterns in the design of automated radio telemetry station arrays involves tradeoffs, which vary by species, geographic area, and study objective. Estimating bird locations through triangulation of the detecting towers requires strategic placement of towers at relatively high densities in areas of high ecological importance. Along straight coastlines that lack islands or peninsulas, we recommend assembling towers on offshore infrastructure, such as buoys or wind turbines, where possible. The geographic coverage and scope of digital VHF telemetry can be further extended through the coordinated efforts of the Motus Wildlife Tracking System. Future studies have the potential to integrate this network with other forms of developing technology (e.g. radar, high definition imagery) for collecting detailed movements of birds in offshore environments.

Key Findings:

- Estimated exposure of Common and Roseate Terns to Federal waters and WEAs peaked during mid-July and August, and primarily occurred during morning hours with fair weather conditions.
- When crossing Federal waters, Common and Roseate terns predominantly occurred below the RSZ (< 25 m). An estimated 4.3% of Common Tern flights and 6.4% of Roseate Tern flights within Federal waters occurred within the RSZ.
- Piping Plovers departing from their breeding grounds in MA and RI primarily used offshore routes to sites in the mid-Atlantic.

- Migratory departures of Piping Plovers peaked in early August, during evenings with favorable atmospheric conditions for crossing the mid-Atlantic Bight (i.e. winds blowing to the southwest, high visibility, little to no precipitation, and high atmospheric pressure)
- Estimated offshore flight altitudes of Piping Plovers over Federal waters primarily occurred above the RSZ (>250 m). An estimated 21.3% of Piping Plover flights in Federal waters occurred within the RSZ.

Contents

Summary.....	i
List of Figures.....	vi
List of Tables.....	xi
List of Appendices.....	xiii
List of Abbreviations and Acronyms.....	xiv
1 Introduction	1
1.1 Risk Assessments and Information Needs for Focal Species in the AOCS	2
1.2 VHF Technology to Study Movements	4
2 Methods	6
2.1 Study Area.....	6
2.1.1 Atlantic OCS and Wind Energy Areas.....	6
2.1.2 Tagging Sites	6
2.2 Study Species	9
2.2.1 Common Tern	9
2.2.2 Roseate Tern.....	9
2.2.3 Piping Plover	10
2.3 Digital VHF Transmitters.....	10
2.4 Capture and Tag Attachment Summaries.....	11
2.4.1 Common and Roseate Terns	11
2.4.2 Piping Plovers	11
2.5 Automated Radio Telemetry Stations	18
2.6 Aerial Telemetry Surveys	21
2.7 Frequency Coordination	25
2.8 Post-processing of Telemetry Data.....	25
2.9 Movement Models.....	26
2.9.1 Background and Motivation of Approach	26
2.9.2 Formulation	30
2.9.3 Near-simultaneous Detections	30
2.9.4 Single Detections	31
2.9.5 Determination of Non-stop Flight	32
2.9.6 Behavioral Flight Constraints	32
2.9.7 Temporal Interpolation Using Brownian Bridge Movement Model.....	32
2.9.8 Calibration and Validation	33

2.9.9	Including Sensor-gnome Receiving Stations	37
2.9.10	Detection Probability	37
2.10	Assessment of Occurrence in Federal Waters and WEAs	37
2.11	Meteorological Conditions.....	38
2.12	Covariate Analysis of Exposure to Federal Waters and WEAs	39
3	Results	40
3.1	Common and Roseate Terns	40
3.1.1	Tagging and Detection Summaries.....	40
3.1.2	Movements in Study Area	41
3.1.3	Aerial Telemetry Surveys	48
3.1.4	Estimated Exposure to Federal Waters	50
3.1.5	Estimated Exposure to Wind Energy Areas.....	70
3.1.6	Altitude Distribution of Terns During Exposure to Federal Waters and WEAs	90
3.2	Piping Plovers	93
3.2.1	Tagging and Detection Summaries.....	93
3.2.2	Migratory Movements in Study Area	94
3.2.3	Exposure to Federal Waters	98
3.2.4	Covariate Analysis of Estimated Exposure to Federal Waters	98
3.2.5	Estimated Exposure to Wind Energy Areas.....	105
3.2.6	Temporal and Meteorological Variation in WEA Exposure	109
3.2.7	Altitude Distribution of Piping Plovers During Exposure to Federal Waters and WEAs ...	116
4	Discussion.....	119
4.1	VHF Tracking Technology.....	119
4.2	Movement Models.....	120
4.3	Common and Roseate Terns	121
4.4	Piping Plovers	124
5	Future Directions.....	125
6	References.....	129

List of Figures

Figure 1. Map of Study Area in Atlantic OCS.....	8
Figure 2. Photos of Common and Roseate Tern trapping and transmitter deployment	15
Figure 3. Photos of Piping Plover trapping and transmitter deployment	17
Figure 4. Automated radio telemetry station on Nantucket NWR (Great Point), Nantucket, MA	19
Figure 5. Map of BOEM automated radio telemetry stations within the Study Area in 2014-2017	20
Figure 6. USFWS amphibious Kodiak aircraft with paired directional (Yagi) antennas used for aerial telemetry surveys in 2014 and 2015.	22
Figure 7. Transect routes flown during aerial telemetry surveys in 2014 and 2015.	23
Figure 8. Radiation pattern of Yagi antenna beam	28
Figure 9. Results of model calibration survey conducted during September 2014 adjacent to two automated radio telemetry towers on Monomoy NWR, MA, USA	35
Figure 10. Model estimated mean and standard deviation of altitude (m, ASL) over time (min) of VHF-tagged kite during September 2014 calibration survey.....	36
Figure 11. Track densities (10-min tracks/km ²) of Common Terns (n=65) from the colony on Monomoy NWR during the breeding and post-breeding periods in 2014.....	43
Figure 12. Track densities (10-min tracks/km ²) of Common Terns (n=142) from the colony on Great Gull Island during the breeding and post-breeding periods in 2014 to 2017 (pooled).	44
Figure 13. Track densities (10-min tracks/km ²) of Common Terns (n=59) from colonies in Buzzards Bay during the breeding and post-breeding periods in 2015 to 2017 (pooled).....	45
Figure 14. Track densities (10-min tracks/km ²) of Roseate Terns (n=90) from the colony on Great Gull Island during the breeding and post-breeding periods in 2015 to 2017 (pooled).	46
Figure 15. Track densities (10-min tracks/km ²) of Roseate Terns (n=60) from colonies in Buzzards Bay during the breeding and post-breeding periods in 2016 and 2017 (pooled).....	47
Figure 16. Locations of tagged Common and Roseate Terns detected during aerial telemetry surveys in 2014 and 2015.	49
Figure 17. Boosted GAM prediction for the partial contribution of the date of year covariate (x-axis) to the likelihood (log-transformed odds ratio) of exposure to Federal waters among Common Terns (y-axis) in 2014, 2015, 2016, and 2017 (pooled).....	52
Figure 18. Boosted GAM prediction for the partial contribution of the date of year by sex interaction term (x-axis) to the likelihood (log-transformed odds ratio) of exposure to Federal waters among Common Terns (y-axis) in 2014, 2015, 2016, and 2017 (pooled).....	53
Figure 19. Boosted GAM prediction for the partial contribution of the nesting colony location (buzz = Buzzards Bay, ggi = Great Gull Island, mny = Monomoy NWR) covariate (x-axis) to the likelihood (log-transformed odds ratio) of exposure to Federal waters among Common Terns (y-axis) in 2014, 2015, 2016, and 2017 (pooled).	54

Figure 20. Boosted GAM prediction for the partial contribution of the hour of day (EST) covariate (x-axis) to the likelihood (log-transformed odds ratio) of exposure to Federal waters among Common Terns (y-axis) in 2014, 2015, 2016, and 2017 (pooled).	55
Figure 21. Boosted GAM prediction for the partial contribution of the atmospheric pressure covariate (x-axis) to the likelihood (log-transformed odds ratio) of exposure to Federal waters among Common Terns (y-axis) in 2014, 2015, 2016, and 2017 (pooled).	56
Figure 22. Boosted GAM prediction for the partial contribution of the wind speed covariate (x-axis) to the likelihood (log-transformed odds ratio) of exposure to Federal waters among Common Terns (y-axis) in 2014, 2015, 2016, and 2017 (pooled).	57
Figure 23. Boosted GAM prediction for the partial contribution of the air temperature covariate (x-axis) to the likelihood (log-transformed odds ratio) of exposure to Federal waters among Common Terns (y-axis) in 2014, 2015, 2016, and 2017 (pooled).	58
Figure 24. Boosted GAM prediction for the partial contribution of the year covariate (x-axis) to the likelihood (log-transformed odds ratio) of exposure to Federal waters among Common Terns (y-axis) in 2014, 2015, 2016, and 2017.	59
Figure 25. Boosted GAM prediction for the partial contribution of the date of year covariate (x-axis) to the likelihood (log-transformed odds ratio) of exposure to Federal waters among Roseate Terns (y-axis) in 2015, 2016, and 2017 (pooled).	62
Figure 26. Boosted GAM prediction for the partial contribution of the date of year by sex interaction term (x-axis) to the likelihood (log-transformed odds ratio) of exposure to Federal waters among Roseate Terns (y-axis) in 2015, 2016, and 2017 (pooled).	63
Figure 27. Boosted GAM prediction for the partial contribution of the hour of day (EST) covariate (x-axis) to the likelihood (log-transformed odds ratio) of exposure to Federal waters among Roseate Terns (y-axis) in 2015, 2016, and 2017 (pooled).	64
Figure 28. Boosted GAM prediction for the partial contribution of the nesting colony location (buzz = Buzzards Bay, ggi = Great Gull Island) covariate (x-axis) to the likelihood (log-transformed odds ratio) of exposure to Federal waters among Roseate Terns (y-axis) in 2015, 2016, and 2017 (pooled).	65
Figure 29. Boosted GAM prediction for the partial contribution of the atmospheric pressure covariate (x-axis) to the likelihood (log-transformed odds ratio) of exposure to Federal waters among Roseate Terns (y-axis) in 2015, 2016, and 2017 (pooled).	66
Figure 30. Boosted GAM prediction for the partial contribution of the wind speed covariate (x-axis) to the likelihood (log-transformed odds ratio) of exposure to Federal waters among Roseate Terns (y-axis) in 2015, 2016, and 2017 (pooled).	67
Figure 31. Boosted GAM prediction for the partial contribution of the wind support covariate (x-axis) to the likelihood (log-transformed odds ratio) of exposure to Federal waters among Roseate Terns (y-axis) in 2015, 2016, and 2017 (pooled).	68
Figure 32. Boosted GAM prediction for the partial contribution of the wind direction covariate (x-axis) to the likelihood (log-transformed odds ratio) of exposure to Federal waters among Roseate Terns (y-axis) in 2015, 2016, and 2017 (pooled).	69
Figure 33. Boosted GAM prediction for the partial contribution of the air temperature covariate (x-axis) to the likelihood (log-transformed odds ratio) of exposure to Federal waters among Roseate Terns (y-axis) in 2015, 2016, and 2017 (pooled).	70

Figure 34. Movement tracks and composite probability density across WEAs of Common Terns (n=30) with estimated exposure to WEAs, 2016 and 2017.	73
Figure 35. Frequency distribution of WEA exposure events (n=30) by date for Common Terns from 2015 to 2017 (pooled) by location of tag deployment.	74
Figure 36. Diel variation (hrs, in EST) in timing of WEA exposure events (n=22) of Common Terns tagged on Great Gull Island, NY, categorized by daylight using timing of local sunrise and sunset.	75
Figure 37. Diel variation (hrs, in EST) in timing of WEA exposure events (n=8) of Common Terns tagged in Buzzards Bay, MA, categorized by daylight using timing of local sunrise and sunset.	76
Figure 38. Circular histogram of wind direction (degrees clockwise from N) during WEA exposure events (n=30) of Common Terns from 2015 to 2017.	77
Figure 39. Frequency distribution of wind speed (m/s) during WEA exposure events (n=30) of Common Terns from 2015 to 2017.	78
Figure 40. Frequency distribution of wind support (m/s) during WEA exposure events (n=30) of Common Terns from 2015 to 2017.	79
Figure 41. Frequency distribution of visibility (m) during WEA exposure events (n=30) of Common Terns from 2015 to 2017.	79
Figure 42. Frequency distribution of precipitation accumulation (kg/m ²) during of WEA exposure events (n=30) of Common Terns from 2015 to 2017.	80
Figure 43. Frequency distribution of precipitation air temperature (°C) during of WEA exposure events (n=30) of Common Terns from 2015 to 2017.	80
Figure 44. Frequency distribution of barometric pressure (Pa) during of WEA exposure events (n=30) of Common Terns from 2015 to 2017.	81
Figure 45. Movement tracks and composite probability density across WEAs of Roseate Terns (n=8), with estimated exposure to WEAs, 2016 and 2017.	83
Figure 46. Frequency distribution in calendar date of WEA exposure events (n=8) of Roseate Terns in 2016 and 2017 (pooled) by location of tag deployment.	84
Figure 47. Diel variation (hrs, in EST) in timing of WEA exposure events (n=8) of Roseate Terns, categorized by daylight using timing of local sunrise and sunset.	85
Figure 48. Circular histogram of wind direction (degrees clockwise from N) during WEA exposure events (n=8) of Roseate Terns in 2016 and 2017.	86
Figure 49. Frequency distribution of wind speed (m/s) during WEA exposure events (n=8) of Roseate Terns in 2016 and 2017.	87
Figure 50. Frequency distribution of wind support (m/s) during WEA exposure events (n=8) of Roseate Terns in 2016 and 2017.	88
Figure 51. Frequency distribution of visibility (m) during WEA exposure events (n=8) of Roseate Terns in 2016 and 2017.	88
Figure 52. Frequency distribution of precipitation accumulation (kg/m ²) during of WEA exposure events (n=8) of Roseate Terns in 2016 and 2017.	89

Figure 53. Frequency distribution of air temperature (C) during of WEA exposure events (n=8) of Roseate Terns in 2016 and 2017.	89
Figure 54. Frequency distribution of barometric pressure (Pa) during of WEA exposure events (n=8) of Roseate Terns in 2016 and 2017.....	90
Figure 55. Model-estimated flight altitude ranges (m) of Common Terns	92
Figure 56. Model-estimated flight altitude ranges (m) of Roseate Terns.....	93
Figure 57. Model estimated migratory tracks of Piping Plovers tagged in Massachusetts (red) and Rhode Island (blue) in 2015 (A), 2016 (B), and 2017 (C).....	97
Figure 58. Boosted GAM prediction for the partial contribution of the date of year covariate (x-axis) to the likelihood (log-transformed odds ratio) of exposure to Federal waters among Piping Plovers (y-axis)....	100
Figure 59. Boosted GAM prediction for the partial contribution of the wind direction covariate (x-axis, in degrees clockwise from Geographic North that the wind is blowing towards) to the likelihood (log-transformed odds ratio) of exposure to Federal waters among Piping Plovers (y-axis).....	101
Figure 60. Boosted GAM prediction for the partial contribution of the hour of day covariate (x-axis, in EST) to the likelihood (log-transformed odds ratio) of exposure to Federal waters among Piping Plovers (y-axis).....	102
Figure 61. Boosted GAM prediction for the partial contribution of surface air temperature (x-axis, in degrees Celsius) to the likelihood (log-transformed odds ratio) of exposure to Federal waters among Piping Plovers (y-axis).	103
Figure 62. Boosted GAM prediction for the partial contribution of wind support (x-axis, representing tailwind component in m/s) to the likelihood (log-transformed odds ratio) of exposure to Federal waters among Piping Plovers (y-axis).	104
Figure 63. Boosted GAM prediction for the partial contribution of year (x-axis) to the likelihood (log-transformed odds ratio) of exposure to Federal waters among Piping Plovers (y-axis).....	105
Figure 64. Migratory tracks and composite probability density across WEAs of Piping Plovers (n=19) with estimated exposure to WEAs, 2015 to 2017.....	108
Figure 65. Frequency distribution in calendar date of WEA exposure events (n=35) of Piping Plovers from 2015 to 2017 (pooled) by location of tag deployment.....	109
Figure 66. Diel variation (hrs, in EST) in timing of WEA exposure events (n=22) of Piping Plovers tagged in Massachusetts, categorized by daylight using timing of local sunrise and sunset.	110
Figure 67. Diel variation (hrs, in EST) in timing of WEA exposure events (n=13) of Piping Plovers tagged in Rhode Island, categorized by daylight using timing of local sunrise and sunset.	111
Figure 68. Circular histogram of wind direction (degrees clockwise from N) during WEA exposure events (n=35) of Piping Plovers from 2015 to 2017.	112
Figure 69. Frequency distribution of wind speed (m/s) during WEA exposure events (n=35) of Piping Plovers from 2015 to 2017.....	113
Figure 70. Frequency distribution of wind support (m/s) during WEA exposure events (n=35) of Piping Plovers from 2015 to 2017.....	114

Figure 71. Frequency distribution of visibility (m) during WEA exposure events (n=35) of Piping Plovers from 2015 to 2017.	115
Figure 72. Frequency distribution of precipitation accumulation (kg/m ²) during of WEA exposure events (n=35) of Piping Plovers from 2015 to 2017.	115
Figure 73. Frequency distribution of precipitation air temperature (°C) during of WEA exposure events (n=35) of Piping Plovers from 2015 to 2017.	115
Figure 74. Frequency distribution of barometric pressure (Pa) during of WEA exposure events (n=35) of Piping Plovers from 2015 to 2017.	116
Figure 75. Model-estimates flight altitude ranges (m) of Piping Plovers	118
Figure 76. Block Island offshore wind turbines	128

List of Tables

Table 1. Dates, start and end times (EST), transects, and weather conditions (wind speed reported in knots) of aerial surveys conducted during 2014 and 2015.	24
Table 2. Model workflow: steps 1-3 govern localization estimation, step 4 interpolates covariate data, and step 5 estimates exposure to Federal waters and WEAs	29
Table 3. Number of adult Common Terns tagged at nesting colonies in MA (Monomoy NWR, Buzzards Bay) and NY (Great Gull Island), 2014-2017	41
Table 4. Number of adult Roseate Terns tagged at nesting colonies in MA (Buzzards Bay) and NY (Great Gull Island), 2015-2017	41
Table 5. Number of adult Common Terns tagged at nesting colonies in MA (Monomoy NWR, Buzzards Bay) and NY (Great Gull Island) that were exposed to Federal waters, 2014-2017. Sample size (N) shows number of individuals tracked per year and location.	50
Table 6. Description and selection frequencies of covariates in binomial Boosted GAM analysis of exposure of Common Terns to Federal waters, 2014 to 2017.	51
Table 7. Number of adult Roseate Terns tagged at nesting colonies in MA (Buzzards Bay) and NY (Great Gull Island) that were exposed to Federal waters, 2015-2017. Sample size (N) shows number of individuals tracked per year and location.	60
Table 8. Description and selection frequencies of covariates in binomial Boosted GAM analysis of exposure of Roseate Terns to Federal waters, 2015 to 2017.....	61
Table 9. Number of adult Common Terns tagged at nesting colonies in MA (Monomoy NWR, Buzzards Bay) and NY (Great Gull Island) with estimated exposure to BOEM Wind Energy Areas, 2014-2017. Sample size (N) of individuals tracked per year appears in top row.....	71
Table 10. The number of estimated exposure events by Common Terns at BOEM Lease Areas within the Study Area during breeding and post-breeding dispersal 2014-2017. Sample size (N) of individuals tracked from each tagging location appears in top row.	71
Table 11. The number of estimated exposure events by Common Terns at BOEM Planning Areas within the Study Area during breeding and post-breeding dispersal 2014-2017. Sample size (N) of individuals tracked from each tagging location appears in top row.	72
Table 12. Summary statistics of meteorological conditions during WEA exposure events (n=30) of Common Terns from 2015 to 2017.	78
Table 13. Number of adult Roseate Terns tagged at nesting colonies in MA (Buzzards Bay) and NY (Great Gull Island) with estimated exposure to Wind Energy Areas, 2015-2017. Sample size (N) of individuals tracked per year appears in top row.....	81
Table 14. The number of estimated exposure events by Roseate Terns at BOEM Lease Areas within the Study Area during breeding and post-breeding dispersal 2015-2017. Sample size (N) of individuals tracked from each tagging location appears in top row.	82
Table 15. The number of estimated exposure events by Roseate Terns at BOEM Planning Areas within the Study Area during breeding and post-breeding dispersal 2015-2017. Sample size (N) of individuals tracked from each tagging location appears in top row.	82

Table 16. Summary statistics of meteorological conditions during WEA exposure events (n=8) of Roseate Terns from 2016 to 2017.....	87
Table 17. Model-estimated flight altitudes (m) of Common Terns during exposure to Federal waters and WEAs during the day and night, with sample size (number of 10-min time intervals) and frequency of estimated occurrence within the rotor-swept zone (25-250 m).....	91
Table 18. Model-estimated flight altitudes (m) of Roseate Terns during exposure to Federal waters and WEAs during the day and night, with sample size (number of 10-min time intervals) and frequency of estimated occurrence within the rotor-swept zone (25-250 m).....	91
Table 19. Tag deployment and detection summaries of adult Piping Plovers tagged at nesting areas in Massachusetts and Rhode Island, 2015-2017.....	94
Table 20. Number of adult Piping Plovers tagged from nesting areas in Massachusetts and Rhode Island that were exposed to Federal waters, 2015-2017	98
Table 21. Description and selection frequencies of covariates in binomial Boosted GAM analysis of exposure of Piping Plover to Federal waters, 2015-2017.....	99
Table 22. Number of adult Piping Plovers tagged from nesting areas in Massachusetts and Rhode Island with estimated exposure to BOEM Wind Energy Areas, 2015-2017	106
Table 23. The number of estimated exposure events by Piping Plovers at BOEM Lease Areas within the Study Area during fall migration, 2015-2017. Sample size (N) of individuals tracked from each tagging location appears in top row.	106
Table 24. The number of estimated exposure events by Piping Plovers at BOEM Planning Areas within the Study Area during fall migration, 2015-2017. Sample size (N) of individuals tracked from each tagging location appears in top row.	107
Table 25. Summary statistics of meteorological conditions during WEA exposure events (n=35) of Piping Plovers from 2015 to 2017.....	113
Table 26. Model-estimated flight altitudes (m) of Piping Plovers during exposure to Federal waters and WEAs during the day and night, with sample size (number of 10-min time intervals) and frequency of estimated occurrence within the rotor swept zone (25-250 m).....	117

List of Appendices

Appendix A. Comparing satellite and digital radio telemetry to estimate space and habitat use of American Oystercatchers in Massachusetts

Appendix B. Post-breeding dispersal and staging of Common and Arctic Terns throughout the western North Atlantic

Appendix C. Assessing the effects of digital VHF transmitters on nesting Common Terns

Appendix D. Metadata for BOEM tag deployments

Appendix E. Metadata for BOEM automated radio telemetry stations

Appendix F. Summary of global data from nano-tagged birds that were tagged by partners in the Motus network and detected by BOEM radio telemetry stations

Appendix G. Detection probability of BOEM automated radio telemetry stations

Appendix H. Summary of geospatially referenced detection data from all Common Terns, Roseate Terns, and Piping Plovers in this study submitted to BOEM as a supplemental material to this report

Appendix I. Summary of spring (northbound) migration data from Piping Plovers tagged during spring of 2017 in the Bahamas

Appendix J. Common Tern satellite telemetry pilot study

Appendix K. Summary of exposure of Common and Roseate Terns at the Block Island Wind Farm

List of Abbreviations and Acronyms

AHY	After Hatch Year
asl	above sea level
ASY	After Second Year
BGAM	Boosted Generalized Additive Model
BOEM	Bureau of Ocean Energy Management
COP	Construction and Operations Plan
dBm	decibel-milliwatts
DOI	US Department of the Interior
ESA	US Endangered Species Act
ESP	Environmental Studies Program
EST	Eastern Standard Time
ft	foot/feet
GMT	Greenwich Mean Time
GOMSWG	Gulf of Maine Seabird Working Group
GW	Gigawatts
HY	Hatch Year
K	Kelvin
kg	Kilogram
km	Kilometer
m	Meter
MBTA	Migratory Bird Treaty Act
min	minute(s)
Motus	Motus Wildlife Tracking System
MW	Megawatts
NARR	North American Regional Reanalysis
NEPA	National Environmental Policy Act
NWR	National Wildlife Refuge
OCS	Outer Continental Shelf
Pa	Pascal
PFR	Plastic Field Readable
PI	Principle Investigator
PO	Project Officer
RSZ	Rotor Swept Zone
SD	Standard Deviation
SY	Second Year
US	United States
USFWS	US Fish and Wildlife Service
USGS	US Geological Survey
UTM	Universal Transverse Mercator
VHF	Very High Frequency
WEA	Wind Energy Area

1 Introduction

The Bureau of Ocean Energy Management (BOEM) is responsible for managing energy and mineral resources on the Outer Continental Shelf (OCS) of the United States. The OCS extends from the outer limit of each state's jurisdictional waters (approximately 3 nautical miles or 5.6 km offshore) to the outer limit of the US Exclusive Economic Zone (approximately 200 nautical miles or 370 km offshore).

Since 2009, BOEM's Office of Renewable Energy Programs has issued twelve commercial wind energy leases and one research lease in the Atlantic OCS, from waters offshore of Massachusetts to North Carolina, totaling approximately 5,492 km² (BOEM 2018). Additional areas offshore of New York (7,188 km²), Massachusetts (1,577 km²), North Carolina (750 km²), and South Carolina (3,462 km²) are in the planning stages for future designation as lease areas (BOEM 2018). Herein, Wind Lease Areas and Wind Planning Areas are collectively referred to as Wind Energy Areas (WEAs).

Concurrently, several Atlantic coast states are developing plans to site additional wind energy facilities within their jurisdictional waters. The first offshore wind energy facility in the US, consisting of five 6-MW turbines within state waters off the coast of Block Island, RI, officially began operation in December of 2016. Several states have passed legislative requirements for power purchase agreements to procure energy from offshore wind (e.g., 5 GW capacity by 2030 in Maine, 1.6 GW capacity by 2027 in Massachusetts, 2.4 GW capacity by 2030 in New York, 1.1 GW capacity by 2028 in New Jersey), or to mandate that a proportion of electricity come from renewable sources (e.g., 25% by 2025 in New Hampshire, 38.5% by 2035 in Rhode Island, 25% by 2025 in Delaware, 25% by 2020 in Maryland, 15% by 2025 in Virginia, 12.5% by 2021 in North Carolina; Musial et al. 2017).

With large nearshore and offshore areas of the US Atlantic under consideration for development, both site specific and regional-scale studies are critical for understanding potential exposure of migratory birds to WEAs (BOEM 2017). Current understanding of the effects of offshore wind turbines on birds comes primarily from studies in western Europe, where large-scale offshore wind energy facilities have been in operation since the 1990s (Langston 2013). These studies have broadly categorized adverse effects to birds from offshore wind turbines as: 1) acting as barriers to movement (e.g. between foraging and roosting sites, along migration routes); 2) destruction, modification, or displacement of habitat; and 3) direct mortality from collisions with infrastructure or pressure vortices (Exo et al. 2003; Drewitt and Langston 2006; Fox et al. 2006). However, the magnitude of these effects are highly species and site specific, highlighting the importance of conducting fine-scale movement studies on priority species in areas of wind energy potential (Furness et al. 2013).

In the Federal waters of the U.S., assessments of the potential effects of development on migratory birds and their habitats are conducted in accordance with the National Environmental Policy Act (NEPA) and the Migratory Bird Treaty Act (MBTA). In addition, information regarding potential adverse effects to species listed as "Threatened" or "Endangered" under the US Endangered Species Act (ESA) is needed for Risk Assessments and Section 7 consultations between BOEM and the USFWS.

Preliminary assessments have identified three ESA-listed bird species that occur in the Atlantic OCS and that could be adversely affected by wind energy development: the Roseate Tern (*Sterna dougallii*) of the Federally-Endangered northeastern US breeding population, the Piping Plover (*Charadrius melodus*) of the Federally-Threatened US Atlantic coast breeding population, and the Red Knot (*Calidris canutus rufa*) of the Federally-Threatened *rufa* subspecies (Burger et al. 2011). Since 2013, BOEM and the USFWS have worked in partnership to address information gaps on the offshore movements of these three species using digital VHF tracking technology. Results from the Red Knot study are available in BOEM ESP 2018-046 (Loring et al. 2018). The present study pertains to the Roseate Tern, Piping Plover, and the non-ESA listed Common Tern.

Common and Roseate Terns are colonial seabirds that nest sympatrically on islands off the US Atlantic coast (Nisbet et al. 2014). Both species occur in the Atlantic OCS during the breeding period and migrate across the Atlantic OCS while traveling between northern breeding grounds and the southern non-breeding range that extends along the coast of South America (Nisbet et al. 2014, Nisbet et al. 2017). The Roseate Tern was listed as "Endangered" under the ESA in 1987 (USFWS 1987). The Common Tern is considered a USFWS "Species of Conservation Concern" (Kushlan et al. 2002) and listed as a Threatened or Special Concern species by the states comprising its U.S. Atlantic coast breeding range (Maine to South Carolina, USA, Nisbet et al. 2017).

The Common Tern is also a species of interest because it shares similar life-history characteristics and often occurs in association with the Roseate Tern during breeding, post-breeding dispersal, and pre-migratory staging periods (Safina and Burger 1985; Trull et al. 1999; Nisbet et al. 2014; Althouse et al. 2016; Nisbet et al. 2017). In 2013 and 2014, Common Terns were initially tagged for this study to evaluate the safety and effectiveness of VHF transmitters, prior to deployment on the taxonomically similar but Federally-listed Roseate Tern. From 2015 to 2017, when the study expanded to include Roseate Terns, we continued tracking the movements of Common Terns to assess variation in exposure to Federal Waters and WEAs between the two species. Previous assessments indicated that Common and Roseate Terns may share similar levels of risk to collision and displacement effects of offshore wind turbines (Robinson Willmott et al. 2013), although these assessments are subject to high uncertainty due to lack of empirical data (Burger et al. 2011).

Piping Plovers are migratory shorebirds that nest along the U.S. Atlantic coast and may occur in the Atlantic OCS during migration between breeding areas and wintering areas in the southeastern US and Caribbean (Burger et al. 2011). The Piping Plover was listed as "Threatened" under the U.S. ESA in 1985 (USFWS 1985).

1.1 Risk Assessments and Information Needs for Focal Species in the AOCS

Risk assessments of avian exposure to offshore wind energy facilities require species-specific information about: 1) spatial and temporal movement patterns, 2) flight altitudes, and 3) behavioral avoidance of turbines (Fox et al. 2006). Information on flight altitudes is used to assess risk of exposure to the RSZ of offshore wind turbines. Herein, we assume that the RSZ occurs from 25 m to 250 m asl, however there is some variability in the range of rotor-swept altitudes among different wind energy facilities. For example,

the RSZ of current turbines at the Block Island Wind Farm in Rhode Island is 29 to 189 m asl (6 MW), whereas the RSZ of 10 MW wind turbines planned in offshore waters of Massachusetts is 31 to 212 m asl (D. Bigger, pers. comm.).

Preliminary assessments of risks to focal species from potential development within the Atlantic OCS have identified priority information gaps and uncertainties (Burger et al. 2011). Roseate and Common Terns occur in the Atlantic OCS during breeding, post-breeding, and migration, although specific information on their movement patterns is lacking (Burger et al. 2011). During the breeding and post-breeding periods, there is some evidence that flight altitudes of Roseate Terns are usually below the RSZ; however, wide variation (0-41%) in the estimated numbers of Common Terns flying within the RSZ has been reported across studies (Burger et al. 2011; Furness et al. 2013). There is very little information on the routes and flight altitude of Common and Roseate Terns during migration (Burger et al. 2011), although data from geolocator studies show that migration of both species occurs offshore (Nisbet et al. 2011; Mostello et al. 2014). Ship-based surveys have detected Common Terns greater than 50 km off the coast of Virginia during their northerly migration, when they return to breeding colonies (Goyert et al. 2016). During the post-breeding season, Roseate Terns have been detected by ship-based observers over 100 km from shore (237 km east of Cape Cod), and Common Terns up to 350 km from shore, within the Atlantic OCS (Goyert et al. 2014).

Overall, very little empirical data are available to inform risk assessments of Piping Plovers in the Atlantic OCS (Burger et al. 2011). Until the present study, there was no information on whether Piping Plovers migrate along the coast or offshore (Burger et al. 2011), although individuals wintering in the Caribbean must cross the Atlantic OCS at some point during migration (Haig and Plissner 1993; O'Connell et al. 2011). There are no empirical data on flight altitudes of Piping Plovers during migration (Burger et al. 2011). Information on the migratory routes and altitudes of Piping Plovers in the Atlantic OCS is critical for evaluating risks of offshore wind energy development to this species (Burger et al. 2011).

In addition to understanding spatial and seasonal variation of exposure to the Atlantic OCS, information on temporal variation is needed to identify timing of potential risk windows (Fox et al. 2006). Risk of collision is potentially higher at night due to reduced visibility of turbines (Exo et al. 2003) and attraction or disorientation effects from artificial lighting on turbine towers (Richardson 2000; Drewitt and Langston 2006). Previous risk assessments indicate that more information is needed on the diurnal versus nocturnal flight patterns of Common and Roseate Terns in the Atlantic OCS, as most information to date has been collected by aerial and boat-based observations that are limited to surveying during daylight (Robinson Willmott et al. 2013). There is no information on diel variation in the migration ecology of Piping Plovers in the Atlantic OCS (Burger et al. 2011).

Information about meteorological conditions associated with offshore flights is also important for risk assessments, as birds may be at higher risk of collision with offshore wind turbines during inclement weather (high winds, precipitation, low visibility) due to impaired visibility and avoidance response (Exo et al. 2003). Migratory birds may also descend into the RSZ during periods of limited visibility, low cloud ceiling, and/or inclement weather (Hüppop et al. 2006).

In order to assess potential risks to populations, information is needed on demographic variation in exposure, including breeding population, age, and sex (Allison et al. 2008). Data on demographic variation in movement patterns of individually-marked birds can be obtained through tracking studies (Burger and Shaffer 2008). In this study, we used digital VHF tracking technology to quantify the movements of Common Terns, Roseate Terns, and Piping Plovers to Federal Waters and WEAs in the Atlantic OCS in relation to temporal variation, meteorological conditions, and demographic variation. This aim of this analysis is to address some of the key information gaps on the offshore movements of focal species and inform future risk assessments of developing offshore wind energy facilities within the Atlantic OCS.

1.2 VHF Technology to Study Movements

For small-bodied species of terns and shorebirds, VHF technology remains one of the sole options for tracking movements of individuals at high spatial and temporal resolution over extended durations. Conventional VHF telemetry has been a standard technique in wildlife tracking studies since the 1960s (Cochran et al. 1965) and involves affixing individuals with lightweight radio transmitters (minimally <1 g), and tracking their signals with specialized antennas and receiving units (Kenward 1987). Conventional VHF technology is based on a system where each transmitter operates on a unique frequency and receivers are programmed to cycle through frequencies sequentially, resulting in a trade-off between overall sample size and detection probability of individual transmitters (Kenward 1987).

Recent advances in the development of digital VHF technology now make it possible to simultaneously monitor thousands of uniquely coded transmitters on a single VHF frequency (Taylor et al. 2017). The use of digital VHF transmitters with automated radio telemetry stations allows thousands of individuals to be monitored continuously and autonomously. Configurations of automated radio telemetry stations are customizable and thus vary widely, but in general consist of one or more receiving antennas elevated on a structure (typically a stand-alone mast) and connected to an automated receiving unit that records detection data from all transmitters within range of the station (typically within 15 km; Taylor et al. 2017). Detection range of automated radio telemetry stations generally increases with the height and gain of the transmitting and the receiving antennas (Cochran 1980). However, since VHF waves emitted by transmitters travel within line-of-sight, factors such as topography, vegetation, and electronic noise may block, reflect, or attenuate the signal (Kenward 1987).

In 2013, we conducted pilot studies to test the safety and effectiveness of using digital VHF technology for tracking local to regional movements of American Oystercatchers (*Haematopus palliatus*) and Common Terns with an array of eight automated radio telemetry stations in the eastern Nantucket Sound region of Massachusetts. As part of this study, individual American Oystercatchers were double-tagged with a digital VHF transmitter and an ARGOS satellite transmitter to compare estimates of length of stay, home ranges, and habitat characteristics on the breeding grounds (Loring et al. 2017a, Appendix A). Our pilot work with Common Terns was coordinated with researchers conducting digital VHF tracking studies on Common and Arctic Terns (*Sterna paradisaea*) at three additional nesting colonies in the Gulf of Maine and Atlantic Canada, providing an opportunity to test the utility of using coordinated, digital VHF tracking technology at a regional scale (Loring et al. 2017b; Appendix B). In addition, we conducted a study on tag retention, behavior and reproductive success of tagged adult Common Terns that

demonstrated the safety and effectiveness of using a glue and suture tag attachment method for medium-term (2 to 3 month) deployments on *Sterna* terns (Loring 2016; Appendix C).

In 2014, the pilot study was expanded to track Common Terns from multiple colonies across the Southern New England continental shelf region, extending the Study Area from Cape Cod, MA to Long Island, NY. This study demonstrated the effectiveness of using nanotag tracking technology to assess exposure of Common Terns to multiple WEAs throughout the study area, and address information gaps on timing, demographic, and meteorological conditions associated with offshore flights (Loring 2016).

The pilot work in 2014 led to the expansion of the study in 2015 to include ESA-Listed Roseate Terns and Piping Plovers. From 2015 and 2017, we expanded our array of automated radio telemetry stations to include a total of 33 coastal and island sites distributed from Cape Cod, Massachusetts to Back Bay, Virginia. We selected sites that were: 1) in close proximity to key areas used by focal species within the Study Area; 2) adjacent to BOEM Lease Areas and Planning Areas within the Study Area; 3) in direct line of sight to offshore waters to maximize reception; and 4) within detection range of one or more adjacent towers to facilitate triangulation. Triangulation is a technique used to estimate 2-dimensional (x, y) animal locations using signal strength and bearings from signals received by directional antennas from multiple towers simultaneously. In addition, we piloted the use of automated radio stations on three different types of boats (passenger ferry, whale watching boat, NOAA Research vessel), and we conducted a series of aerial telemetry surveys to relocate tagged birds offshore.

Beginning with our pilot work in 2013, we have coordinated our tracking efforts with the Motus Wildlife Tracking System (Motus; www.motus.org), a collaboration of researchers using digital VHF transmitters and automated radio telemetry stations to track the movements of birds and bats from the Canadian High Arctic to South America (Taylor et al. 2017). Motus provides a system to coordinate data sharing among automated radio telemetry studies on a common frequency, allowing all tagged individuals to be detected by all stations in the network. Since its formal inception as a program of Bird Studies Canada in 2014, the Motus network has expanded to include over 300 automated radio telemetry stations distributed across the Western Hemisphere that are operated in collaboration among 120 different research efforts (Taylor et al. 2017).

For this study, we used data from the targeted BOEM-funded array and the broader Motus network to provide a spatially-explicit, empirical assessment of exposure risk. We defined exposure as the degree to which Common Terns, Roseate Terns, and Piping Plovers use targeted areas of the Atlantic OCS, from Cape Cod, MA to southern VA that are under consideration for the development of offshore wind energy facilities. As part of this study, we developed new quantitative methods to model movements of tagged birds throughout the digital VHF telemetry array. This included estimates of altitude when signals were received simultaneously by multiple receiving stations. We applied these models to assess exposure of our focal species to Federal waters and WEAs of the Atlantic OCS, relative to meteorological, temporal, and demographic covariates.

Our specific objectives were to:

- (1) Develop spatially-explicit, 3-dimensional models to estimate movements of Common Terns, Roseate Terns and Piping Plovers in the Atlantic OCS Study Area during breeding and post-breeding periods;

(2) Estimate the exposure of Common Terns, endangered Roseate Terns and threatened Piping Plovers to Federal Waters, and to each BOEM Lease Area and BOEM Planning Area in the Atlantic OCS Study Area, during breeding and post-breeding periods.

(3) Quantify effects of meteorological conditions (e.g., wind speed, wind direction, barometric pressure, temperature, visibility, precipitation), temporal variation (time of day, date), and demographic variation (breeding population, sex, reproductive success) on occurrence of Common Terns, Roseate Terns and Piping Plovers within Federal waters and WEAs within the Atlantic OCS Study Area.

2 Methods

2.1 Study Area

2.1.1 Atlantic OCS and Wind Energy Areas

The Study Area extends along the US Atlantic Coast and adjacent OCS waters. Along the coast, the Study Area is bounded by Cape Cod, MA to the north and Back Bay, VA to the south (Fig. 1).

Currently (February 2019), there are 11 BOEM Commercial Renewable Energy Lease Areas within the Study Area, as well as one Research Renewable Energy Lease Area (Fig. 1). These BOEM Renewable Energy Lease Areas are located in Rhode Island Sound and adjacent offshore waters of Massachusetts (2,106 km²), New York Bight (321 km²), and adjacent waters offshore of New Jersey (1,391 km²), Delaware (390 km²), Maryland (322 km²) and Virginia (467 km²). In total, their combined area covers 4,997 km² of the Atlantic OCS. Additional BOEM Planning Areas (under consideration for designation as lease areas) are located within the Study Area in Federal waters off the coast of Massachusetts (1,578 km²) and New York (7,188 km²).

2.1.2 Tagging Sites

All tagging was conducted during the breeding period and tracking continued through post-breeding dispersal and migratory departure. We tagged Common and Roseate Terns at their largest nesting colonies within the US Atlantic, with the Roseate Tern sites collectively harboring over 90% of the northeastern US breeding population (Nisbet et al. 2014). We tagged Piping Plovers from breeding populations within the northern portion of the Study Area to track their southbound flights during fall migration.

2.1.2.1 Monomoy National Wildlife Refuge (NWR), Massachusetts

Monomoy NWR (41°36'31" N, 69°59'12" W) is a 30-km² barrier beach and island complex located in the southeastern Cape Cod region of Massachusetts, USA. Monomoy NWR supports one of the largest Common Tern colonies on the Atlantic coast, with over 8,500 nesting pairs in 2014 (GOMSWG 2014). In 2014 and 2015, we tagged Common Terns within the nesting colony on Monomoy NWR. From 2015 to 2017, we tagged Piping Plovers on Monomoy NWR and adjacent South Beach in Chatham, MA

(41°37'24"N, 69°57'58"W). In 2017, these sites collectively supported 61 pairs or about 9% of the Massachusetts population of 668 pairs of Piping Plovers (Levasseur et al. 2017).

2.1.2.2 Great Gull Island, New York

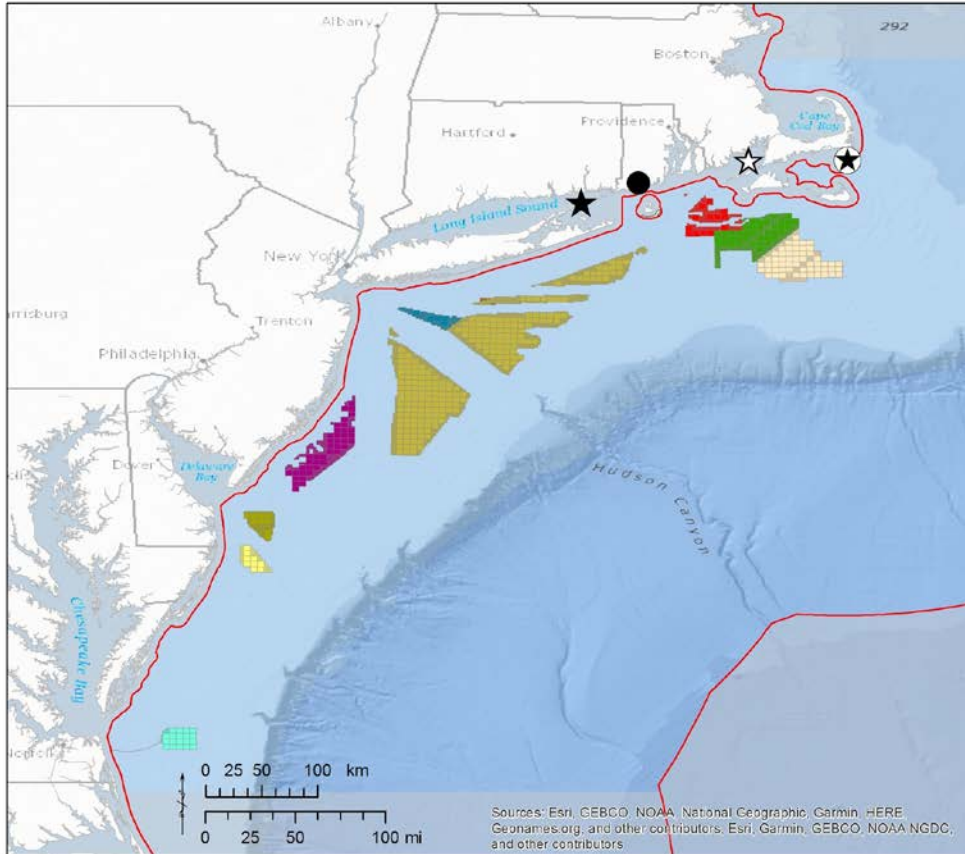
Great Gull Island (41°12'23" N, 72°06'25" W) is a 0.08 km² offshore island in eastern Long Island Sound, NY, that supports one of the largest concentrations of nesting Common Terns (approximately 9,500 pairs) and Roseate Terns (approximately 1,800 pairs) in the Western Hemisphere (H. Hays and G. Cormons, unpubl. data) and is managed by the Great Gull Island Project with the American Museum of Natural History. On Great Gull Island, we tagged Common Terns from 2014 to 2017 and Roseate Terns from 2015 to 2017.

2.1.2.3 Buzzards Bay, Massachusetts

From 2016 to 2017, we tagged Common and Roseate Terns from three islands (Bird, Ram, and Penikese) in Buzzards Bay, Massachusetts. These islands are managed by the Massachusetts Natural Heritage and Endangered Species Program and collectively supported over 6,500 Common Terns and approximately 2,600 pairs of Roseate Terns in 2016 (Mostello et al. 2018). Bird Island (41°40'10 N, 70°43'02"W) is a 0.006 km² island located < 2 km off the coast of Marion, MA. Ram Island (41°37'05"N, 70°48'16"W) is a 0.01 km² island located < 1 km off the coast of Mattapoisett, MA. Penikese Island (41°27'05"N, 70°55'03"W) is 0.3 km² island located near the western entrance of Buzzards Bay, within the Elizabeth Islands chain.

2.1.2.4 Coastal Rhode Island

From 2015 to 2017, we tagged Piping Plovers within nesting areas at several sites along the southern coast of Rhode Island. Nesting Piping Plovers at these sites are monitored by the USFWS, although individual sites are owned and managed by various Federal, state, and NGO entities and have varying levels of public use and access. Across all sites in RI, the highest trapping effort for Piping Plovers was on Trustom Pond NWR (41°22'11"N, 71°34'52"W) along a 2.1 km section of barrier beach habitat where public access is limited to below the mean high tide line during the nesting period (1 April to 15 September; USFWS 2002). Trustom Pond NWR contains the highest nesting population of Piping Plovers in Rhode Island, accounting for 31% of nesting pairs in monitored by USFWS staff in 2018 (J. White, USFWS, Rhode Island Wildlife Complex, Charlestown, RI, unpubl. data).



Legend

BOEM Wind Lease Areas

- RI/MA OCS-A 0486 and 0487
- MA OCS-A 0500 and 501
- NY OCS-A 0512
- NJ OCS-A 0498 and 0499
- DE OCS-A 0482 and 0519
- MD OCS-A 0490
- VA OCS-A 0483 and 0497

U.S. Federal Waters

- 3 - 200 nautical mile boundary

BOEM Wind Planning Areas

- Massachusetts PSN
- New York Bight Call Area
- New York Proposed Commercial Lease

Block Island Wind Farm

-

Tagging Sites

- ☆ Common and Roseate Terns (Buzzards Bay, MA)
- ★ Common and Roseate Terns (Great Gull Island, NY)
- ⊛ Common Terns and Piping Plovers (Monomoy NWR, MA)
- Piping Plovers (coastal RI)

Figure 1. Map of Study Area in Atlantic OCS

Stars show locations of Common and Roseate Tern tagging sites, and circles show locations of Piping Plover tagging sites. Federal waters of the U.S Atlantic are delineated by the red boundary (3 to 200 nautical miles). Within this boundary, all current (July 2018) BOEM Wind Energy Areas and Planning Areas are shown as polygons.

2.2 Study Species

2.2.1 Common Tern

Common Terns are globally-distributed, mid-sized (110 to 145 g) seabirds that breed throughout the Northern Hemisphere and winter along tropical and subtropical coasts (Nisbet et al. 2017). Along the northern Atlantic coast of North America, Common Terns nest colonially on islands and barrier beaches from Newfoundland and Labrador, Canada to South Carolina, USA (Nisbet et al. 2017). Available evidence suggests that Common Terns wintered in at least four sites on the north and east coasts of South America from Guyana to Argentina, with a stopover site in Puerto Rico (Nisbet et al. 2011a). Common Terns forage by plunge diving for small fish of various species in open waters, often over shoals, tide rips, or marine predators (e.g. *Thunnus* spp., cetaceans) that drive bait to the surface (Duffy 1986, Safina 1990, Goyert et al. 2014). Previous studies have shown that during the breeding season, Common Terns typically forage within about 20 to 30 km of their nest sites (Safina 1990, Duffy 1986, Thaxter et al. 2012, Nisbet et al. 2017). During their northerly migration, Common Terns have been observed greater than 50 km off the coast of Virginia and Massachusetts (Goyert et al. 2016, Veit et al. 2016). In southern New England, adults arrive at their nesting sites in late April to May and nest through mid-July (Nisbet et al. 2017). Common Terns nest within sand to cobble substrates, typically laying a two to three egg clutch (Nisbet et al. 2017). Peak hatch occurs between June and early July, and chicks fledge within 22 to 29 days of hatching (Nisbet et al. 2017). Prior to migration, mixed flocks of Common and Roseate Terns stage at sites along the U.S. Atlantic coast from Maine through New Jersey (Shealer and Kress 1994, Nisbet et al. 2017), with large flocks of over >10,000 terns reported on Cape Cod, Massachusetts (Trull et al. 1999). They also use this post-breeding, pre-migratory season to forage far offshore (up to 350 km from the coast, within the Atlantic OCS), where they rest on the water (Goyert et al 2014). Studies using archival light-level loggers (geolocators) revealed that Common Terns migrate offshore across the western North Atlantic (Nisbet et al. 2011). Available studies indicate that Common Terns typically fly at altitudes of 1 to 30 m (Johnston and Cook 2016, Borkenhagen et al. 2018), but may ascend to altitudes of 1,000 m to 3,000 m during migration (Alerstam 1985). Common Terns are a long-lived species (maximum known age: 29 years) with a mean annual adult survival rate ranging from 0.80 to 0.88 (Brenton et al. 2014, Nisbet et al. 2017).

2.2.2 Roseate Tern

Roseate Terns are a mid-sized (95 to 130 g) seabird with a scattered tropical and temperate distribution (Nisbet et al. 2014). In North America, there are two populations of Roseate Terns: the Federally-endangered northeastern population, and the Federally-threatened Caribbean population. The wintering ranges for both populations are poorly understood, with known wintering sites distributed from Guyana to eastern Brazil along the coast of South America and staging areas near Puerto Rico and the Dominican Republic (Hays et al. 1997; Mostello et al. 2014). Individuals from the northeastern population of Roseate Terns only nest in mixed-species colonies in sympatry with Common Terns, on a limited number of islands distributed from Maritime Canada to Long Island, NY, with only three colonies that have over 200 nesting pairs (Bird and Ram Islands in MA and Great Gull Island in NY; Nisbet et al. 2014). Like Common Terns, Roseate Terns also forage by plunge-diving for prey fish in nearshore and offshore waters, often in association with shoals, tide rips, or marine predators (Duffy 1986, Nisbet et al. 2014, Goyert 2014). In the western North Atlantic, Roseate Terns are known to specialize on sand-lance

(*Ammodytes* spp.; Nisbet et al. 2014; Goyert 2015) and previous studies have estimated their foraging ranges as approximately 20 to 30 km from their nest sites during the breeding period (Duffy 1986, Heinemann 1992, Burger et al. 2011, Thaxter et al. 2012). Peak hatch occurs between June and early July, and chicks fledge within 22 to 30 days of hatching (Nisbet et al. 2014). During the post-breeding period (late July through September), thousands of Common Terns and nearly the entire Northeast population of Roseate Terns have been shown to concentrate together at relatively undisturbed coastal sites on outer Cape Cod and Nantucket to feed and roost prior to their southward migration (Trull et al. 1999). They also occur far offshore (over 100 km) during this pre-migratory period, where they have been observed foraging and resting on the water (Goyert et al. 2014). Peak migratory departure of Roseate Terns from the western North Atlantic region occurs in early September (Nisbet et al. 2014). Like Common Terns, recent a study using geolocators revealed that, during fall migration, Roseate Terns from nesting areas in the western North Atlantic migrated offshore directly to the West Indies en route to wintering areas in South America (Mostello et al. 2014). Roseate Terns are a long-lived species (maximum known age >25 years) with a mean annual adult survival rate of 0.84 (Spendelov et al. 2008, Nisbet et al. 2014).

2.2.3 Piping Plover

Piping Plovers are small-bodied (43 to 63 g) migratory shorebirds. The species breeds only in North America, in three federally-listed populations: Great Lakes (Endangered), the Northern Great Plains (Threatened) and Atlantic Coast (Threatened; Elliott-Smith and Haig 2004). On the Atlantic coast of North America, their breeding range extends from the Canadian Maritimes to North Carolina, and their wintering range occurs from the US mid Atlantic to the Gulf of Mexico, with some individuals scattered throughout the Caribbean (Elliott-Smith and Haig 2004). In coastal areas, Piping Plovers typically nest on open sandy beaches and forage on a variety of invertebrates along the shoreline and intertidal zone (Elliott-Smith and Haig 2004). Along the Atlantic coast, the migratory routes that Piping Plovers follow have not been fully described (Elliott-Smith and Haig 2004). Spring migration to Atlantic coast breeding sites begins in mid to early March, with birds arriving at southern New England breeding sites through early May (Elliott-Smith and Haig 2004). On the US Atlantic Coast, Piping Plovers nest in shallow scrapes and lay an average of four eggs. Peak hatch typically occurs in June, and chicks fledge within about 35 days (Elliott-Smith and Haig 2004). The post-breeding dispersal period occurs through late August. Piping Plovers are thought to depart on migration in small groups, although large flocks (approx. 100 birds) are sometimes observed at coastal sites during fall (Elliott-Smith and Haig 2004). Prior to the present study, few data were available on the migratory routes that Atlantic Coast Piping Plovers use during fall migration (Elliott-Smith and Haig 2004).

2.3 Digital VHF Transmitters

In this study, we tracked the movements of Common Terns, Roseate Terns, and Piping Plovers using digital VHF transmitters (“nanotags”, Lotek Wireless, Ontario, Canada). Each Common and Roseate Tern in the study was fitted with Lotek NTQB-4-2 nanotag. The transmitter body measured 12 x 8 x 8 mm and had a 18-cm antenna. The NTQB-4-2 nanotags deployed on terns were coated with a waterproofing material and custom-fit with 1-mm tubes at the front and back of the transmitter body for attachment, bringing the total tag weight to 1.5 g. The transmitter and attachment materials weighed <2% of the body mass of tagged Common and Roseate terns.

In 2015 and 2016, each Piping Plover in the study was fitted with a Lotek NTQB-4-2 nanotag (1.1 g; 12 x 8 x 8 mm). In 2017, each Piping Plover within the study was fitted with a Lotek NTQB-3-2 nanotag (0.67 g; 12 x 6 x 5 mm). Both tag models used on Piping Plovers had a 16.5-cm antenna. The transmitter and attachment materials weighed <3% of the body mass of tagged Piping Plovers (<2% for the 0.67 g model).

All transmitters in the study were programmed to continuously transmit signals on a shared frequency of 166.380 MHz from activation through the end of battery life. Burst intervals (time between transmissions) were specific to each transmitter and ranged from 4 to 6 seconds. The expected life of the NTQB-4-2 nanotags ranged from 146 days (4 second burst interval) to 187 days (6 second burst interval). The expected life of the NTQB-3-2 nanotags ranged from 72 days (4 second burst interval) to 92 days (6 second burst interval). Tag deployment metadata for each nano-tagged bird in this study are provided in Appendix D.

2.4 Capture and Tag Attachment Summaries

2.4.1 Common and Roseate Terns

From 9 June to 12 July, staff at nesting colonies used walk-in treadle traps to capture adult Common and Roseate Terns at their nests, within approximately 1 to 5 days of their hatch date (Fig. 2). All banding activities were conducted by colony managers at each tagging site. Terns that were not previously banded were marked with an incoloy (at Monomoy and Buzzards Bay colonies) or steel (at Great Gull Island colony) U.S. Geological Survey (USGS) band on the tarsometatarsus. At Monomoy and Great Gull Island, the opposite tarsometatarsus was marked with a wrap-around a plastic field readable (PFR) band engraved in with a unique 3-digit alphanumeric code (Fig. 2). Common Terns banded at Monomoy NWR in 2014 were marked with a black PFR band engraved with a white alphanumeric code. Roseate Terns banded on Great Gull Island from 2015 to 2017 were marked with either a yellow PFR with a black alphanumeric code (2015) or a dark blue PFR band with a white alphanumeric code (2016 and 2017). Morphometric measurements collected on each bird included bill length (± 0.01 mm), head and bill length (± 0.01 mm), flattened wing chord (± 1 mm), and mass (± 0.1 g). From each bird, three to five contour feathers were collected for molecular-based determination of gender (Avian Biotech, Gainesville, FL).

Following banding, we attached a digital 1.5 g VHF transmitter ('Avian NanoTag'; Lotek Wireless, Inc., Newmarket, Ontario, Canada) to the dorsal inter-scapular region using cyanoacrylate adhesive and two sutures (Prolene: 45-cm length, 4.0, BB taper point needle, catalog # 8581H) that were inserted subcutaneously and secured to the end-tubes of the transmitter (Fig. 2). Total handling time, from capture to release, ranged from 20 to 40 min per individual.

2.4.2 Piping Plovers

From 9 May through 27 June, we captured adult Piping Plovers at their nest sites during the incubation phase. In some of our trapping areas, site managers placed circular wire anti-predator exclosures over selected nests to minimize egg depredation, and we used different types of traps depending on whether or not target nests were exclosed. For nests with no exclosures, we trapped adult plovers using walk-in

funnel traps at active nests (Cairns 1977; Fig. 3). We used modified trap for enclosed nests by attaching hardware cloth with a mist-net funnel to the exterior of the enclosure.

We banded each plover with a single, dark blue Darvic leg band on the right tibiotarsus and a green, three-digit alpha-numeric coded flag unique to each individual on the opposite tibiotarsus (Fig. 3). Coded flags were issued in collaboration with researchers at Virginia Tech as part of a larger population dynamics study. All individuals were measured using standard protocols, and in most cases, included tarsus (± 0.01 mm), culmen (± 0.01 mm), flattened wing chord (± 1 mm), and mass (± 0.1 g). From each bird, three to five contour feathers were collected for molecular-based determination of gender (Avian Biotech, Gainesville, FL). Nanotags were attached by clipping a small area of feathers from the interscapular region and gluing the tag to the feather stubble and skin with a cyanoacrylate gel adhesive (Fig. 3). Handling time, from capture to release, was approximately 15 to 30 min per bird. Field staff surveyed each nesting area 3 to 5 days per week to monitor the nesting success and tag retention of all tagged Piping Plovers within the study. There was no evidence that trapping or tagging plovers affected their productivity as measured by the number of chicks fledged per nesting attempt (Stantial et al. 2018).

A.



B.



C.



Figure 2. Photos of Common and Roseate Tern trapping and transmitter deployment

A) Walk-in treadle traps deployed at nest sites of Common Terns; B) attaching nanotag to interscapular region of Common Tern using sub-cutaneous sutures; C) Roseate Tern with nanotag (interscapular region), metal USGS band (left tarsometatarsus) and plastic field readable band (right tarsometatarsus). Photos: Peter Paton.

A.



B.



Figure 3. Photos of Piping Plover trapping and transmitter deployment

A) Deploying walk-in funnel trap on a Piping Plover nest; B) Piping Plover with a nanotag (interscapular region), dark blue Darvic band (right tibiotarsus) and green coded flag (left tibiotarsus). Photos: Peter Paton.

2.5 Automated Radio Telemetry Stations

We tracked the signals of nano-tagged birds using an array of automated radio telemetry stations. Typical station specifications consisted of a 12.2-m radio antenna mast supporting six, nine-element (3.3 m) Yagi antennas mounted in a radial configuration at 60-degree intervals (Fig. 4). At some sites, stations consisted of up to four Yagi antennas, or a single omni-directional antenna, attached to existing structures. At each station, the antenna(s) were connected to ports on a receiving unit (Lotek SRX-600, Lotek Wireless, Ontario, Canada) via coaxial cable (TWS-200). The receivers were programmed to automatically log several types of data from each antenna, including: tag ID number, date, time stamp, antenna (defined by monitoring station and bearing), and signal strength (linear scale: 0 to 255). Each receiving station was operated 24 hours per day using one 140-watt solar panel and two 12-volt deep-cycle batteries.

Detection range of each station varied with the height of the station above sea level (asl) and with altitude of the transmitting bird. The maximum estimated detection range of stations 12.2 m asl was approximately 20 km to birds flying at 25 m altitude (lower limit of RSZ of offshore wind turbines), and approximately 40 km to birds flying at 250 m altitude (upper limit of RSZ of offshore wind turbines). Birds flying at migratory altitudes (1,000 m) may be detected at ranges exceeding 80 km (Loring et al. 2018).

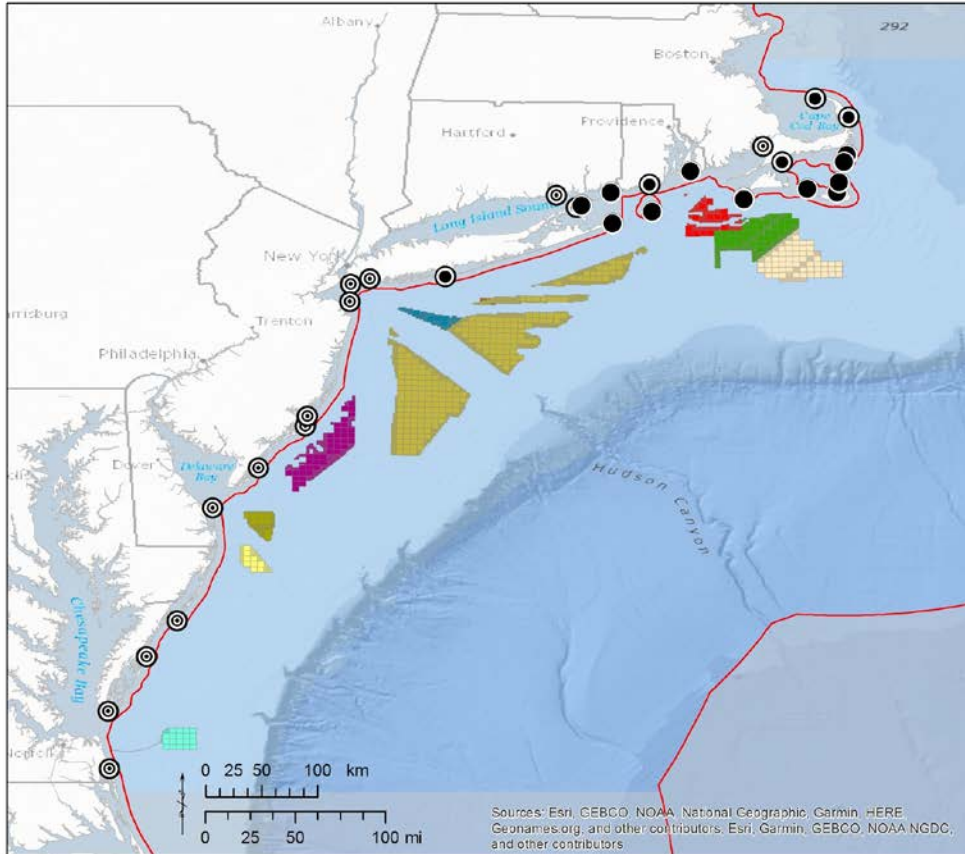
In 2014, we operated an array of eleven, land-based automated radio telemetry towers at coastal sites ranging from Cape Cod, MA to Long Island, NY (Fig. 5). In addition, at each tern tagging site (Monomoy NWR and Great Gull Island), we operated receiving stations that were configured to monitor to track local movements of nano-tagged terns at the breeding colony. We also operated two mobile receiving stations: (1) on a passenger ferry that traveled along a north-south route across Nantucket Sound, and (2) on a NOAA research vessel (R/V Henry Bigelow) that regularly traveled from Newport, RI to sites throughout the northwest Atlantic, including George's Bank, approximately 100 km east of Cape Cod, MA.

In 2015, we expanded the array to include five additional land-based telemetry towers in Massachusetts, Rhode Island, and New York. We continued to run a receiving station on a passenger ferry in Nantucket Sound, and added an additional boat-based receiving station on a whale watching boat based out of Nantucket, MA. At the end of the 2015 season, due to logistical issues, we decommissioned two land-based stations (Monomoy tern colony and Eel Point, Nantucket) and two-boat based stations (passenger ferry and NOAA ship).

During 2016, we added 14 land-based telemetry towers at high-priority sites ranging from Cape Cod, MA to Back Bay VA. The expanded array of 30 land-based telemetry stations, and the station on the whale watching boat in Nantucket Sound, remained in operation through the fall of 2017. To date (February 2019), the majority of the tracking towers are still in operation to support the Motus Wildlife Tracking Network. A detailed description of the locations, specifications, and operational dates of each receiving station appears in Appendix E.



Figure 4. Automated radio telemetry station on Nantucket NWR (Great Point), Nantucket, MA
Station consisted of a radial Yagi antenna array atop a guyed, 12.2 m mast with a solar powered automated receiving unit at the base (photo: Matt Malin).



Legend

BOEM Wind Lease Areas

- RI/MA OCS-A 0486 and 0487
- MA OCS-A 0500 and 501
- NY OCS-A 0512
- NJ OCS-A 0498 and 0499
- DE OCS-A 0482 and 0519
- MD OCS-A 0490
- VA OCS-A 0483 and 0497

U.S. Federal Waters

- 3 - 200 nautical mile boundary

BOEM Wind Planning Areas

- Massachusetts PSN
- New York Bight Call Area
- New York Proposed Commercial Lease

Block Island Wind Farm

-

BOEM Tracking Stations (years operated)

- 2014 - 2017
- ⊙ 2015 - 2017
- ⊗ 2016 - 2017

Figure 5. Map of BOEM automated radio telemetry stations within the Study Area in 2014-2017

Black and white points show locations of BOEM telemetry stations operated from 2014-2017, symbolized by years of operation. Federal waters of the U.S Atlantic are delineated by the red boundary (3 to 200 nautical miles). Within this boundary, all current (July 2018) BOEM Wind Energy Areas and Wind Planning Areas are shown as polygons.

2.6 Aerial Telemetry Surveys

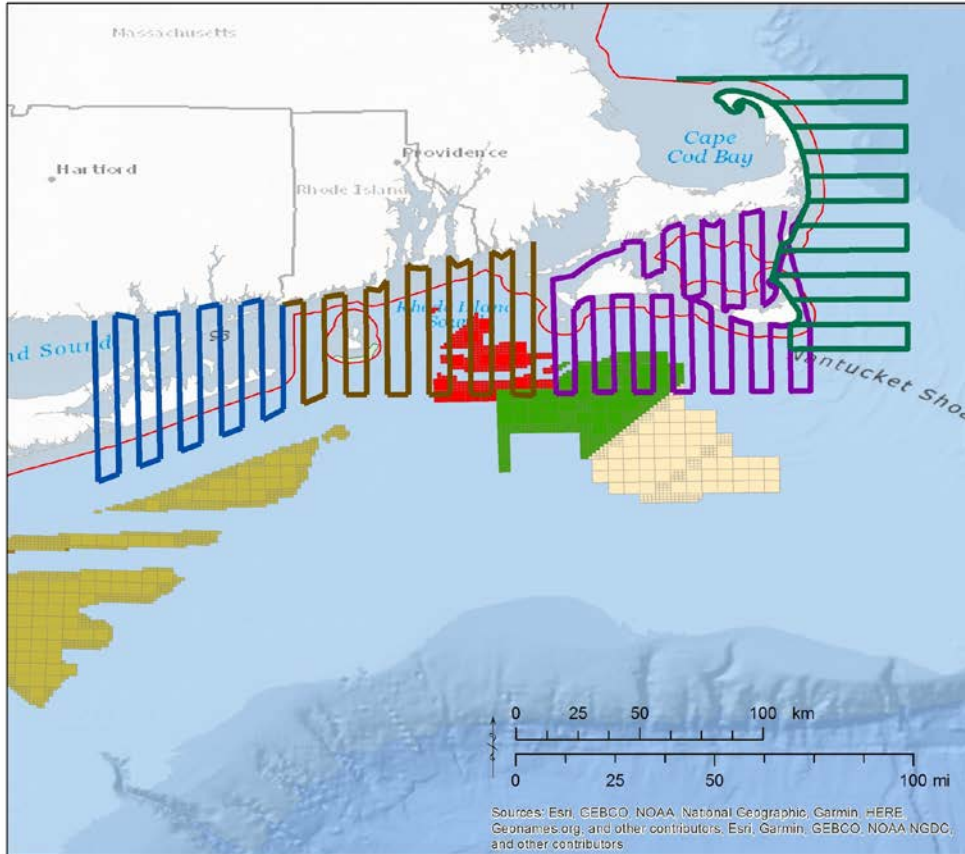
In 2014 and 2015 we conducted telemetry surveys in a USFWS amphibious Kodiak aircraft to relocate tagged Common and Roseate terns across the Study Area during the post-breeding dispersal period. We used a pair of 4-element, Yagi antennas mounted on each strut of the aircraft at an angle of approximately 45° (Fig. 6). The antennas connected to a switch-box used to toggle between antennas so that signals could be isolated on one side of the aircraft and boxed in to localize individuals. We used an SRX-600 set to data-logging mode to monitor and record all detections of individuals within range. We quantified detection range of the airplane to detect nanotags to targets on land and in flight, by strategically placing test beacons in the following configurations: 1) on the ground in open, coastal areas; 2) atop a 1.5 m fiberglass pole on a moored boat; and 3) on a kite flying over an open coastal area at an altitude of approximately 30 ft. Maximum range of the aircraft receiver to detect tags under various conditions was 3 km to tags on the ground and atop a 1.5 m fiberglass pole on a moored boat, and 6 km to tags flying on a kite at 30 ft. altitude.

Telemetry surveys were flown at a constant airspeed of 110 knots and altitude of 750 ft, covering over 3,000 km of transects from eastern Long Island Sound, NY to Cape Cod, MA (Fig. 7). Transect lines off the eastern shore of Cape Cod, MA (where no BOEM Wind Energy or Lease Areas are present, but terns are known to forage) were spaced at 6 km, and transect lines across Nantucket Sound, Rhode Island Sound, and Block Island Sound (in the vicinity of BOEM WEAs and Lease Areas) were spaced at 3 km. We completed a total of six equipment calibration flights and sixteen aerial surveys in 2014 and 2015 (Table 1).

During aerial surveys, the pilot-biologist (left front seat) and observer (right front seat) simultaneously collected survey counts of all terns observed over water within a strip width of 1,500 m (750 m on each side of the plane), using strut-marks to estimate the transect bounds. Counts of Common and Roseate terns were pooled by genus (*Sterna*) due to the difficulty of reliably separating these two species from the plane at tracking altitudes (750 ft). Counts of all other birds, marine mammals, and sea turtles were also recorded, with individuals identified to the lowest possible taxon. Behavior of birds was recorded as flying, foraging, or sitting on the water. Observation conditions were recorded on a 5-point Likert scale, where 1=worst conditions, 3=average conditions, and 5=best conditions. Surveys were discontinued if winds exceeded 20 knots or observation conditions deteriorated and persisted to 2 or lower on the Likert scale. All survey data are archived in the Northwest Atlantic Seabird Catalog (USFWS 2018).



Figure 6. USFWS amphibious Kodiak aircraft with paired directional (Yagi) antennas used for aerial telemetry surveys in 2014 and 2015.



Legend

BOEM Wind Lease Areas

RI/MA OCS-A 0486 and 0487

MA OCS-A 0500 and 501

BOEM Wind Planning Areas

Massachusetts PSN

New York Bight Call Area

New York Proposed Commercial Lease

Block Island Wind Farm

U.S. Federal Waters

3 - 200 nautical mile boundary

Aerial Survey Transects

Long Island Sound

Rhode Island Sound

Nantucket Sound

Cape Cod and Nantucket

Figure 7. Transect routes flown during aerial telemetry surveys in 2014 and 2015.

Table 1. Dates, start and end times (EST), transects, and weather conditions (wind speed reported in knots) of aerial surveys conducted during 2014 and 2015.

Date	Departure Time	Return Time	Transects	Weather
8/1/2014	17:45	18:15	Calibration	Cloudy, light wind (<5)
8/2/2014	12:00	13:15	Calibration	Light wind (<5), cloudy, light rain
8/4/2014	12:45	17:30	Nantucket Sound	Partly cloudy, light wind (<5)
8/5/2014	10:10	14:27	Cape Cod and Nantucket	Partly cloudy, fog, light wind (<5)
8/11/2014	15:10	15:50	Calibration	Partly cloudy, SW wind 5-10
8/12/2014	11:20	14:50	Cape Cod and Nantucket	Partly cloudy, S wind 5-15
8/18/2014	10:50	15:22	Rhode Island Sound	Sunny, NW wind (5-10)
8/19/2014	10:20	14:30	Long Island Sound	Sunny, light wind (<5)
8/25/2014	11:13	14:50	Cape Cod and Nantucket	Sunny, NE wind (5-10)
8/27/2014	12:05	17:00	Calibration	Sunny, SW wind 10-15 gusts 20
8/28/2014	11:00	16:16	Nantucket Sound	Sunny, N wind 10-15 gusts 22
8/30/2014	11:20	16:45	Cape Cod and Nantucket	Sunny, E wind 5-10
7/13/2015	17:15	18:55	Calibration	Partly cloudy, SW wind 10-15
8/2/2015	10:53	14:15	Cape Cod and Nantucket	Sunny, SW wind 5-10
8/3/2015	9:15	15:00	Nantucket Sound	Partly cloudy, SW wind 15-17
8/8/2015	11:40	16:30	Long Island Sound	Partly cloudy, N wind 10
8/9/2015	9:30	11:30	Rhode Island Sound	Partly cloudy, NE wind 10-13, fog
8/16/2015	10:50	14:26	Cape Cod and Nantucket	Partly cloudy, SW wind 5-10
8/17/2015	9:50	11:30	Rhode Island Sound	Sunny, light wind (<5)
8/18/2015	9:47	12:42	Rhode Island Sound	Sunny, SW wind 10-15
8/26/2015	10:30	12:30	Cape Cod and Nantucket	Sunny, SW wind 10
8/27/2015	10:45	14:55	Calibration	Sunny, light wind (<5)

2.7 Frequency Coordination

We conducted this study in collaboration with the Motus Wildlife Tracking System (www.motus.org). All transmitters were programmed to transmit on the Motus Network frequency of 166.380 MHz and were uniquely identifiable by a unique combination of the digital ID code and burst rate interval. In 2016, the Motus Network comprised over 300 automated radio telemetry stations from Arctic Canada to northern South America and over 4,000 nano-tagged individuals representing a variety of taxa of birds and bats (Taylor et al. 2017).

Below, we define key terms used to describe different types of data in the Motus Network database:

- 1) Principal Investigator (PI) stations: automated radio telemetry stations operated by the Principal Investigator of tracking study. Within this report, we refer to automated radio telemetry stations that were funded by BOEM as “BOEM stations”.
- 2) Global stations: automated radio telemetry stations operated by cooperators in the Motus network.
- 3) Target transmitters: transmitters deployed by the PI of the tagging study.
- 4) Non-target transmitters: transmitters deployed by cooperators in the Motus network.

By participating in the Motus Network, we obtained detailed detection data (including: bird ID, location, time, date, receiving antenna, signal strength value) for target transmitters deployed on Common Terns, Roseate Terns, and Piping Plovers in this study that were detected by global stations operated by partners within the Motus Network. In addition, the BOEM stations were programmed to detect all active non-target transmitters deployed by partners in the Motus network. Access to and use of detection data from non-target transmitters recorded on BOEM stations are pursuant to the Motus Collaboration Policy (Motus Wildlife Tracking System 2016). The Collaboration Policy states that PIs control access and use of detailed detection data from their target transmitters on both their PI stations as well as all global stations. However, basic metadata from tags and receiving stations from all projects (location, deployment dates and species), as well as daily summaries of tag detections at each receiving station are publicly available. The basic open-access dataset from non-target data collected by BOEM stations is available on the Motus website (www.motus.org) and provided in tabular format as supplementary material to this report (Appendix F).

2.8 Post-processing of Telemetry Data

To post-process detection data collected by the BOEM automated radio telemetry stations, we used a filtering algorithm in the Sensorgnome Package (Brzustowski 2015) within program R (v.3.0.2) to remove false detections from the raw VHF telemetry data. The algorithm was based on the following default parameters applied to each unique transmitter: minimum of three consecutive bursts required to comprise a 'run' (run length), a maximum of 20 consecutive missed bursts allowed within each run, and a maximum deviation of four milliseconds from a tag's unique burst interval between its consecutive bursts (Brzustowski 2015). These parameters were selected according to conservative recommendations from Motus network developers (Taylor et al. 2017).

Data from global automated radio telemetry stations operated by cooperators in the Motus network were processed and disseminated by Bird Studies Canada. We visually inspected the processed global data and identified remaining spurious detection data by quantifying speed and distance of movements between automated radio telemetry stations. We found that some of the global towers showed higher rates of false positive detections than others, which led to our taking a conservative approach in minimizing false detection rate. The source of the false positives was unclear but was likely from nearby transmitting VHF or cellular antennas (Taylor et al. 2017) and was more prevalent at sites located in developed areas such as marinas. Due to the high rate of false-positive detections from certain global sites with a high level of interference, we applied a more stringent filter (relative to default) to these data that required a minimum of seven consecutive bursts required to comprise a 'run'. The electromagnetic noise is assumed to be white noise which is uncorrelated in the time domain, so selecting a minimum number of seven consecutive bursts ensured that received signals were from the transmitter and not environmental noise.

2.9 Movement Models

The first main objective of our study was to develop spatially-explicit, 3-dimensional models to estimate movements of Common Terns, Roseate Terns and Piping Plovers in the Atlantic OCS during the breeding period, post-breeding dispersal, and fall migration. Our specific aim was to develop movement models that simultaneously: 1) account for observation error; 2) estimate likely paths taken in continuous time (rates, direction); and, 3) estimate behavioral states (on land, direct flight).

2.9.1 Background and Motivation of Approach

Networks of automated radio telemetry arrays provide a unique opportunity to estimate detailed 3-dimensional trajectories for tagged individuals across broad geographic ranges and flight altitudes. However, the theory behind such estimation and its application across broad scales remains in development. The principal challenges are to infer detailed flight trajectories from spatiotemporally scattered detection events, and to distinguish between detections either along receiving antenna beams (i.e. within $\sim 35^\circ$ of main antenna axes for 11.1 dBd Yagi antennas) or along 'off-beam' detections. Additionally, triangulation is only applicable within short time frames, given near-simultaneous detection between separate but proximate arrays. Most studies of avian movement using fixed VHF tower arrays have therefore involved selecting sequences of detections and analyzing these on a case by case basis, under the assumption that detections occur along a main-beam (Taylor et al. 2017). Bird trajectories are then inferred in two ways: by location or by signal strength. Some studies calculate a weighted average among locations of towers for sequences of detections (Woodworth et al. 2015; Duijns et al. 2017), sometimes augmented by manual identification of characteristic signal strength patterns from movement along or across main beams (Brown et al. 2016). Other studies infer flight bearings via the ratio of signal strength between receiving antennas during selected near-simultaneous detection events (Smolinski et al. 2013). In contrast, our approach integrates tower location with signal strength, while accounting for other transmitter properties (e.g., beam orientation, altitude), for a three-dimensional perspective.

Given the continental-wide span of the Motus system and complicated nature of signal propagation over heterogeneous terrain, this poses a challenging problem from the location model perspective. In this study, we advanced the development of approaches used to estimate transmitter location and altitude

explicitly, based on a two-beam radio propagation model (Janaswamy 2001; Janaswamy et al. 2018). This approach allows for completely automated location estimation across many individuals, and accounts explicitly for variation relative to the beam orientation and flight altitudes (Janaswamy 2001; Janaswamy et al. 2018). Compared with using a traditional direct-transmission propagation model (Friis 1946), this new formulation accounts for variability in the relationship between predicted signal strength and flight altitude, which differs for signals received along the main beam, side or back lobes (Fig. 8). For a single given signal received in the absence of near-simultaneous detections, the inherent uncertainty in a bird's location can theoretically reach up to 80 km horizontally and several kilometers vertically (i.e., in altitude; McLaren et al. *in prep.*).

Given the inherently nonlinear inverse relationship between signal strength and location, we integrated estimates of both location and flight altitude, which required a set of constraints to choose between possible solutions (Janaswamy 2001; Janaswamy et al. 2018). Preliminary results were based on a simplified beam equation, which allowed for exact matching between nearly simultaneously detected signals. This tended to predict locations that zig-zagged between main beams of detecting receivers, and occasionally predicted large jumps in minimum altitudes, due to gaps in occurrences of near-simultaneous detections. This implied that additional constraints were needed to account for ambiguity and unreliability in signal strength. For example, variation in signal strength can be strongly influenced by factors such as meteorological conditions and reflectance effects, as well as any limitations of the two-beam propagation model.

In the present study, we accounted more fully for the vertical structure in the Janaswamy et al. (2018) method, applied constraints based on known flight characteristics of focal species, and created a framework that accounted for measurement and model uncertainty by assessing the variation in received versus predicted signal strength among detecting antennas. In this way, we estimated the most likely flight path in three dimensions, as well as the uncertainty in this estimate, based on both predicted signal strengths among receiving arrays and known flight characteristics. Also, and importantly, since the model could compare received signal strength between distinct antennas from a single receiving station, this increased the potential to resolve locations in comparison to traditional triangulation methods, which cannot resolve trajectories without near-simultaneous detections from spatially separated receiving stations.

Our model workflow proceeds in six steps, outlined in detail below and in Table 2. In the first two model steps, we derived the most consistent estimated locations among plausible detections, based on their signal strength (Sections 2.9.2-2.9.4) and based on behavioral constraints (Sections 2.9.5-2.9.6). Specifically, the target's location was determined to be the weighted mean among sequential locations, weighted by the inverse-square discrepancy in signal strength among all near-simultaneous detections, and resulting in the lowest discrepancy between measured and predicted signal strength. The constraints involved differentiating between local movements (at nesting or stopover areas) and non-stop flight (regional or migratory) movements according to (1) limits to a bird's possible flight speeds in the horizontal and vertical and (2) the assumption that during directed flight, a bird limits variation in its horizontal and vertical speed (Section 2.9.6). Because these detections occurred at irregular intervals, the third step interpolated the estimated locations to one-minute time steps, using a Brownian Bridge movement model (Horne et al. 2007). Choosing a time window represents a trade-off between the advantage of adding more information (detections) to co-locate position, and the disadvantage of the

bird's actual position changing within the time window. Maximal flight speeds were chosen to be 10 m s^{-1} for the terns (Wakeling and Hodgson 1992) and 12 m s^{-1} for the Piping Plover (Hedenström et al 2013; Stantial and Cohen 2015). The 1-minute time step was selected to estimate location estimates at approximately a 1-km scale (given maximal flight speeds), which we felt was an appropriate resolution for assessing macro-scale exposure to WEAs throughout the Study Area.

In the fourth model step, meteorological data (approximately 32-km spatial resolution and 3-hour temporal resolution) were spatiotemporally-interpolated to each one-minute record, and orientation and airspeed were derived from flight speed and wind data (Kemp et al. 2012). Meteorological data were downloaded from the National Centers for Environmental Prediction North American Regional Reanalysis (NARR; National Oceanic and Atmospheric Administration 2017). In the fifth model step, occurrence in WEAs and in Federal waters was quantified using the output from the Brownian Bridge model, as well as the standard deviation of location estimates in the horizontal plane, as described in Section 2.10. Finally, in the sixth model step, we extracted the magnitude of all meteorological and flight speed related covariates to assess incidence in Federal waters and WEAs, including flight direction and heading, wind support, and crosswinds (Section 2.11).

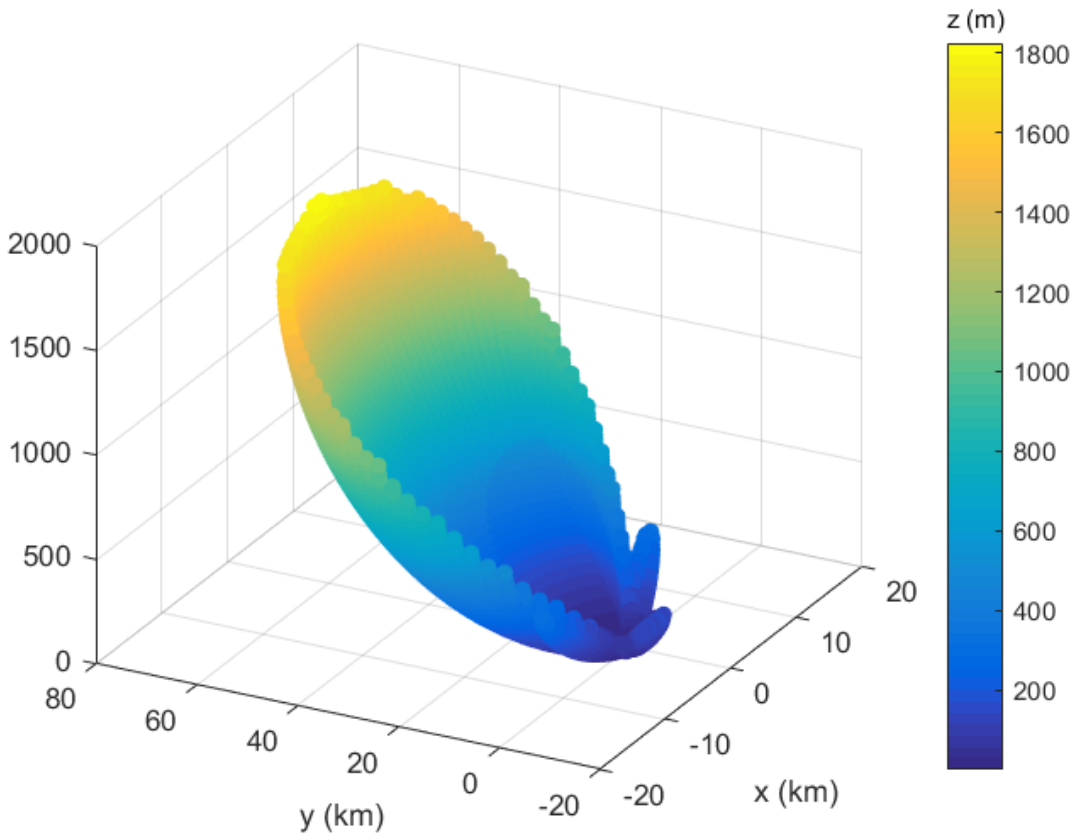


Figure 8. Radiation pattern of Yagi antenna beam

Possible locations, measured in distance from an automated radio telemetry tower with a Lotek SRX-600 receiver (set to standard gain of 80) to a source (i.e., target bird), depicted for a typical received signal (30 on a scale of 0-255), according to the two-ray propagation model. The main beam is oriented along the y-axis at x=0, with the tower mast located x=0 and y=0, crossbeam distance x (km), along-beam distance y (km) and vertical receiver height (z) in m.

Table 2. Model workflow: steps 1-3 govern localization estimation, step 4 interpolates covariate data, and step 5 estimates exposure to Federal waters and WEAs

Step	Action	Section	Method
1a	Determine periods of non-stop flight	2.9.5	Based on thresholds for inter-tower distance (default minimum, 20 km) and species-appropriate inferred flight speed
1b	Determine locations with near-simultaneous detection (default time window <1 minute)	2.9.3	Consistency of signal strength for each location and detecting beam (see Fig. 8) within appropriate flight altitude bounds, given species and flight mode
1c	Re-determine periods of non-stop flight based on output 1b	2.9.5	(see above and Sections 2.9.5 and 2.9.6)
2a	Determine locations from other ('single') detections	2.9.4	Height range interpolated from step 1b, (maximal vertical speed 2 m/s for piping plovers and 0.5 m/s for terns locations based on main beam and tower locations
2b	Refine periods of non-stop flight based on output 2a	2.9.5	(see above and Sections 2.9.5 and 2.9.6)
2c	Refine non-stop flight locations from step 2b in accordance with behavioral constraints	2.9.5	Constrained by species-appropriate flight speed (see Sections 2.9.5 and 2.9.6) and minimized discrepancy in both the location estimates and in the bird's acceleration (default: minimizing 50% sum of square location discrepancy and acceleration)
3a	Interpolate to one-minute time step	2.9.7	Brownian Bridge model based on standard deviation in horizontal position
3b	Incorporate aerial survey detections (terns only)	2.9.7	Add aerial survey location estimates, assuming standard measurement errors of 10 km in the horizontal and 10 m in the vertical.
4	Add dynamic weather covariates	2.11	Spatiotemporally interpolated NARR data
5a	Determine incidence in Federal waters	2.10	Mean estimate location within FW and standard errors from Step 2b < 30 km in x and y
5b	Determine incidence in WEAs	2.10	Mean estimate location within WEAs and standard errors from Step 2b < 30 km in x and y. Given the more directed movements of migratory shorebirds vs. terns, incidence in WEAs among Piping Plovers was refined by considering only non-stop movements

2.9.2 Formulation

For directional receivers like the Yagi element arrays deployed in this study, received signal strength (in dBm, normalized to a transmitter- and receiver-specific gain factor) varies with the two-dimensional and three-dimensional ranges (i.e. distance to receiver; r and R , respectively), radial angle ψ between receiver and transmitter, and the heights z of the (bird) transmitter and H of the receiving tower. To account for altitude effects as well as ground-reflected signals (multipath), Janaswamy et al. (2018) incorporated the two-beam model and applied this to the known radiation pattern of Yagi receivers. In this multipath formulation, the received signal is predicted to vary sinusoidally with flight altitude z , at least as long as the horizontal range r exceeds the vertical height z :

Equation 1

$$\xi^2 = g^2(\psi) \sin^2(k_0 H \cdot z/R) / (k_0 R)^2$$

Here $g(\psi)$ governs the shape of the directional beam and k_0 (m^{-1}) represents the wavenumber in free-space (Janaswamy 2001). The sinusoidal dependence of flight altitude z on signal strength in Equation 1, and Fig. 8, together illustrate how significant signal gain with height is possible, resulting in possible long-range (>50 km) detection of high-flying birds, and adding to the complexity of distinguishing flight altitudes based on signal strength.

For horizontal ranges much larger than the vertical range ($z \ll r$), Equation 1 can be simplified and inverted to determine the transmitter (bird) height (z) above the ground as a function of horizontal range, r :

Equation 2

$$z = \frac{r}{k_0 H} \sin^{-1}(k_0 r \cdot \xi / g(\psi))$$

This formulation (McLaren et al. *in prep.*) allows for efficient calculation and assessment of plausible locations in three dimensions while retaining the vertical structure of Equation (1).

2.9.3 Near-simultaneous Detections

In the first model step, we derived estimated target (i.e., bird) locations, and uncertainty in these locations, for all detections from separate towers or antennas within a time window of 60 seconds (hereafter, near-simultaneous detections). Near-simultaneous detections help reduce the inherent ambiguity in signal strength (Fig. 8). A one-minute time window ensures that exposure to the WEAs is adequately assessed without compromising the accuracy of estimated locations (since the terns and Piping Plovers are predicted to cover less than 1-km per minute), whereas shorter time windows reduce the number of near-simultaneous detections and thereby the accuracy of location estimates.

To account for measurement and model errors, we used Equation 2 to evaluate the degree of correspondence among all received signals within the time window, considering all plausible horizontal

ranges r and axial angles ψ : for each detection within the 1-minute time window, we searched through 2,880 candidate horizontal locations (radial distances between 100 m and 50 km, and every 0.5° radially) to determine the consistency of each location given the other detections. For each detected signal and candidate horizontal location (and corresponding vertical location, via Equation 2), the mean discrepancy in signal strength from all other detections was calculated (based on what their signal strength would be at this location using Equation 1). Estimated locations that fell outside of the possible bounds on vertical location were excluded. Among the remaining locations (typically 500-100 for each detection), we then chose the median location among those having the lowest 10% discrepancy in signal strength, and the mean of these best location estimates among all detections as the best ('mean') estimated location within the time window. Selecting the most representative value in the 10% most probable set of points was found to improve both the kite validation (Section 2.9.8) and the smoothness of non-stop flight trajectories, especially once these were constrained to conform to non-stop flight (see 2.9.5-2.9.6). To assess exposure to Federal waters and WEAs, uncertainty around this 'mean' location was quantified by the standard deviation in horizontal coordinates and the upper and lower quartile in vertical height. For updating locations to conform to dynamic flight constraints (Section 2.9.5), 5-95% confidence intervals in both the horizontal and vertical were also retained.

2.9.4 Single Detections

We refer to single detections by separate towers or antennas as those that occurred greater than 60 seconds apart. In these cases (i.e., in the absence of near-simultaneous detections), localization was estimated following one of two procedures: (1) numerical estimation of straight-line trajectories from a sequence of single-antenna detections (i.e. a computational version of that employed by e.g. Brown et al. 2017), or (2) estimation of the most likely location of a single detection based on received signal strength and interpolated near-simultaneous location estimates. Specifically, (1) when three or more consecutive detections from (only) a single antenna 'beam' occurred within a span of 30 minutes, a straight-line trajectory was fit among candidate locations to minimize the discrepancy in single strength (log-transformed ξ squared) within the species-specific bounds for horizontal speed (see sections 2.9.5 and 2.9.6), using MATLAB routine `fmincon`. An initial trajectory was used in the optimization procedure according to a linearized version of Equation 2 (or, equivalently, assuming, $z \ll r$). Additionally, among these 'sequential' single-beam detections, a constant vertical (climb) speed was also fit whenever initiation of non-stop flight was inferred (see Section 2.9.5) or if such a sequence occurred as final detections (the final 10 minutes for terns and 15 minutes for Piping Plovers, reflecting the latter's stronger tendency for directed flight during migration). Finally, horizontal uncertainty was quantified in these cases by an interpolation of the horizontal uncertainty between the closest simultaneous detections, or of the closest simultaneous detection if only one occurred. Alternatively, (2) when fewer than 3 consecutive single detections occurred within 30 minutes, birds were presumed to be located along the main-beam (within 30 degrees of the main axis) and on the same side of the beam as the horizontally interpolated location from previous or following near-simultaneous detection. As with near-simultaneous location estimation, 2880 candidate horizontal locations were tested for consistency with measured signal strength, being within the visible horizon and vertical bounds, and proximity to the interpolated location between any previous or subsequent location estimates derived from near-simultaneous detections.

2.9.5 Determination of Non-stop Flight

Refining the movement trajectories of birds through time and space required differentiation between stopover behavior and non-stop flight (Kranstauber et al. 2012; Jonsen 2016). The reasons for this are two-fold: (1) initial estimates for current locations can only be interpolated from previous or subsequent location estimates if they involve non-stop flight, and (2) given the potentially large range in flight altitudes and associated horizontal locations for any given signal strength (Fig. 8), using biologically reasonable bounds in altitude greatly improved model performance (see Poessel et al. 2018 for an analogue using GPS measurements). During non-stop flight, modeled flight altitudes were bounded by a minimum of 10 m and maximum 50 m for terns (Everaert and Stienen 2008) and between 10 m and 1000 m for Piping Plovers (Williams and Williams 1990). During flight in other ('staging') periods, a minimum of 1 m and maximum of 50 m was assumed for terns and between 1 m and 30 m for Piping Plovers, which tend to fly at lower altitudes outside of migration (Dirksen et al. 2000; Stantial and Cohen 2015). Non-stop flight periods were determined iteratively in the model, beginning by deriving proxy flight speeds based on inter-tower distances and the timing of subsequent detections. To reduce the risk of misidentifying simultaneous detections during stopover as non-stop flight, initial classification of non-stop flight during the first model step was restricted to detection events involving receivers separated by at least 20 km. Also, because initial ground speed estimates will be influenced by proximity to detecting receivers, wind effects and measurement imprecision, the range of (estimated) flight speeds during non-stop events was broadened for each species (4-20 m/s for terns and 4-30 m/s for Piping Plovers). Non-stop flight periods were subsequently updated and refined using the improved location estimates derived for multiple detections (step one) and single detections (step two). To prevent misclassification of brief stopovers between two non-stop flight bouts, any interim period implying less than 2 m/s for longer than two hours was considered as a stopover as opposed to non-stop flight.

2.9.6 Behavioral Flight Constraints

Location estimates during non-stop flight sequences were further refined, based on known characteristics of flight for each species, to ensure that flight trajectories were feasible, smooth and behaviorally consistent. Specifically, following initial location estimation of both near-simultaneous and single detections, location estimates were adjusted, within the 5% and 95% bounds of the candidate locations, to ensure that (i) vertical speeds, i.e. as implied by estimated changes in flight altitude between detections, were less than 2 m/s in magnitude for Piping Plovers (Hedenström and Alerstam 1994) and 0.25 m/s for terns, (ii) horizontal speeds remained within 5-20 m/s for terns and 3-30 m/s for Piping Plovers, the relatively broader ranges accounting for straightness of flight paths, wind conditions and proximity to towers and (iii) the total horizontal and vertical acceleration were minimized given constraints (i) and (ii). The uncertainty in each dimension was retained according to the standard deviations in the x and y components, and both the interquartile range and the 5 to 95% quantiles in the vertical dimension among all candidate vertical locations.

2.9.7 Temporal Interpolation Using Brownian Bridge Movement Model

To estimate occurrence across Federal waters and WEAs, we spatiotemporally interpolated the irregular location estimates and the aerial survey detections into one-minute time steps using a Brownian Bridge model (Horne et al. 2007). Modelled spatial locations were interpolated in three dimensions between all

near-simultaneous and single detections. Uncertainty of one-minute horizontal location estimates was quantified as the root-mean square of estimated variance in location from detections and due to time gaps between detections (via a horizontal flight speed of 10 m/s for terns and 12 m/s for Piping Plovers; see Horne et al. 2007). Vertical uncertainty in one-minute time steps was linearly interpolated between all near-simultaneous and single location estimates. Aerial survey data were presumed to have a horizontal spatial uncertainty of 1 km (based on data from calibration surveys) and vertical uncertainty of 10 m (based on typical flight altitude ranges of Common and Roseate terns during breeding and post-breeding periods).

2.9.8 Calibration and Validation

Since Equation 1 is dependent on the transmitter and receiver properties, signal strength of the SRX-600 receiver (on a scale of 0-255) needed to be calibrated using data from a known location:

Equation 3

$$\tanh^{-1}\left(\frac{Z}{255-Z}\right) = b \cdot \ln\left(\frac{\xi^2}{p_0} + 1\right),$$

where Z represents the SRX-600 receiver signal (0-255), b represents a rate of signal saturation and p_0 is a noise threshold (see Bai 2016 and Janaswamy et al. 2018).

To estimate these two coefficients, two 1.0 g nanotags were attached to a kite that was flown from the back of a motorboat. The motorboat was driven in transects within range of two land-based 12.2 m automated radio telemetry stations, each supporting six, 9-element Yagi antennas mounted in a radial configuration with main beams separated by 60°.

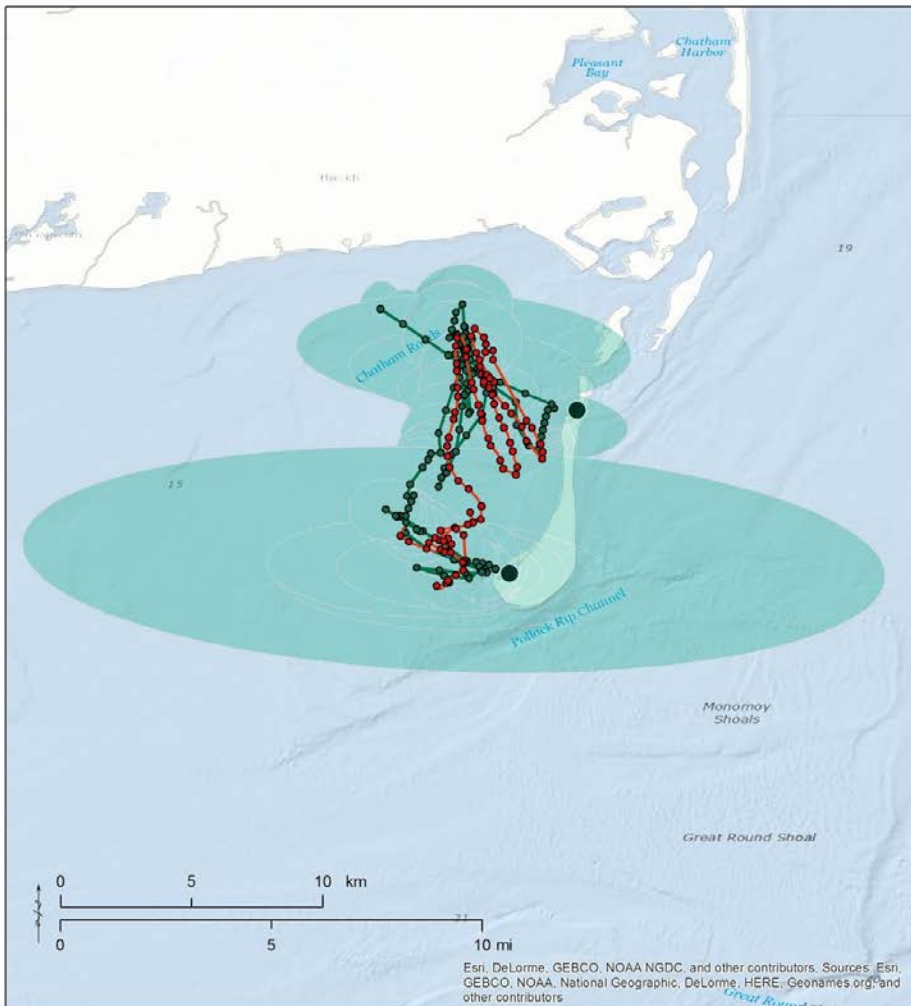
The first (calibration) dataset comprised detections from flying the kite along the main beam of two automated radio telemetry stations, located 6.7 km apart on Monomoy NWR in Massachusetts. We flew the kite at two heights, 30 and 60 m above sea level (asl), to optimize our calibration estimates within rotor height, within limitations of Federal Avian Administration regulations. We aligned the transmitting antennas of two nanotags horizontally and vertically (i.e. parallel and perpendicular to the water surface, respectively). This resulted in horizontal ranges from two detecting towers up to 10 km (maximum distance of transect length), and, between the six antennas on each, all possible bearings between the transmitter and receiver. All detections were pooled and the data calibrated by fitting the coefficients p_0 and b in Equation 3 using non-least squares based on GPS location of the boat, the measured signal strength Z, and predicted signal strength (Equation 2).

Then, to validate the location model and coefficients, we used a second set of surveys for our calibration dataset, which involved a VHF-tagged kite flown at altitudes ranging from 10 to 30 m asl in a zig-zag pattern between the two receiving arrays. This erratic pattern was designed to provide a challenge for the location model, resulting in no near-simultaneous detections between towers (i.e. only between antennas from the same receiving tower, so that this data set would not be analyzable using traditional triangulation methods). To facilitate the kite's erratic movement, we used a shorter time window for fitting single-antenna sequences (5 minutes) and constrained modeled flight to altitudes within 10 to 40 m.

The mean pairwise distance between each tag location (Fig. 9, red points) and corresponding model estimate location (Fig. 9, green points) was 1,351 m (SD 690 m, range 134 to 3,600 m). The mean pairwise difference in the East-West (x) coordinates was 777 m (SD 638 m, range 20 to 3,313 m) and the mean pairwise difference in the North-South (y) coordinates was 909 m (SD 688 m, range 1 to 3,246 m).

The model-estimated standard error in location (shown as green polygon in Fig. 9) was considerably higher than the true error, with a mean in East-West (x) coordinates of 1,316 m (SD 1,433 m, range 585 to 12,377 m) and in North-South (y) coordinates of 1,260 m (SD 392 m, range 761 to 4,270 m).

During the calibration survey, the altitude of the kite/transmitter was not accurately recorded because it varied with the wind, ranging between 10 and 30 m. The mean model estimated kite altitude was 20 m (SD 0.6 m, interquartile range 10 to 40 m; Fig. 10).



Legend

- Automated Radio Telemetry Station
- Calibration data**
- Actual track of test tag
- Actual locations of test tag
- Movement model**
- Estimated track of test tag
- Estimated locations of test tag
- Standard dev. of location estimates

Figure 9. Results of model calibration survey conducted during September 2014 adjacent to two automated radio telemetry towers on Monomoy NWR, MA, USA

Red line shows GPS track of boat towing a kite with a VHF transmitter attached to it flying at approximately 10 to 30 m above sea level (ASL). Red points show GPS locations collected every minute. The green track shows corresponding locations and track estimated by the movement model. Green ellipses show model-estimated error (SD) corresponding to each location estimate.

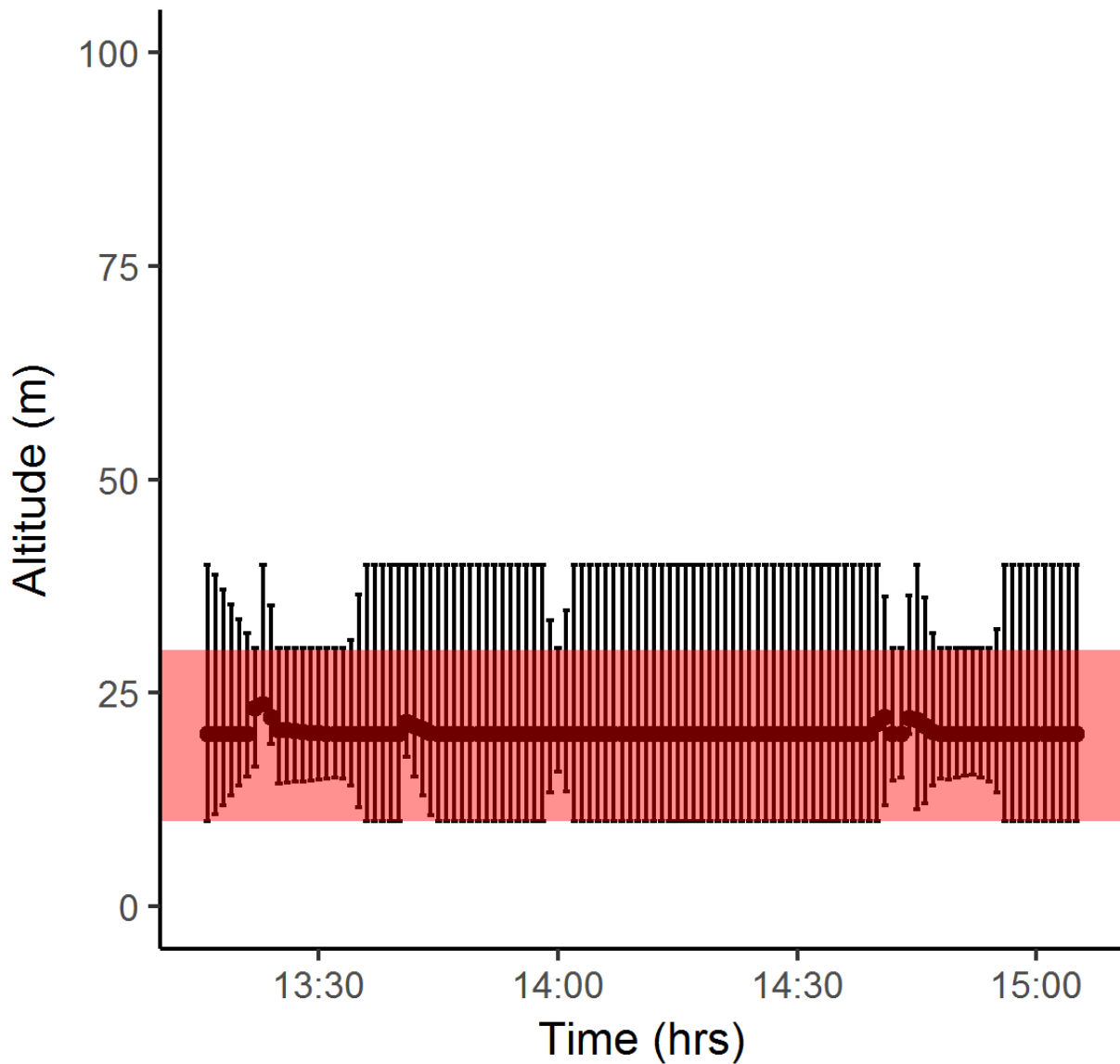


Figure 10. Model estimated mean and standard deviation of altitude (m, ASL) over time (min) of VHF-tagged kite during September 2014 calibration survey

The black error bars represent the predicted interquartile range of plausible altitudes, which depended on the consistency of received signal strength among all detections (modeled altitude was constrained from 10 to 40 m). The dark line represents the most plausible vertical trajectory as solved by the dynamic smoothing. During the survey, actual height of the VHF-tagged kite fluctuated between 10 and 30 m (red shading).

2.9.9 Including Sensorgnome Receiving Stations

Most of the towers in the Study Area were BOEM stations equipped with SRX-600 receivers and gain set to 80. Additional global stations operated by partners in the Motus Network in the region (e.g. New Jersey, North Carolina) used Sensorgnome receivers (Taylor et al. 2017). Sensorgnome measurements are converted from received power to and reported in raw dBm units, which will vary with gain and other settings. To standardize Sensorgnome and SRX-600 signal strength data in order to make use of data collected from target birds at global stations, a gain of 80 was assumed and dBm units transformed to SRX-600 receiver Z units using a simple linear relationship (J. Brzustowski, personal communication):

Equation 4

$$Z = (40G_0 + 44 \cdot dBm + 4565)/11$$

2.9.10 Detection Probability

To assess the efficacy of the BOEM telemetry stations in detecting movements of radio-tagged birds, we analyzed the relative probability of detection by single towers (with multiple-antenna) as a function of range (using Equation 1), and the overall detection probability based on the kite detections. These together allowed us to estimate the overall detection rate from the calibration surveys, given the current configuration of BOEM telemetry stations within the Study Area. The results for these analyses are presented in Appendix G.

2.10 Assessment of Occurrence in Federal Waters and WEAs

Primary objectives of this study were to estimate the occurrence of Common Terns, Roseate Terns, and Piping Plovers in Federal waters, within each BOEM Lease Area, and BOEM Planning Area from Massachusetts to Virginia.

For the BOEM Atlantic Region, we obtained GIS shapefiles of the Submerged Lands Act boundary line, delineating the boundary between state waters (landward) and Federal waters (seaward), and Atlantic OCS WEAs (v. 25 Jul 2018, BOEM 2018). We clipped these shapefiles to the boundaries of the Study Area (Cape Cod, MA to Back Bay, VA), retaining a total of twelve Renewable Energy Lease Areas (by Lease Number) and three Wind Planning Areas (by CAT1 label) in the Study Area bounds (Fig. 5). We also include the boundary of the Renewable Energy Zone in state waters of Rhode Island to evaluate exposure to the Block Island Wind Farm, which is currently the only operating wind energy facility in the US (Northeast Regional Ocean Council 2017).

We assessed occurrence in Federal waters and WEAs within the Study Area using the mean and standard deviations in locations estimates (X and Y, in UTM coordinates) interpolated to a one-minute time step. Interpolations generated from tracking tower detections on long distance offshore flights were sometimes widely separated in time and space, and as a result subjected to artificially low flight speed estimates and large locational error. To address uncertainty in model output, we considered locations as occurring within Federal waters or WEAs when the mean estimated coordinates intersected Federal water polygon and/or WEA, and when the location's X-Y error distribution was less than 30-km. We selected a 30-km

threshold to match the spatial resolution of our meteorological data (described in Section 2.11, below) and to correspond the spatial scale of individual WEAs (ranging from 106 km² to >750 km², BOEM 2018).

We used ArcGIS (v. 10.4.1) to display movement model output by species. To map flight paths of Piping Plovers, we subset all 1-minute locations identified as 'non-stop flight' and applied a smoothing filter (speed-distance-angle) using the R package 'trip' (Sumner 2016), set to the following parameters: max speed = 80 km/hr, maximum step length = 100 m, minimum turning angle = 155 degrees.

To visualize movement patterns of Common and Roseate terns, we used the R package 'sp' (Bivand et al. 2013) to create spatial lines using the 10-minute locations estimates of each individual tern from tag deployment through final detection. We then used the R package 'spatstat' (Baddeley et al. 2015) to create a raster surface representing number of tracks of all terns intersecting each pixel (resolution 1 km²) within the spatial extent of the input tracks. These maps represent the density of 10-min line segments per 1 km² pixel. We created separate line density maps to display variation across species and nesting colonies from tag attachment (during late incubation to early chick rearing period) through emigration from the Study Area, pooled across years.

For each species, we created a probability density map accounting for all WEA exposure events (with standard deviation in estimated horizontal locations < 30 km). We did this by (i) for each time step during an event, based on the mean and standard deviations in estimated location, calculating spatial contours for 10-90% occurrence probability, (ii) spatially interpolating these within time-step contours to probabilities within 500 x 500 m grid cells, (iii) calculating the cumulative exposure probability for each grid cell across time steps, and (iv) estimating total exposure density by summing these probabilities among all events per species.

2.11 Meteorological Conditions

To examine movements relative to meteorological covariates, we obtained satellite-derived North American Regional Reanalysis environmental data for the Study Area (Atlantic coast and OCS from Cape Cod, Massachusetts to Back Bay, VA) in 3-hr time steps and approximately 32-km² spatial resolution (National Oceanic and Atmospheric Administration 2017). The specific meteorological covariates that we included were: wind at a pressure level of 1000 mb (about 100 m above sea level), quantified as wind speed (m/s), Zonal (Eastward) and Meridional (northward) wind components (m/s), and wind direction (the direction wind blows toward, measured clockwise from geographic north); and additionally four other meteorological covariates at surface level values: barometric pressure (Pascal [Pa]), precipitation accumulation (kg/m²), air temperature (Celsius [C]) and visibility (m).

These data were interpolated from their native Lambert conic grid to each location along the predicted trajectory (stored in the model in NAD83 UTM 18N coordinates), using a cubic spline based on the nearest 8 spatial locations, and linearly interpolated in time (MATLAB routines `lambert1` and `latln2val`, respectively) for each individual at each 1-minute location estimate. We also estimated wind support (i.e., tailwind) and crosswind components for each individual at each 1-minute time step, based on equations described in Kemp et al. (2012). These quantities inherently depend on a bird's heading, i.e. how it orients its horizontal body axis relative to the ground, and how they might compensate for any wind drift, i.e.

adjust their heading to incident wind to maintain a preferred or intended direction (see Kemp et al. 2012 and McLaren et al. 2012). For simplicity, and because many of the 1-minute interpolations reflected time spent on the ground, we used measures for wind support and crosswind reflecting full compensation for any wind drift relative to track directions.

Geospatially referenced detection data and corresponding covariates for all birds tagged in this study were submitted to BOEM as a supplement to this report (Appendix H).

2.12 Covariate Analysis of Exposure to Federal Waters and WEAs

For analysis of timing, meteorological conditions, and altitude of flights across Federal Waters and WEAs, we used model location estimates (1-minute time step) for each location that intersected Federal Waters or WEAs and met the criteria for exposure described in Section 2.10.

We used the program R (version 3.4.1, R Core Development Team 2017) and associated packages to summarize and format location data for covariate analyses. For the analysis of exposure to Federal waters, we used the packages 'plyr' (Wickham 2011) and 'lubridate' (Grolemund and Wickham 2011) to calculate the mean of each covariate to the nearest 3-hr bin (i.e. 0:00 hrs, 03:00 hrs, 06:00 hrs, 09:00 hrs, 12:00 hrs, 15:00 hrs, 18:00 hrs, 21:00 hrs) in local Eastern Standard Time (EST). For circular variables (time of day in hours EST and wind direction in degrees relative to true north), we calculated the mean based on the circular distribution (R package 'Circular', Agostinelli and Lund 2017). We then performed an integrated analysis of all covariates (temporal, demographic, and meteorological) to predict movements into Federal waters by species using a regression-based method, boosted GAMs (R package 'mboost' using function 'gamboost'; see also Buhlmann and Hothorn 2007). The boosted approach allows estimation of both the relative 'influence' of covariates to exposure to Federal waters (i.e., the percentage reduction in deviance attributable to each predictor), and of the 'relative' response to these covariates (Hastie et al. 2009).

To fit responses to exposure to Federal waters as influencing discrete events, we used a Binomial logistic regression formulation as the basis of the boosted GAM. In this formulation, probability of exposure is incorporated as an 'inverse log-link', with responses to each covariate presented as partial contributions to the likelihood (log-transformed odds ratio) of an offshore event occurring, i.e. the higher the contribution, the increased predicted likelihood of an exposure event. Responses represent the contribution of a given covariate to the likelihood of exposure, quantified by log-transformed odds ratio of exposure. Additional advantages of this method are that in being additive it fits non-linear and independent responses to each covariate, and that only the most influential covariates are chosen, so that the model performs both model fitting and predictor selection simultaneously, i.e., covariates with little to no influence on exposure to offshore waters are automatically excluded.

The boosted approach iteratively sums simple regressions based on single-covariate 'learner' functions, each chosen to minimize an equivalent loss function based on binomial predictors (see Buhlmann and Hothorn 2007). The additive approach facilitates estimation of the relative 'influence' of each covariate as the number of boosts choosing that covariate, to minimize the current loss. Model parameters were chosen to reduce possible bias and overfitting (Buhlmann and Hothorn 2007): the fit is incremented using small step sizes or "shrinkage" (default 0.25 for terns and 0.3 for plovers) of each iterative sub-model to

the fit, and is also terminated before convergence (i.e., before the fit is maximized; see e.g. Maloney et al. 2012). We used 1,000 boosts per analysis, and verified that this was a reasonable number of iterations using the function `cvrisk` (cross-validated risk) with a species-specific number of separate ‘folds’ (independently sampled fits: 4 for Piping Plovers and 8 for terns).

Learner functions for fitting responses were tailored to the nature of each covariate. Responses to the categorical covariates (sex, location, year and species) were fit using linear learner functions (resulting in fixed effects for each category), responses to each individual were treated as random intercepts, and responses to all the meteorological covariates were fit using cubic p-splines. The package also allowed cyclical responses to the periodic covariates (hour of day and wind direction). Finally, to assess the significance of the predicted covariate responses, we performed bootstrap analysis (using function `confint` with 1,000 model fits) to produce 95% confidence intervals for each covariate response.

To assess the timing of crossing events and meteorological conditions during WEA exposure, we calculated summary statistics of temporal and meteorological variables associated with each exposure event. For circular variables (time of day, in hours EST and wind direction, in degrees relative to true north) we calculated the mean under a circular distribution (R package ‘Circular’, Agostinelli and Lund 2017). To examine exposure relative to daylight, we used the R package ‘mapproj’ (Bivand and Lewin-Koh 2016) to calculate local sunrise and sunset times for each modeled location estimate, interpolated to a 1-minute time step. Exposure events that occurred between the time of local sunrise and the time of local sunset were considered to have occurred during daytime hours. Conversely, exposure that occurred between the time of local sunset and the time of local sunrise were considered to have occurred during nighttime hours. For each remaining variable (wind speed, wind support, crosswind, barometric pressure, precipitation accumulation, temperature, visibility) we report summary statistics (mean, SD, range) across WEA exposure events.

3 Results

3.1 Common and Roseate Terns

3.1.1 Tagging and Detection Summaries

We tagged a total of 266 Common Terns and 150 Roseate Terns for this study over four field seasons (Tables 3 and 4). In 2014, we tagged 65 Common Terns on Monomoy NWR, MA and 51 on Great Gull Island, NY. In 2015, we tagged 31 Common Terns and 30 Roseate Terns on Great Gull Island. In 2016, we tagged 30 Common Terns from nesting colonies in Buzzards Bay, MA (n=25 on Bird Island and n=5 on Penikese Island), 30 Common Terns on Great Gull Island, and 60 Roseate Terns (n=30 on Bird Island, n=30 on Great Gull Island). In 2017, we tagged 29 Common Terns in Buzzards Bay (n=19 on Bird Island, n=10 on Ram Island), 30 Common Terns on Great Gull Island, 30 Roseate Terns in Buzzards Bay (n=19 on Bird Island, n=11 on Ram Island), and 30 Roseate Terns on Great Gull Island. Of the total Common Terns tagged from 2014 to 2017, 58% (n=153) were female, 42% were male, and one individual was of unknown sex. Of the total Roseate Terns tagged from 2015 to 2017, 51% (n=77) were female, 48% (n=72) were male, and one was of unknown sex.

Of the 416 Common and Roseate Terns tagged, 97% were detected by the telemetry array. However, due to incomplete detection data from tag loss and incomplete spatial coverage of the receiving station array (Appendix G), modeled movements are not representative of the entire breeding and post-breeding period for many individuals. Tagging of Common and Roseate Terns ranged from 9 June to 12 July. Tagged Common Terns were tracked within the Study Area for an average of 40 days following tagging (sd 18 days; range 0 to 101 days) and Roseate Terns were tracked for an average of 32 days following tagging (sd 21 days; range 0 to 95 days).

Table 3. Number of adult Common Terns tagged at nesting colonies in MA (Monomoy NWR, Buzzards Bay) and NY (Great Gull Island), 2014-2017

	2014	2015	2016	2017	Total
Monomoy NWR, MA	65	0	0	0	65
Buzzards Bay, MA	0	0	30	29	59
Great Gull Island, NY	51	31	30	30	142
Total	116	31	60	59	266

Table 4. Number of adult Roseate Terns tagged at nesting colonies in MA (Buzzards Bay) and NY (Great Gull Island), 2015-2017

	2015	2016	2017	Total
Buzzards Bay, MA	0	30	30	60
Great Gull Island, NY	30	30	30	90
Total	30	60	60	150

3.1.2 Movements in Study Area

During the breeding and post-breeding period, model-estimated tracks of tagged Common and Roseate Terns primarily occurred from Cape Cod, MA to eastern Long Island Sound, NY (Figs. 10-15). Across all species, sites, and years, track density of tagged terns was highest within 50 km of their nesting colonies. High-use areas of Common and Roseate Terns tagged and nesting on Great Gull Island, NY included Montauk Point on Long Island, NY; Block Island, RI; and Napatree Point in southwestern RI (Figs. 12 and 15). High-use areas of Common and Roseate Terns nesting on islands in Buzzards Bay, MA included western Nantucket Sound and adjacent waters of Vineyard Sound, Muskeget Island in southern Nantucket Sound, and Nomans Land Island in Rhode Island Sound (Figs. 13 and 15). During the post-breeding period, Common and Roseate Terns from Great Gull Island and Buzzards Bay dispersed to staging areas in southeastern Massachusetts, including the outer Cape Cod region (with high densities on Monomoy NWR), Nantucket, and Muskeget Island.

From 2014 to 2017, six Common Terns and one Roseate Tern made long distance (>250 km) movements during the post-breeding period. Two Common Terns from Great Gull Island were tracked to Delaware

Bay during late July of 2014 and 2016, respectively (Fig. 12). In mid-July of 2016, a Common Tern from Buzzards Bay was tracked to Parker River, MA (Fig. 13). During late July through mid-September of 2017, three Common Terns from Buzzards Bay were tracked to Delaware Bay, Virginia, and North Carolina (Fig. 13). One Roseate Tern from Great Gull Island was detected in coastal New Jersey during mid-August of 2016 (Fig. 14).

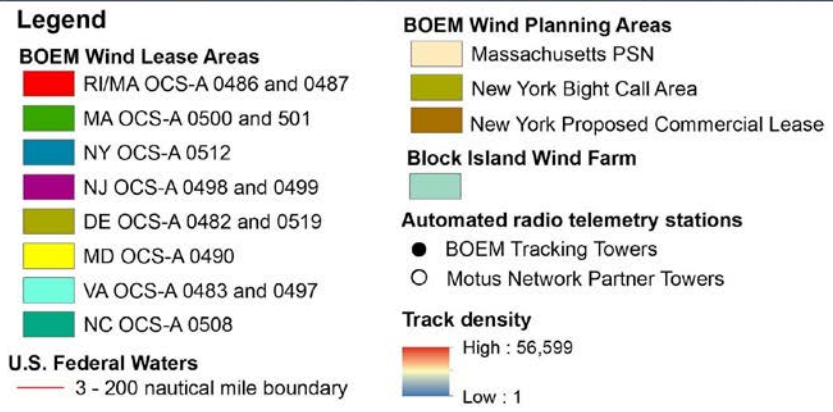
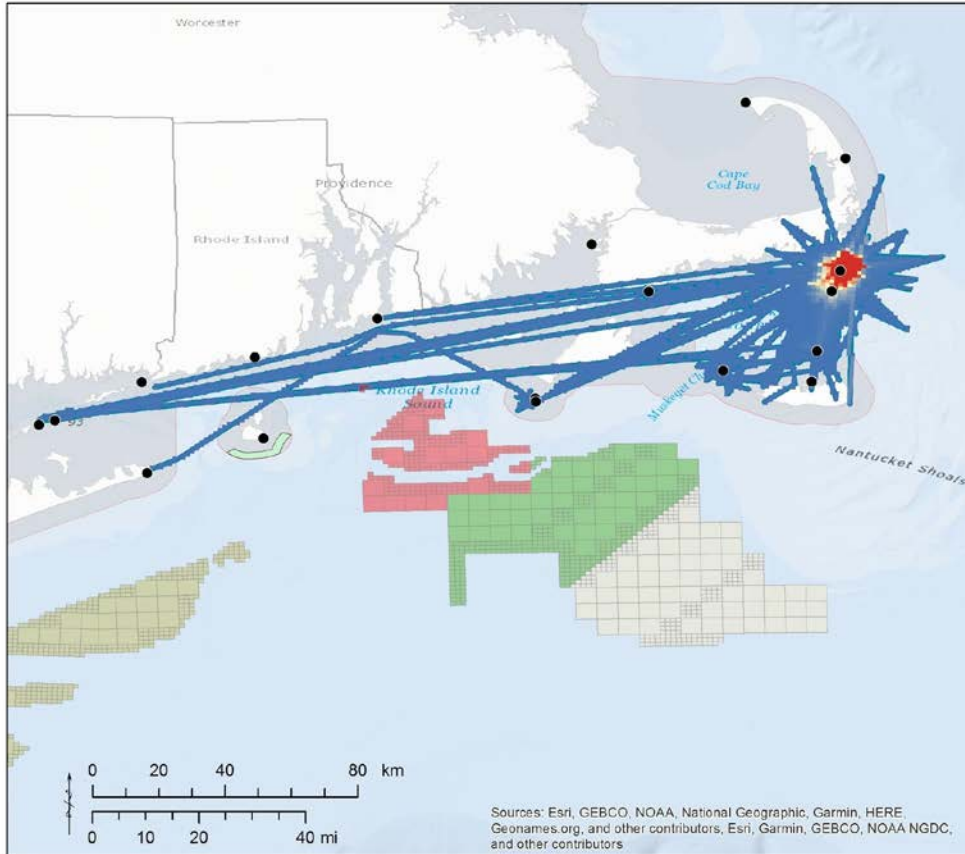


Figure 11. Track densities (10-min tracks/km²) of Common Terns (n=65) from the colony on Monomoy NWR during the breeding and post-breeding periods in 2014.

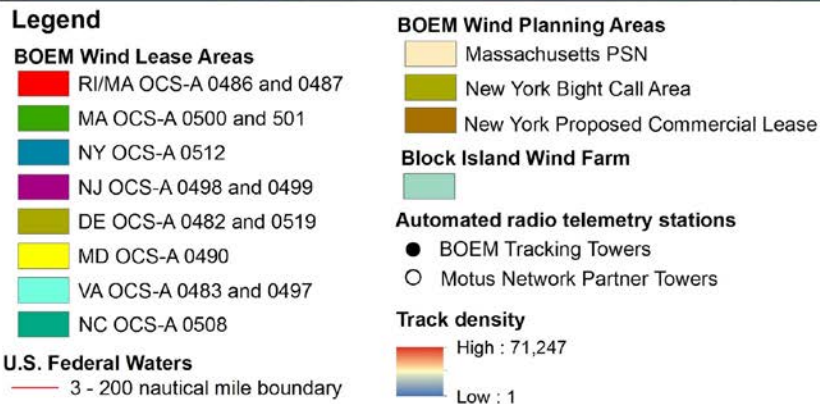
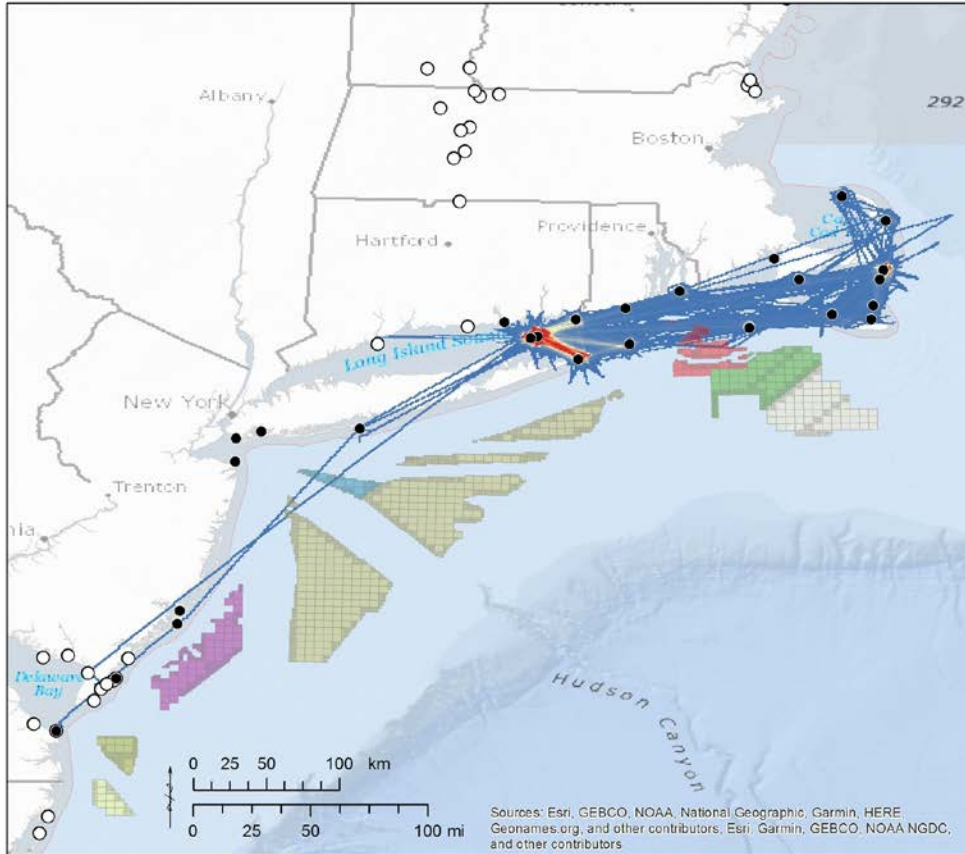


Figure 12. Track densities (10-min tracks/km²) of Common Terns (n=142) from the colony on Great Gull Island during the breeding and post-breeding periods in 2014 to 2017 (pooled).

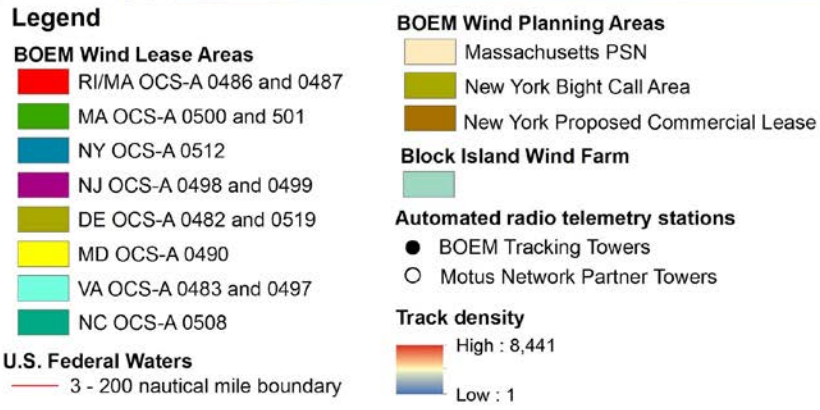
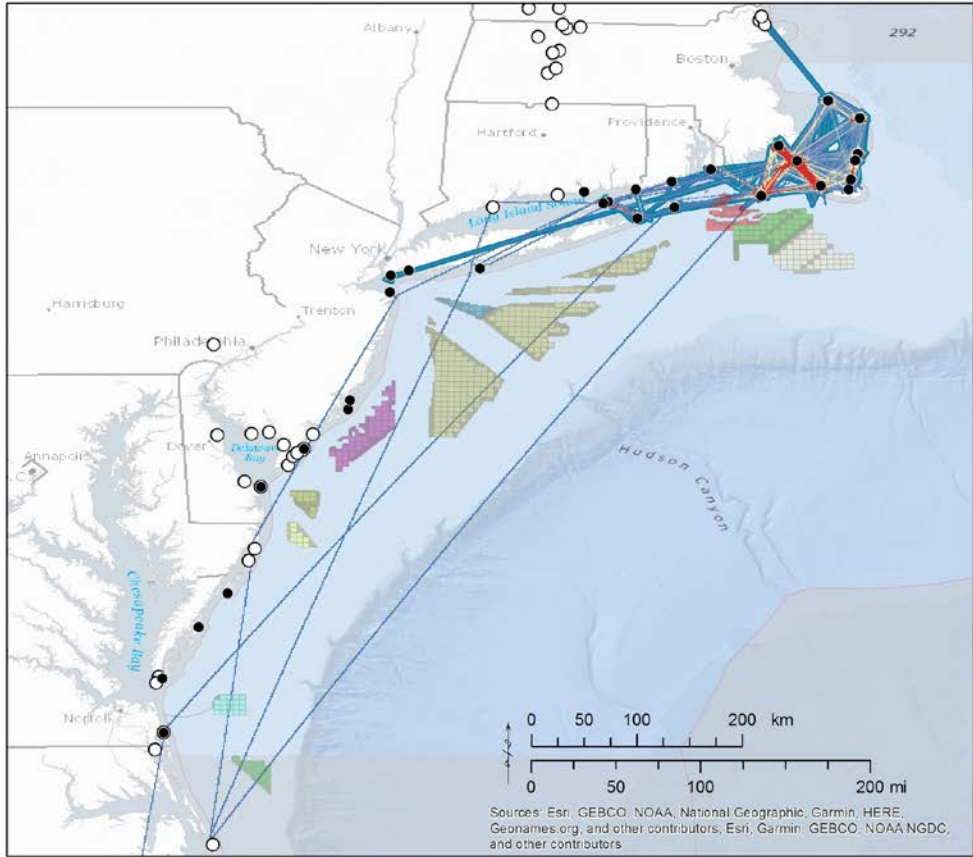


Figure 13. Track densities (10-min tracks/km²) of Common Terns (n=59) from colonies in Buzzards Bay during the breeding and post-breeding periods in 2015 to 2017 (pooled).

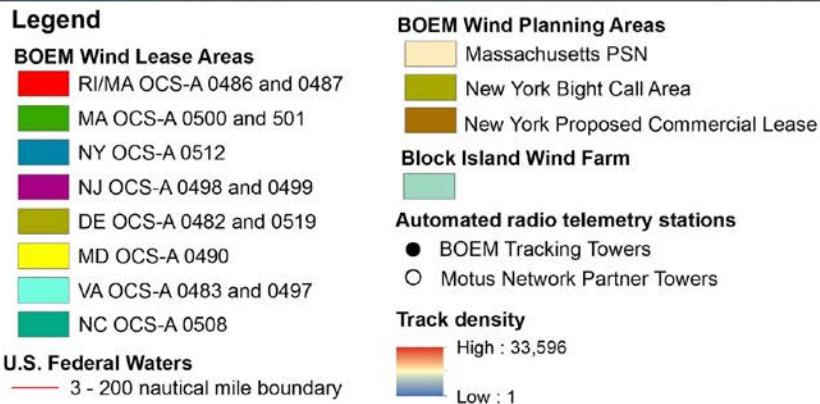
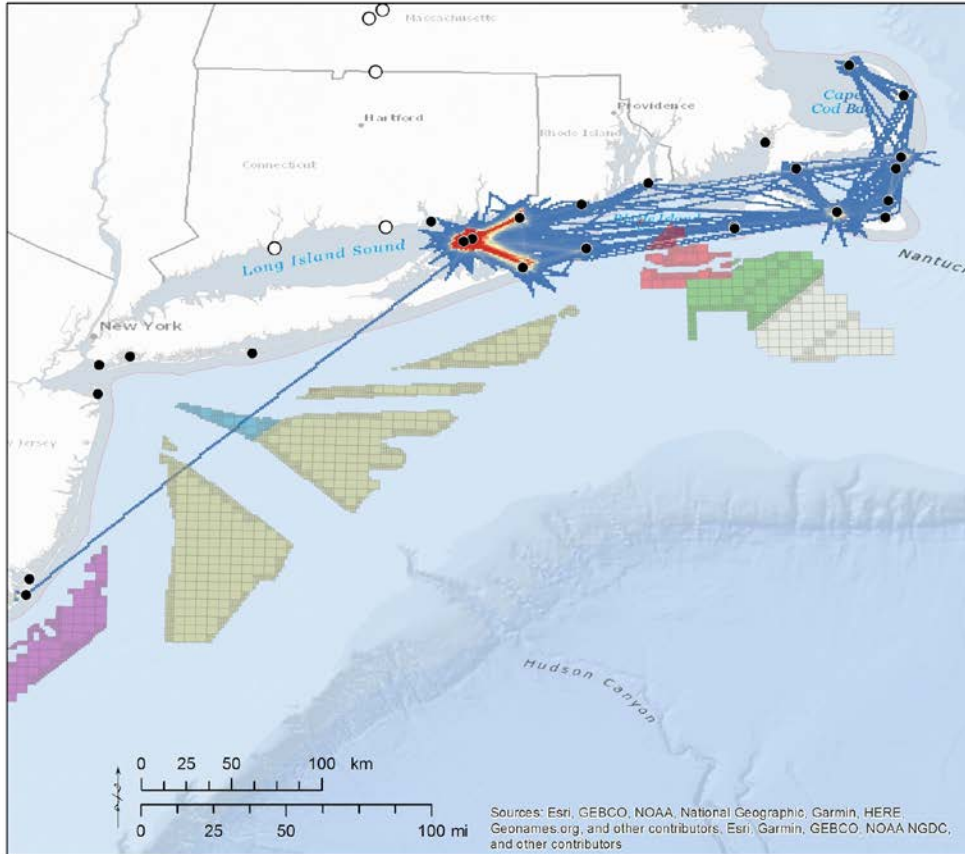


Figure 14. Track densities (10-min tracks/km²) of Roseate Terns (n=90) from the colony on Great Gull Island during the breeding and post-breeding periods in 2015 to 2017 (pooled).

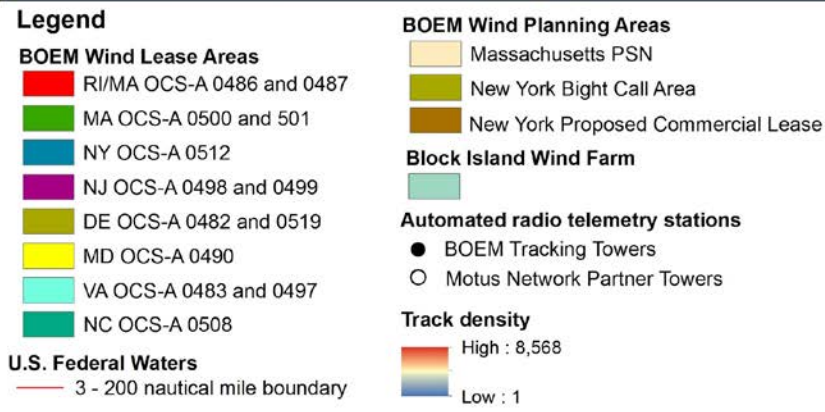
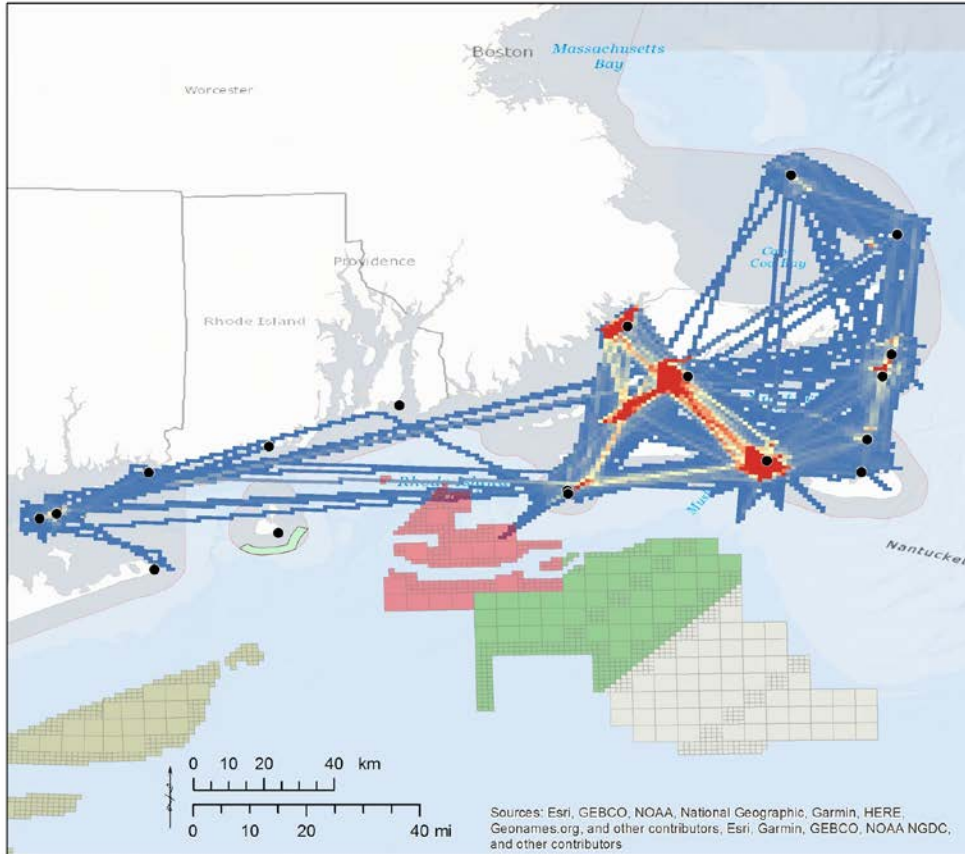
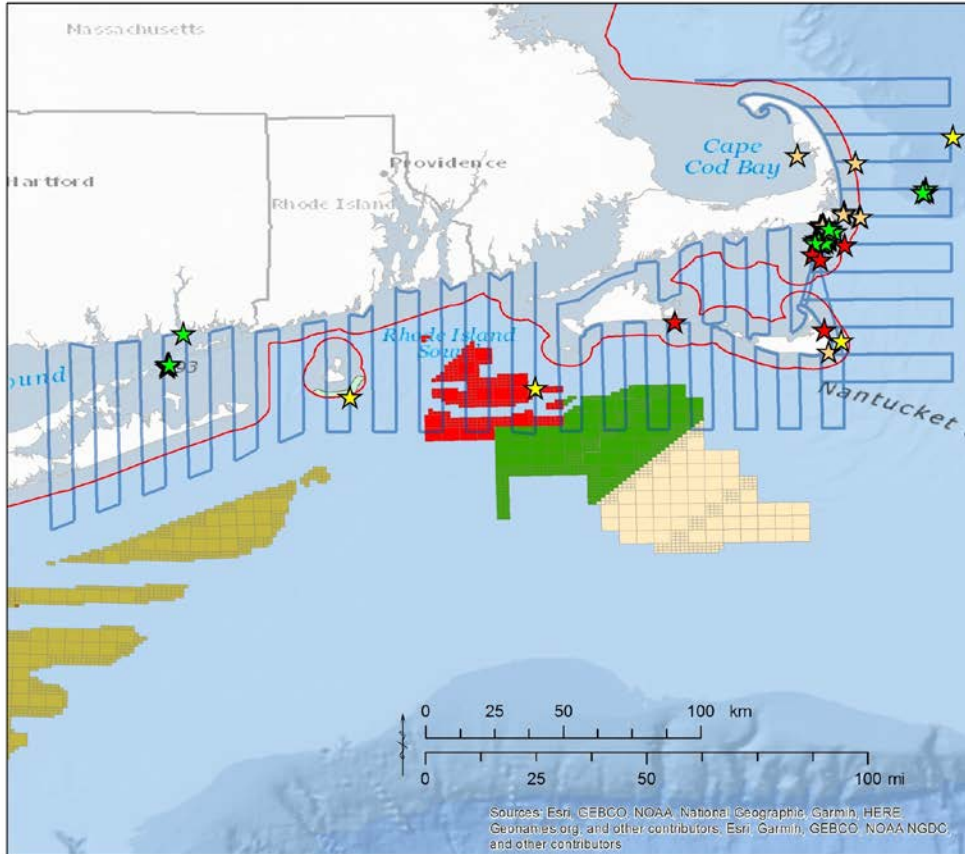


Figure 15. Track densities (10-min tracks/km²) of Roseate Terns (n=60) from colonies in Buzzards Bay during the breeding and post-breeding periods in 2016 and 2017 (pooled).

3.1.3 Aerial Telemetry Surveys

During aerial telemetry surveys conducted in August 2014, we detected a total of 22 Common Terns (7 from Great Gull Island and 15 from Monomoy NWR; Fig. 16). The majority of terns from both colonies were detected in the vicinity of Monomoy NWR. Three Common Terns (two from Monomoy and one from Great Gull Island) were detected in Federal waters, up to 25 km east of Cape Cod, MA. Detections of Common Terns in Federal waters occurred on Aug 5, 12, and 25.

During aerial telemetry surveys conducted in August 2015, we detected a total of 3 Common Terns and 3 Roseate Terns from Great Gull Island (Fig. 16). Two Common Terns were detected in Federal waters. The first was detected approximately 6 km south of Block Island, RI near the Block Island Wind Farm on Aug 9. The second was detected 35 km east of Cape Cod, MA (the farthest extent of the transects) on Aug 16 and subsequently in Rhode Island Sound within BOEM Lease Area OCS-A 0486 on Aug 17. Detections of Roseate Terns primarily occurred within the vicinity of Monomoy NWR. One Roseate Tern was also detected on Martha's Vineyard and Nantucket during surveys on Aug 3 and 16, respectively.



Legend

BOEM Wind Lease Areas

RI/MA OCS-A 0486 and 0487

MA OCS-A 0500 and 501

BOEM Wind Planning Areas

Massachusetts PSN

New York Bight Call Area

New York Proposed Commercial Lease

Block Island Wind Farm

U.S. Federal Waters

3 - 200 nautical mile boundary

Aerial Survey Transects

Locations of tagged terns

☆ Common Terns (Monomoy NWR 2014)

☆ Common Terns (Great Gull Is 2014)

☆ Common Terns (Great Gull Is 2015)

★ Roseate Terns (Great Gull Is 2015)

Figure 16. Locations of tagged Common and Roseate Terns detected during aerial telemetry surveys in 2014 and 2015.

3.1.4 Estimated Exposure to Federal Waters

3.1.4.1 Common Terns

Of the 257 Common Terns detected by the array from 2014 to 2017, 78% (n=201) had estimated exposure to Federal waters within the Study Area (Table 5). Estimated exposure to Federal waters was higher among Common Terns from Buzzards Bay (85%, n=45 of 53) and Great Gull Island (81%, n=112 of 139), relative to those from Monomoy (68%, n=44 of 65). Of the 201 Common Terns with estimated exposure to Federal waters, 62% (n=125) were female and 38% (n=76) were male.

Table 5. Number of adult Common Terns tagged at nesting colonies in MA (Monomoy NWR, Buzzards Bay) and NY (Great Gull Island) that were exposed to Federal waters, 2014-2017. Sample size (N) shows number of individuals tracked per year and location.

	2014 (N=115)	2015 (N=31)	2016 (N=59)	2017 (N=52)	Total (N=257)
Monomoy NWR, MA (N=65)	44	---	---	---	44
Buzzards Bay, MA (N=53)	---	---	23	22	45
Great Gull Island, NY (N=139)	34	28	29	21	112
Total (N=257)	78	28	52	43	201

3.1.4.1.1 Covariate Analysis of Estimated Exposure to Federal Waters

Day of year was the strongest predictor of exposure to Federal Waters among Common Terns, both in terms of selection among boosts (Table 6) and regarding the magnitude of predicted response (Fig. 17). Overall, the probability of exposure increased from tag deployment at the nesting areas (June) through the post-breeding dispersal period (mid-July through Sept; Fig. 17). Interaction terms between day of year and sex revealed that exposure of males to Federal waters peaked during the pre-fledging period (June through early July), whereas females had higher exposure relative to males during the post-fledging period in mid-July through September (Fig. 18). Common Terns from Buzzards Bay had a higher probability of exposure to Federal waters relative to Common Terns from Great Gull Island, and Monomoy NWR, respectively (Fig. 19). The probability of exposure to Federal waters peaked in the morning, from 04:00 to 09:00 hrs EST (Fig. 20). Predicted responses to the meteorological variables indicated increased offshore movements in fair weather, i.e. high pressure (Fig. 21), in wind-speeds that peaked around 10 m/s (Fig. 22). Exposure to Federal waters occurred at the lower range of air temperatures (10-20° C; Fig. 23), associated with early morning conditions. By year, the model predicted lower exposure in 2014 and 2017 relative to 2015 and 2016 (Fig. 24).

Table 6. Description and selection frequencies of covariates in binomial Boosted GAM analysis of exposure of Common Terns to Federal waters, 2014 to 2017.

Covariate (units)	Fitting function	Selection Frequency
Date (Julian)	p-spline	0.23
Bird ID	Random intercept	0.19
Colony	categorical (MNY, GGI, Buzz Bay)	0.19
Hour (EST)	cyclical p-spline	0.13
Pressure (Pa)	p-spline	0.08
Date * Sex	categorical	0.07
Wind speed (m/s)	p-spline	0.06
Air temperature (°C)	p-spline	0.03
Year	categorical (2014, 2015, 2016, 2017)	0.03
Wind support	p-spline	0.00
Sex	categorical (M, F, unknown)	0.00
Visibility (m)	p-spline	0.00
Wind direction (° true N)	cyclical p-spline	0.00
Precipitation (kg/m ²)	p-spline	0.00

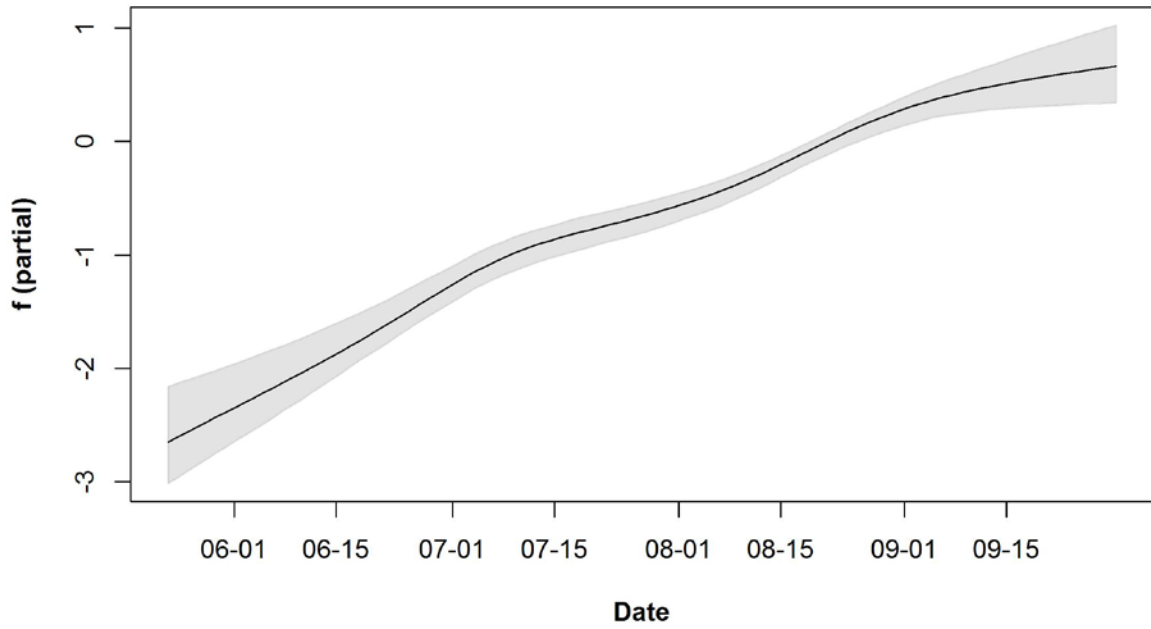


Figure 17. Boosted GAM prediction for the partial contribution of the date of year covariate (x-axis) to the likelihood (log-transformed odds ratio) of exposure to Federal waters among Common Terns (y-axis) in 2014, 2015, 2016, and 2017 (pooled).
The gray-shaded area represents the 95% confidence interval for the response based on 1000 bootstrapped models.

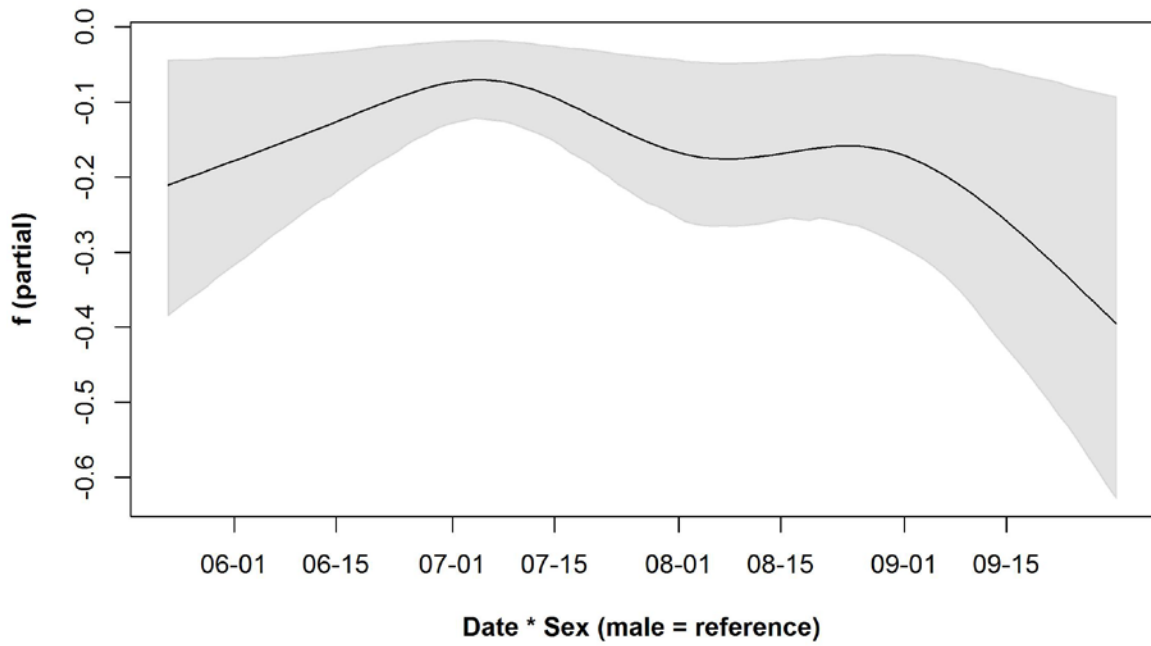


Figure 18. Boosted GAM prediction for the partial contribution of the date of year by sex interaction term (x-axis) to the likelihood (log-transformed odds ratio) of exposure to Federal waters among Common Terns (y-axis) in 2014, 2015, 2016, and 2017 (pooled).

The gray-shaded area represents the 95% confidence interval for the response based on 1000 bootstrapped models.

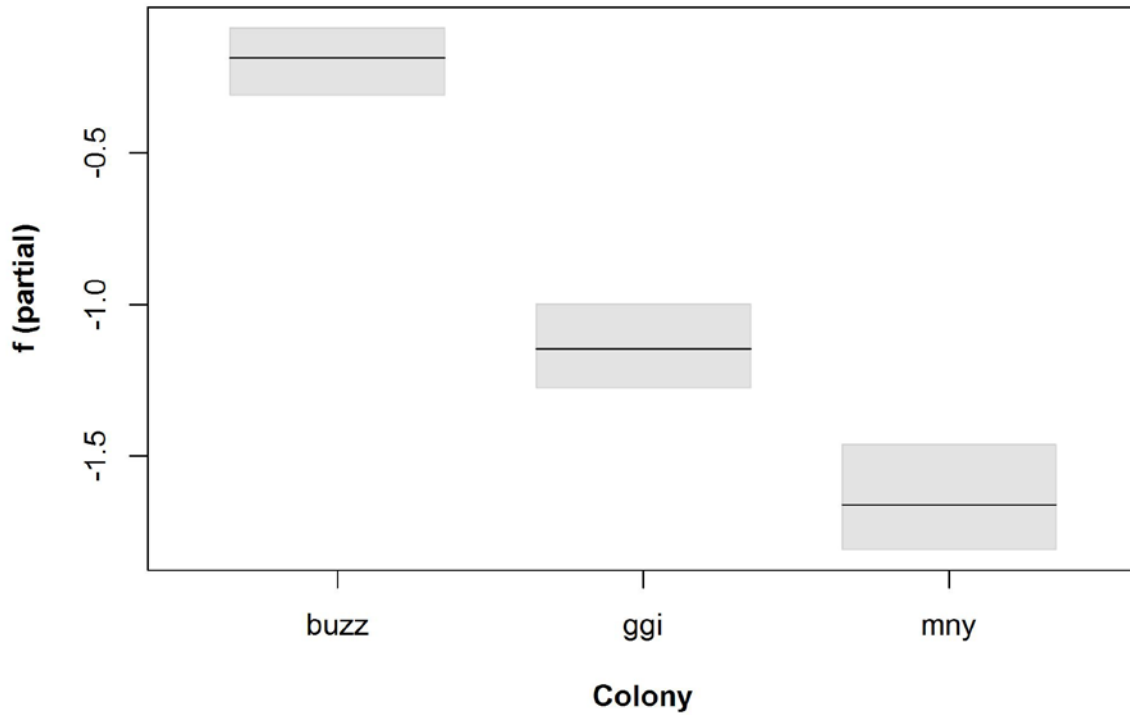


Figure 19. Boosted GAM prediction for the partial contribution of the nesting colony location (buzz = Buzzards Bay, ggi = Great Gull Island, mny = Monomoy NWR) covariate (x-axis) to the likelihood (log-transformed odds ratio) of exposure to Federal waters among Common Terns (y-axis) in 2014, 2015, 2016, and 2017 (pooled).
 The gray-shaded area represents the 95% confidence interval for the response based on 1000 bootstrapped models.

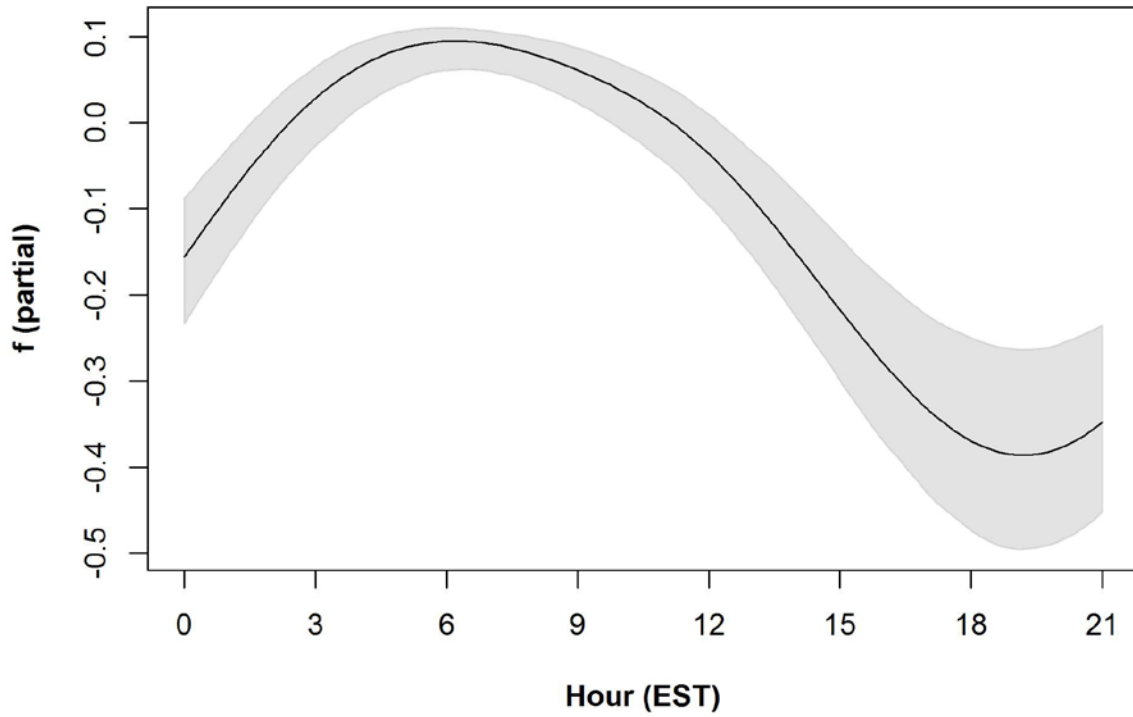


Figure 20. Boosted GAM prediction for the partial contribution of the hour of day (EST) covariate (x-axis) to the likelihood (log-transformed odds ratio) of exposure to Federal waters among Common Terns (y-axis) in 2014, 2015, 2016, and 2017 (pooled). The gray-shaded area represents the 95% confidence interval for the response based on 1000 bootstrapped models.

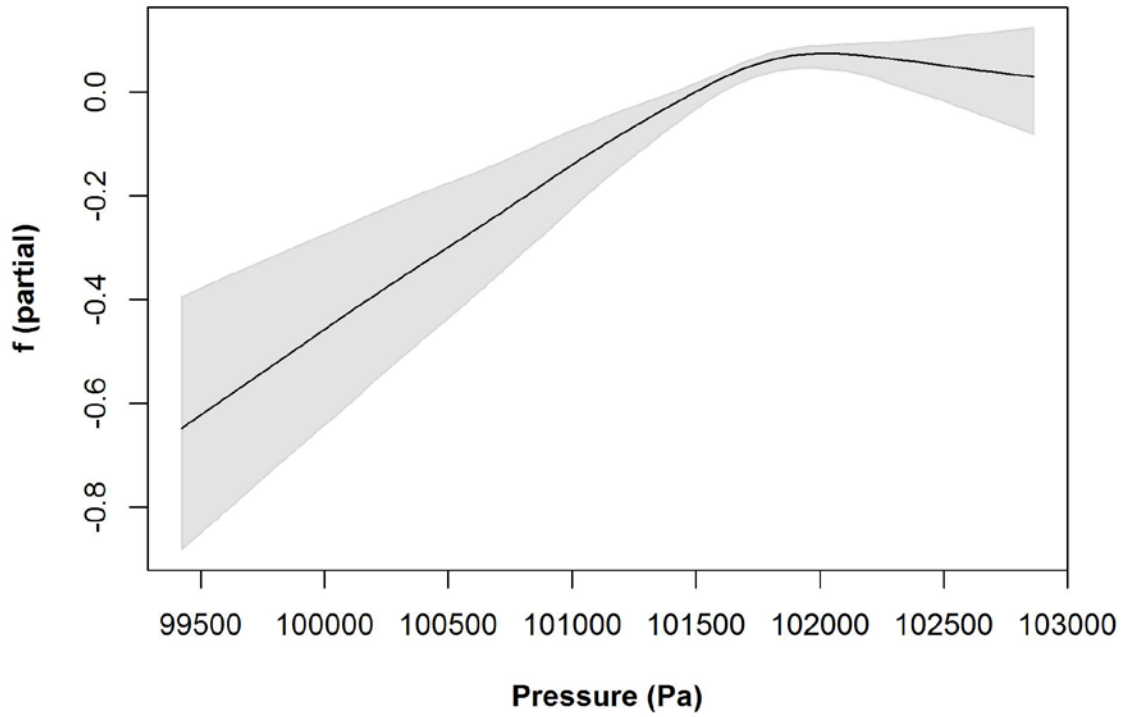


Figure 21. Boosted GAM prediction for the partial contribution of the atmospheric pressure covariate (x-axis) to the likelihood (log-transformed odds ratio) of exposure to Federal waters among Common Terns (y-axis) in 2014, 2015, 2016, and 2017 (pooled).

The gray-shaded area represents the 95% confidence interval for the response based on 1000 bootstrapped models.

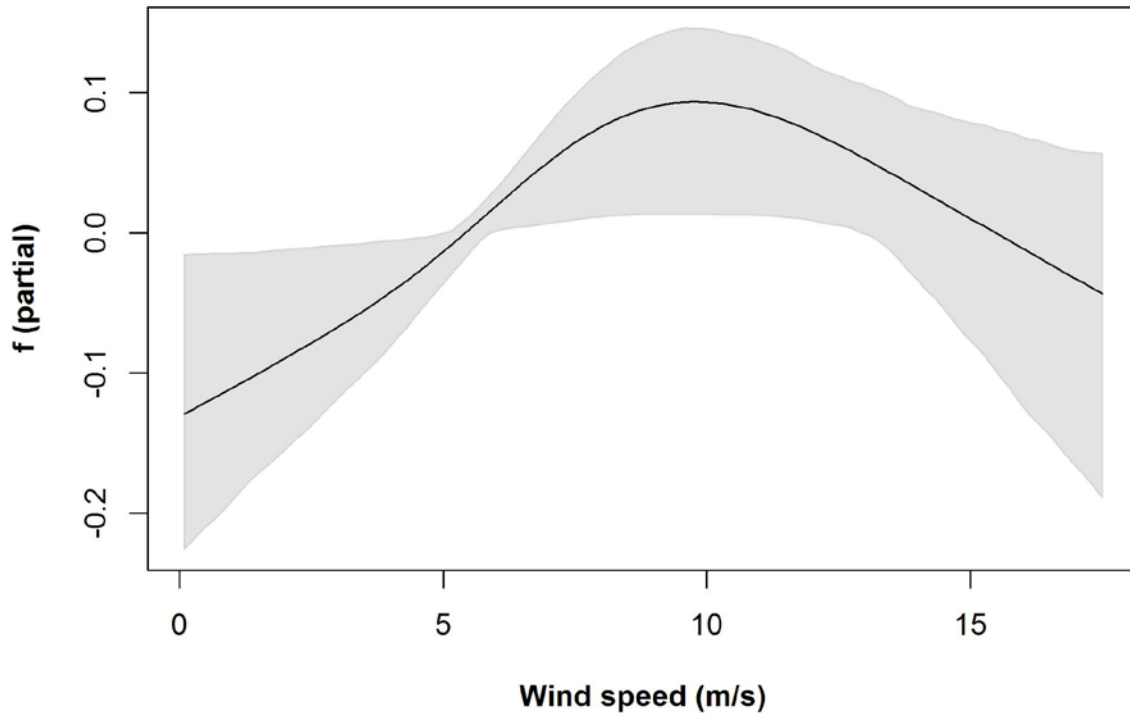


Figure 22. Boosted GAM prediction for the partial contribution of the wind speed covariate (x-axis) to the likelihood (log-transformed odds ratio) of exposure to Federal waters among Common Terns (y-axis) in 2014, 2015, 2016, and 2017 (pooled).

The gray-shaded area represents the 95% confidence interval for the response based on 1000 bootstrapped models.

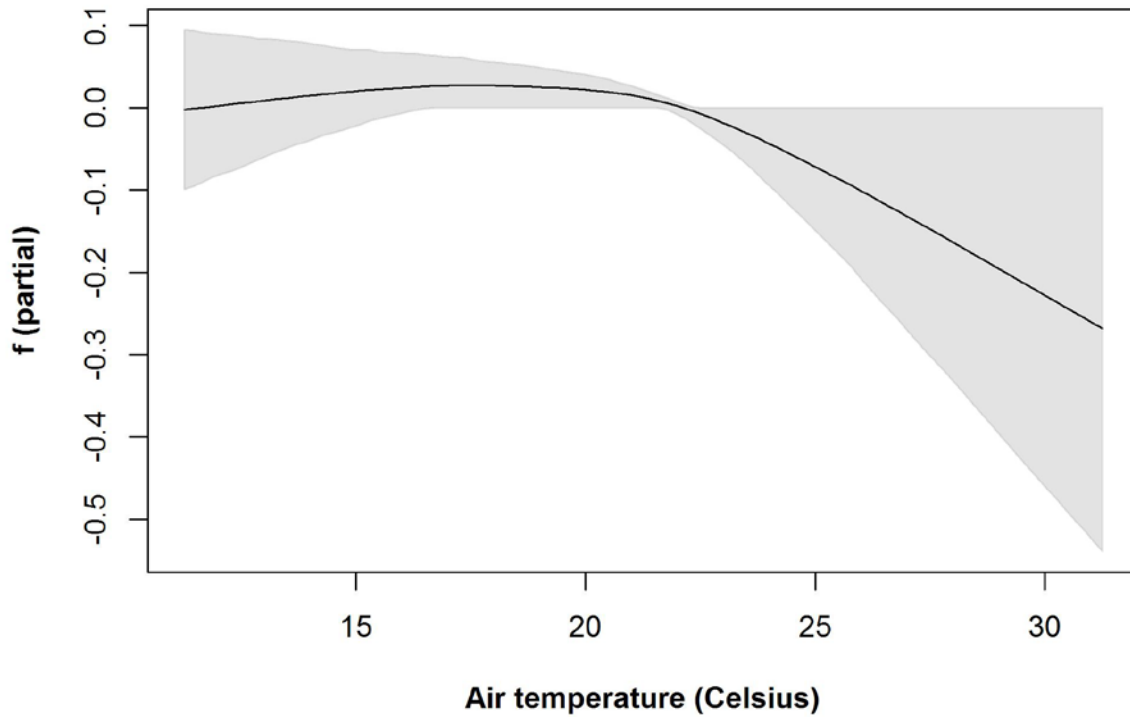


Figure 23. Boosted GAM prediction for the partial contribution of the air temperature covariate (x-axis) to the likelihood (log-transformed odds ratio) of exposure to Federal waters among Common Terns (y-axis) in 2014, 2015, 2016, and 2017 (pooled).

The gray-shaded area represents the 95% confidence interval for the response based on 1000 bootstrapped models.

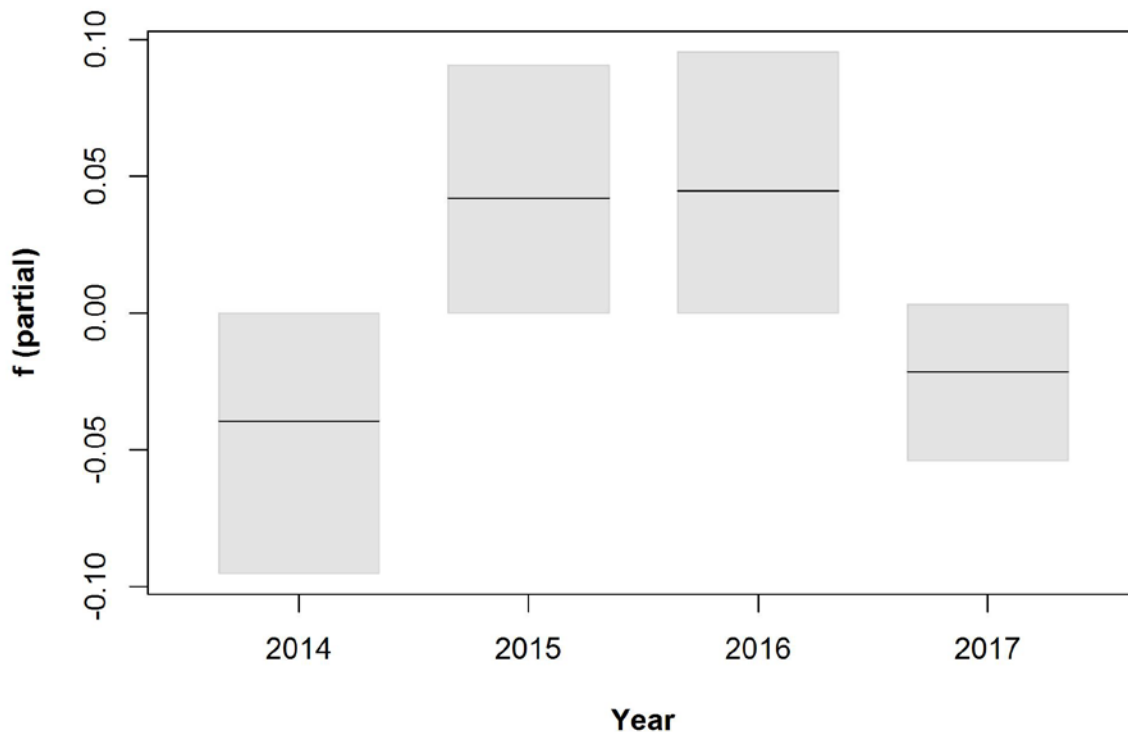


Figure 24. Boosted GAM prediction for the partial contribution of the year covariate (x-axis) to the likelihood (log-transformed odds ratio) of exposure to Federal waters among Common Terns (y-axis) in 2014, 2015, 2016, and 2017.

The gray-shaded area represents the 95% confidence interval for the response based on 1000 bootstrapped models.

3.1.4.2 Roseate Terns

Of the 145 Roseate Terns detected by the array from 2015 to 2017, 59% (n=85) had estimated exposure to Federal waters within the Study Area (Table 7). Estimated exposure to Federal waters was similar among Roseate Terns from Great Gull Island (60%, n=54 of 90) and Roseate Terns from Buzzards Bay (56%, n=31 of 55). Of the 85 Roseate Terns with estimated exposure to Federal waters, 55% (n=47) were female and 44% (n=37) were male.

Table 7. Number of adult Roseate Terns tagged at nesting colonies in MA (Buzzards Bay) and NY (Great Gull Island) that were exposed to Federal waters, 2015-2017. Sample size (N) shows number of individuals tracked per year and location.

	2015 (N=30)	2016 (N=60)	2017 (N=55)	Total (N=145)
Buzzards Bay, MA (N=55)	---	14	17	31
Great Gull Island, NY (N=90)	25	22	7	54
Total (N=145)	25	36	24	85

3.1.4.2.1 Covariate Analysis of Estimated Exposure to Federal Waters

Similar to Common Terns, the covariate analysis of Roseate Tern exposure to Federal waters revealed that day of year was the strongest predictor, both in terms of selection among boosts (Table 8) and regarding the magnitude of predicted response (Fig. 25). Overall, the probability of exposure increased from tag deployment at the nesting areas (June) through the post-breeding dispersal period (mid-July through Sept; Fig. 25). Interaction terms between day of year and sex revealed that exposure of males to Federal waters was highest from the June through July, spanning the pre-fledging period through early post-breeding dispersal, whereas females had higher exposure relative to males during the post-breeding period in August and September (Fig 26). Like Common Terns, the probability of exposure to Federal waters among Roseate Terns peaked in the morning, from 04:00 to 09:00 hrs EST (Fig. 27). Roseate Terns from Buzzards Bay had a higher probability of exposure to Federal waters relative to Roseate Terns from Great Gull Island (Fig. 28). Predicted responses to the meteorological variables indicated increased offshore movements in fair weather, i.e. high pressure (Fig. 29), at wind-speeds greater than 5 m/s (Fig. 30), with a relatively weak association with headwinds (i.e. negative wind support, Fig. 31) blowing from the southwest (Fig. 32). As with Common Terns, exposure to Federal waters occurred at the lower range of air temperatures (10-20° C), associated with early morning conditions (Fig. 33).

Table 8. Description and selection frequencies of covariates in binomial Boosted GAM analysis of exposure of Roseate Terns to Federal waters, 2015 to 2017.

Covariate (units)	Fitting function	Selection Frequency
Date (Julian)	p-spline	0.30
Bird ID	Random intercept	0.22
Pressure (Pa)	p-spline	0.11
Date * Sex	categorical	0.08
Hour (EST)	cyclical p-spline	0.08
Colony	categorical (GGI, Buzz Bay)	0.07
Wind speed (m/s)	p-spline	0.05
Air temperature (°C)	p-spline	0.03
Wind direction (° true N)	cyclical p-spline	0.03
Wind support	p-spline	0.03
Year	categorical (2014, 2015, 2016, 2017)	0.00
Sex	categorical (M, F, unknown)	0.00
Visibility (m)	p-spline	0.00
Precipitation (kg/m ²)	p-spline	0.00

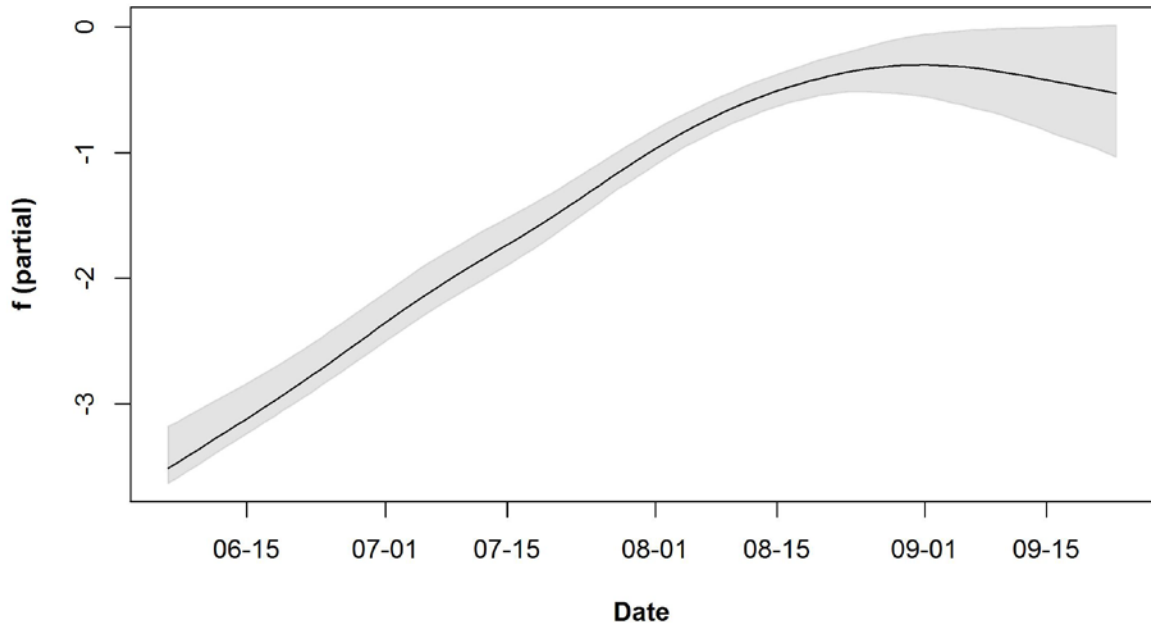


Figure 25. Boosted GAM prediction for the partial contribution of the date of year covariate (x-axis) to the likelihood (log-transformed odds ratio) of exposure to Federal waters among Roseate Terns (y-axis) in 2015, 2016, and 2017 (pooled).
The gray-shaded area represents the 95% confidence interval for the response based on 1000 bootstrapped models.

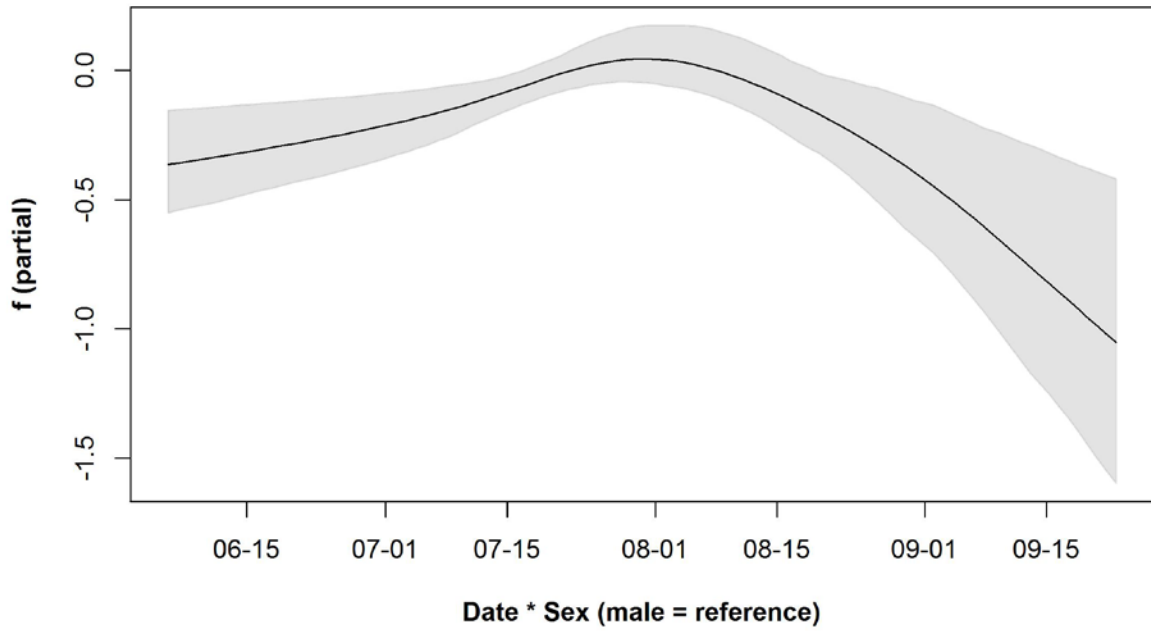


Figure 26. Boosted GAM prediction for the partial contribution of the date of year by sex interaction term (x-axis) to the likelihood (log-transformed odds ratio) of exposure to Federal waters among Roseate Terns (y-axis) in 2015, 2016, and 2017 (pooled). The gray-shaded area represents the 95% confidence interval for the response based on 1000 bootstrapped models.

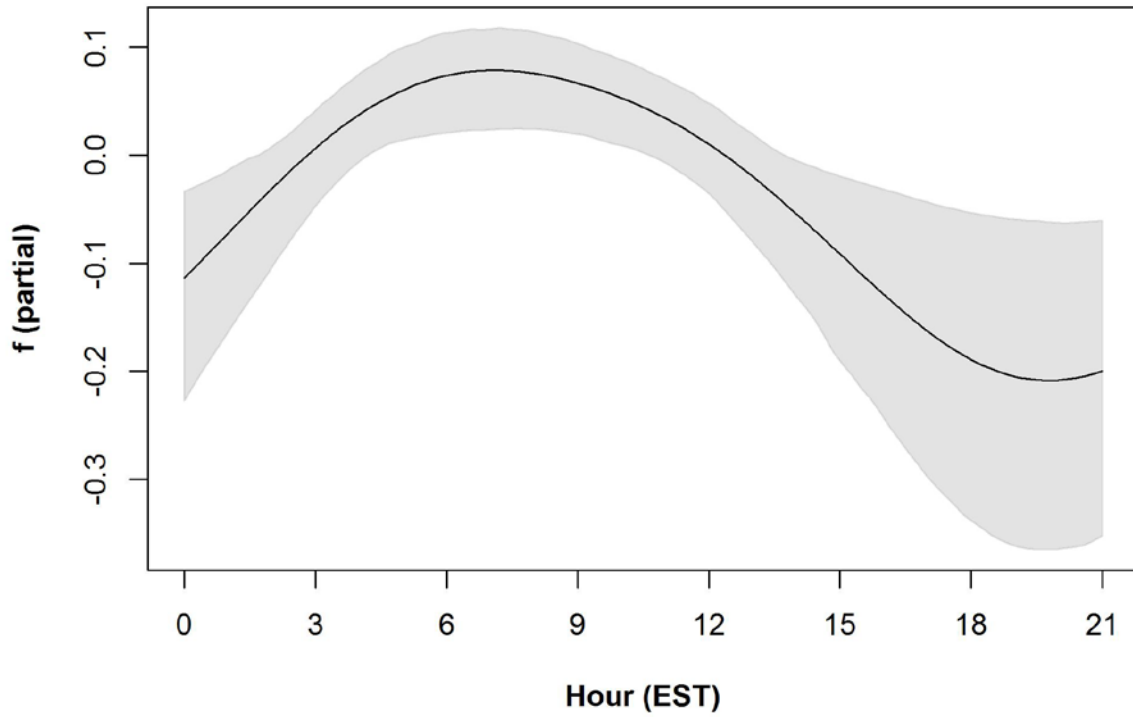


Figure 27. Boosted GAM prediction for the partial contribution of the hour of day (EST) covariate (x-axis) to the likelihood (log-transformed odds ratio) of exposure to Federal waters among Roseate Terns (y-axis) in 2015, 2016, and 2017 (pooled).
The gray-shaded area represents the 95% confidence interval for the response based on 1000 bootstrapped models.

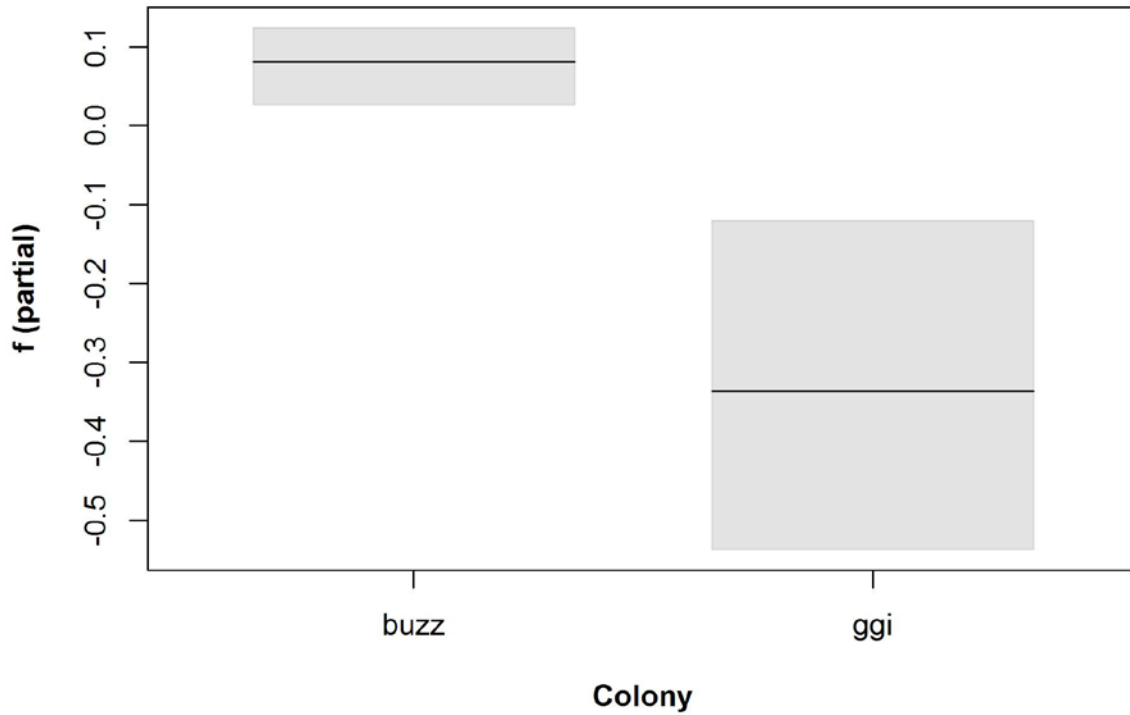


Figure 28. Boosted GAM prediction for the partial contribution of the nesting colony location (buzz = Buzzards Bay, ggi = Great Gull Island) covariate (x-axis) to the likelihood (log-transformed odds ratio) of exposure to Federal waters among Roseate Terns (y-axis) in 2015, 2016, and 2017 (pooled).

The gray-shaded area represents the 95% confidence interval for the response based on 1000 bootstrapped models.

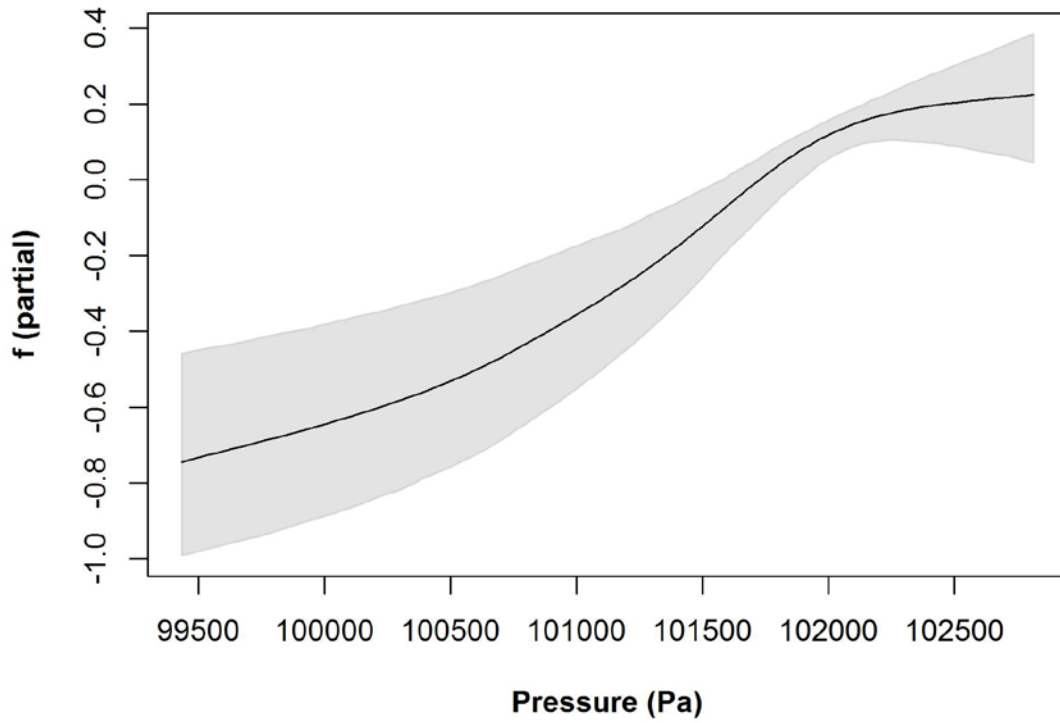


Figure 29. Boosted GAM prediction for the partial contribution of the atmospheric pressure covariate (x-axis) to the likelihood (log-transformed odds ratio) of exposure to Federal waters among Roseate Terns (y-axis) in 2015, 2016, and 2017 (pooled). The gray-shaded area represents the 95% confidence interval for the response based on 1000 bootstrapped models.

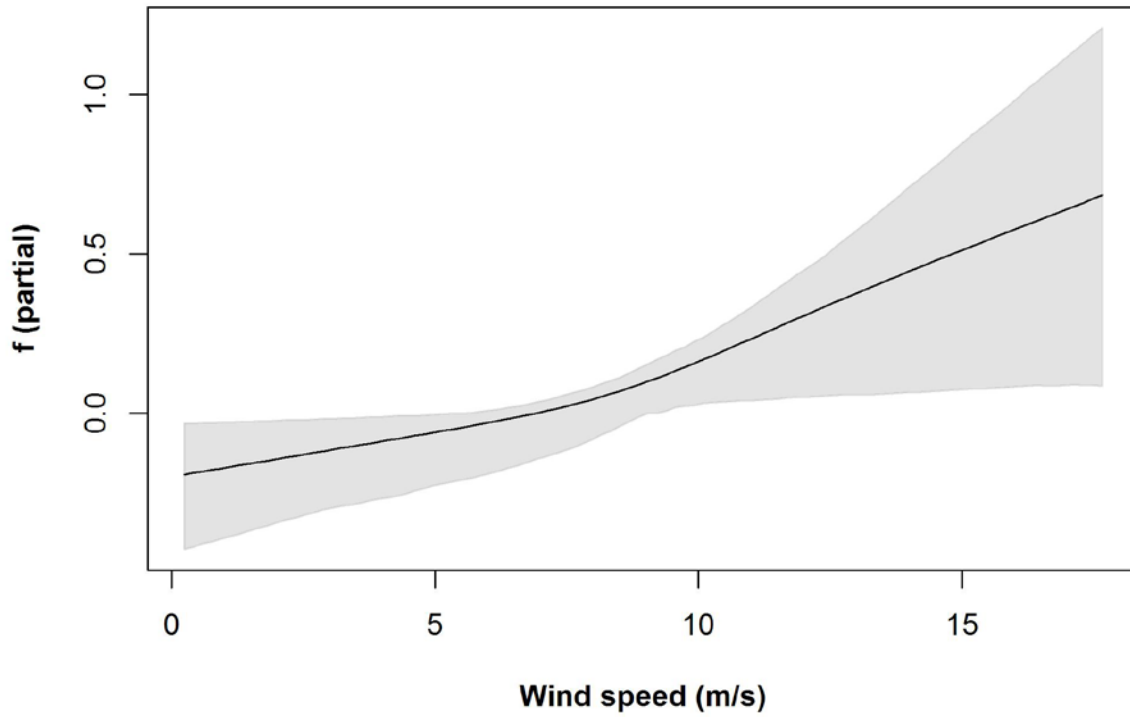


Figure 30. Boosted GAM prediction for the partial contribution of the wind speed covariate (x-axis) to the likelihood (log-transformed odds ratio) of exposure to Federal waters among Roseate Terns (y-axis) in 2015, 2016, and 2017 (pooled).

The gray-shaded area represents the 95% confidence interval for the response based on 1000 bootstrapped models.

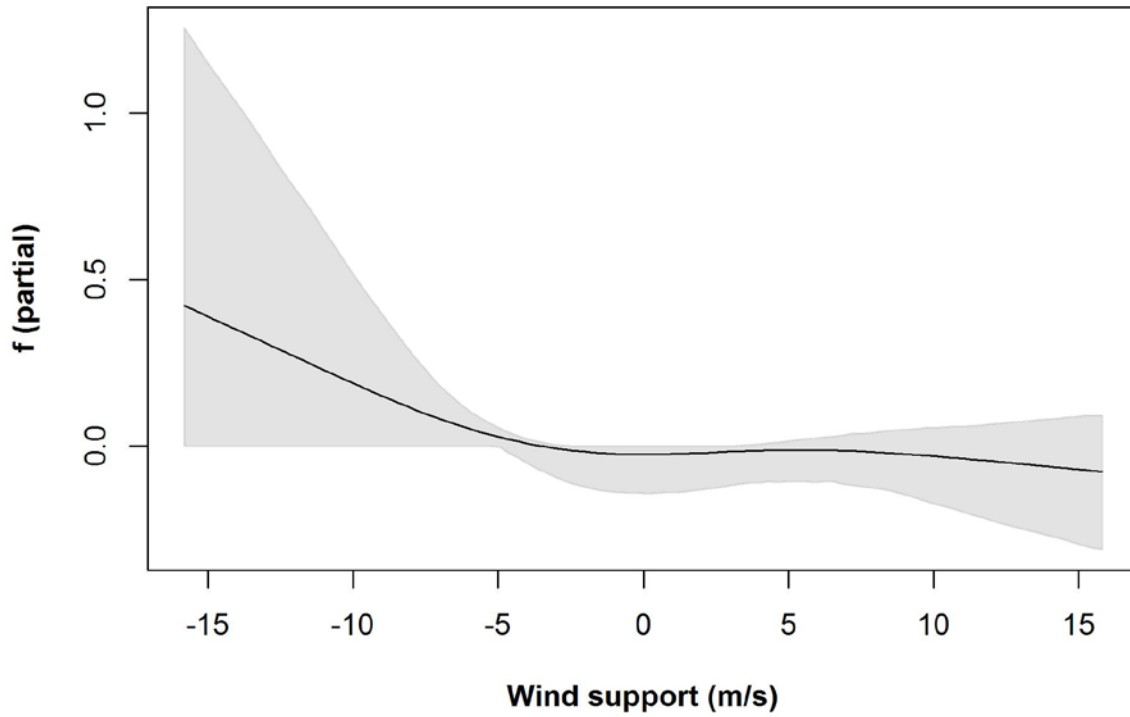


Figure 31. Boosted GAM prediction for the partial contribution of the wind support covariate (x-axis) to the likelihood (log-transformed odds ratio) of exposure to Federal waters among Roseate Terns (y-axis) in 2015, 2016, and 2017 (pooled).
The gray-shaded area represents the 95% confidence interval for the response based on 1000 bootstrapped models.

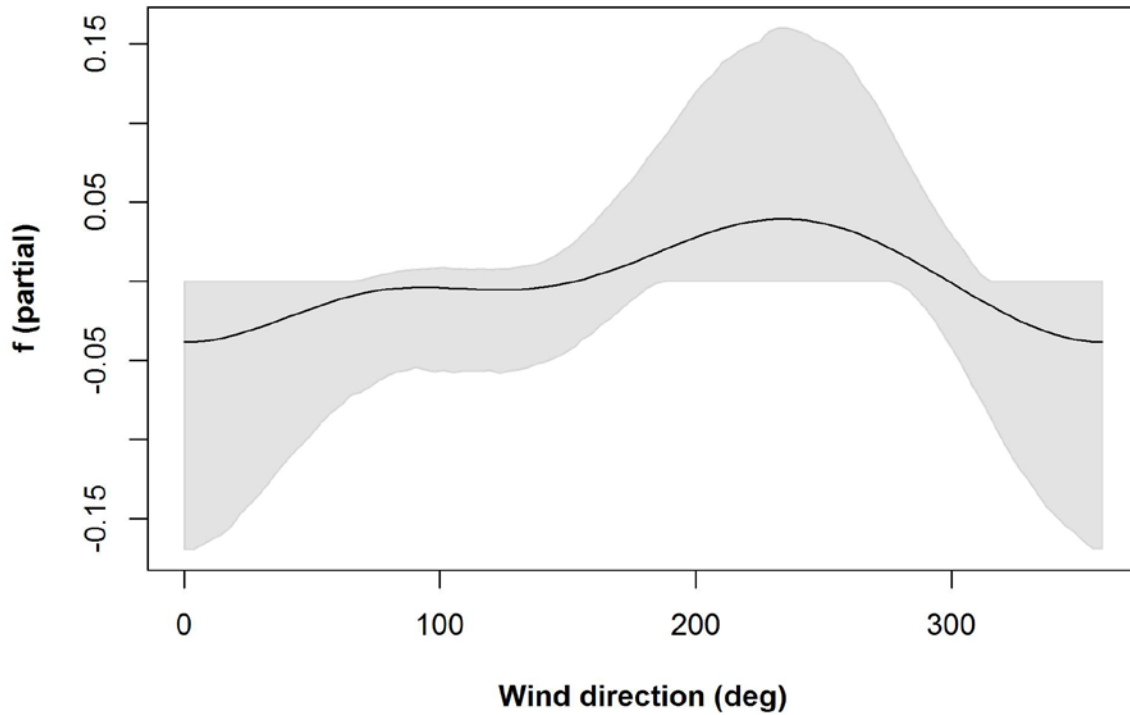


Figure 32. Boosted GAM prediction for the partial contribution of the wind direction covariate (x-axis) to the likelihood (log-transformed odds ratio) of exposure to Federal waters among Roseate Terns (y-axis) in 2015, 2016, and 2017 (pooled).
The gray-shaded area represents the 95% confidence interval for the response based on 1000 bootstrapped models.

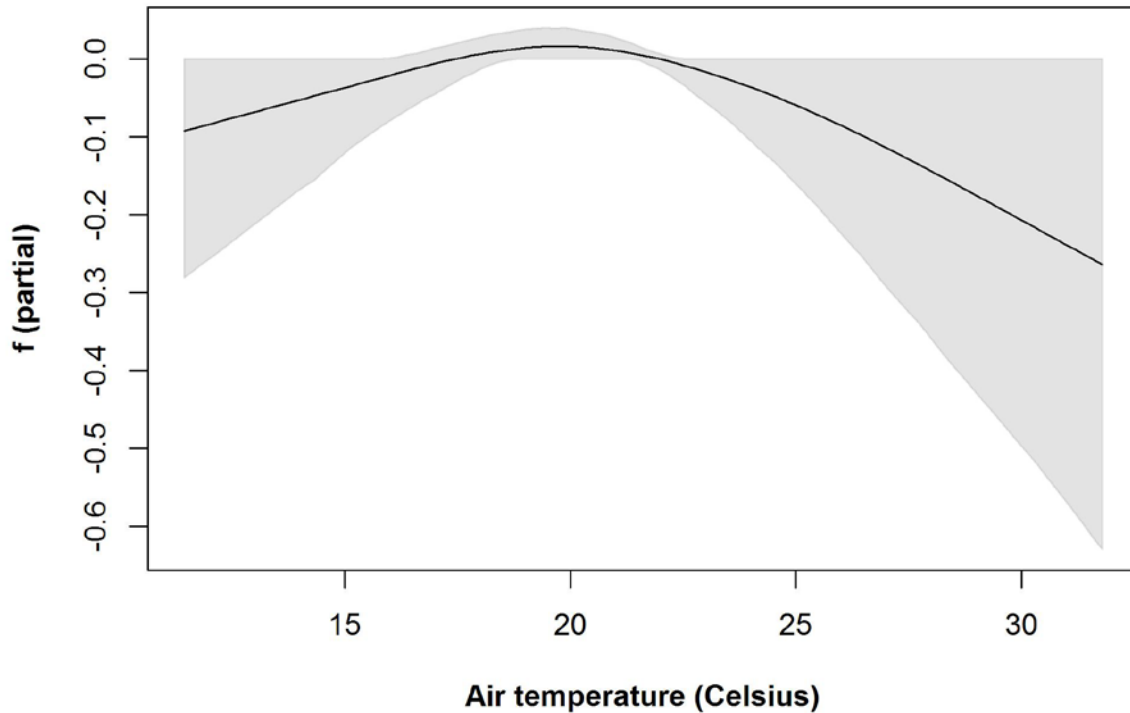


Figure 33. Boosted GAM prediction for the partial contribution of the air temperature covariate (x-axis) to the likelihood (log-transformed odds ratio) of exposure to Federal waters among Roseate Terns (y-axis) in 2015, 2016, and 2017 (pooled).

The gray-shaded area represents the 95% confidence interval for the response based on 1000 bootstrapped models.

3.1.5 Estimated Exposure to Wind Energy Areas

3.1.5.1 Common Terns

Of the 257 Common Terns detected by the array from 2014 to 2017, 12% (n=30) had estimated exposure to BOEM WEAs within the Study Area (Table 9, Fig. 31). The highest number of estimated exposure events at BOEM WEAs occurred in 2014 by Common Terns from Great Gull Island (50%, n=15 of 30). Overall, the estimated number of exposure events were higher for females (77%, n=23) versus males (23%, n=7).

Among BOEM Lease Areas, highest number of estimated exposure events by Common Terns (73%, n=22 of 30), occurred at OCS-A 0486 in Rhode Island Sound, predominantly from terns from the Great

Gull Island colony (Table 10). Additional exposure was estimated at the New York Lease Area (6%, n=2 of 30) and Virginia Lease Area (3%, n=1 of 30). Among BOEM planning areas, the highest number of exposure events by Common Terns (10%, n=3 of 30) occurred at New York Bight Call Area (Table 11).

Table 9. Number of adult Common Terns tagged at nesting colonies in MA (Monomoy NWR, Buzzards Bay) and NY (Great Gull Island) with estimated exposure to BOEM Wind Energy Areas, 2014-2017. Sample size (N) of individuals tracked per year appears in top row.

	2014 (N=115)	2015 (N=31)	2016 (N=59)	2017 (N=52)	Total (N=257)
Monomoy NWR, MA	0	---	---	---	0
Buzzards Bay, MA	---	---	3	5	8
Great Gull Island, NY	15	3	3	1	22
Total	15	3	6	6	30

Table 10. The number of estimated exposure events by Common Terns at BOEM Lease Areas within the Study Area during breeding and post-breeding dispersal 2014-2017. Sample size (N) of individuals tracked from each tagging location appears in top row.

BOEM Lease Number	BOEM Lease Area Name	MNY (N=65)	GGI (N=139)	Buzz Bay (N=53)	Total (N=257)
OCS-A 0486	Rhode Island/Massachusetts Lease Area – North	0	19	3	22
OCS-A 0487	Rhode Island/Massachusetts Lease Area - South	0	0	0	0
OCS-A 0500	Massachusetts Lease Area	0	0	0	0
OCS-A 0501	Massachusetts Lease Area	0	0	0	0
OCS-A 0512	New York Lease Area	0	1	1	2
OCS-A 0499	New Jersey Lease Area - North	0	0	0	0
OCS-A 0498	New Jersey Lease Area - South	0	0	0	0
OCS-A 0482	Delaware Lease Area - GSOE	0	0	0	0
OCS-A 0519	Delaware Lease Area - Skipjack	0	0	0	0
OCS-A 0490	Maryland Lease Area	0	0	0	0
OCS-A 0483	Virginia Lease Area	0	0	1	1
OCS-A 0497	Virginia Research Lease	0	0	0	0
	Total	0	20	5	25

Table 11. The number of estimated exposure events by Common Terns at BOEM Planning Areas within the Study Area during breeding and post-breeding dispersal 2014-2017. Sample size (N) of individuals tracked from each tagging location appears in top row.

BOEM Planning Area Name	MNY (N=65)	GGI (N=139)	Buzz Bay (N=53)	Total (N=257)
Massachusetts PSN	0	0	0	0
New York Bight Call Area	0	1	2	3
New York Proposed Commercial Lease	0	0	0	0
Total	0	1	2	3

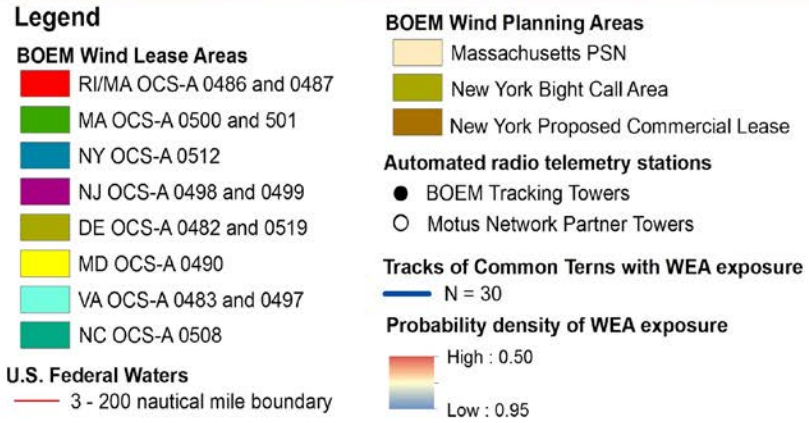
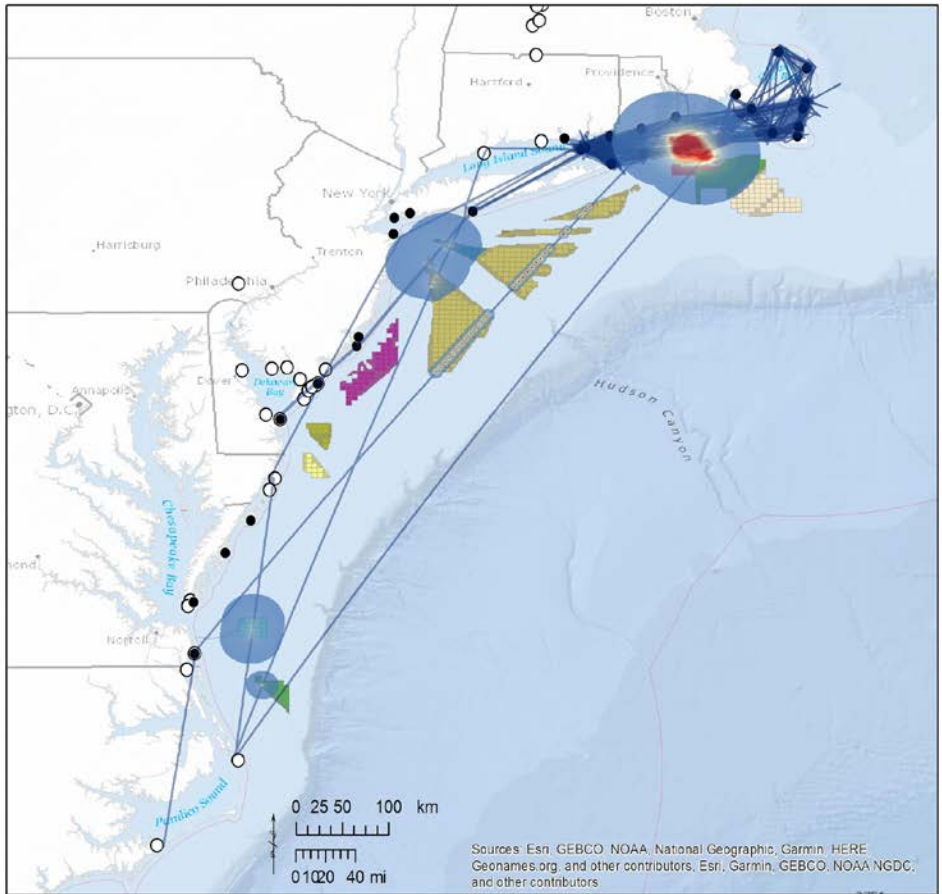


Figure 34. Movement tracks and composite probability density across WEAs of Common Terns (n=30) with estimated exposure to WEAs, 2016 and 2017.

Estimated exposure of Common Terns to WEAs occurred from July 1 through September 20, with peak exposure in late July (Fig. 35). Estimated WEA exposure events by Common Terns from Great Gull Island primarily occurred during the day (70%, n=16) versus night (30%, n=7), with peak exposure near sunrise (5:00 to 6:00 hrs EST; Fig. 36). Common Terns from Buzzards Bay had slightly higher estimated exposure at night (56%, n=5), versus day (44%, n=4), with peak exposure between 22:00 hrs to 23:00 hrs EST (Fig. 37). Estimated WEA exposure occurred during northeast or southwest winds (Fig. 38) with a mean speed of 5.27 m/s (Fig. 39) and positive wind-support (mean 1.99 m/s, Fig. 40). Flights across WEAs generally occurred during favorable weather conditions, with high visibility (mean 17,810 m; Fig. 41), little to no precipitation (mean 0.06 kg/m²; Fig. 42), mild air temperatures (mean 21.70° C; Fig. 43), and high atmospheric pressure (mean 101,450 Pa, Fig. 44). However, there was some evidence of estimated WEA exposure during inclement weather, including low visibility (< 500 m), precipitation (1.03 kg/m²), and high winds (14.43 m/s; Table 12).

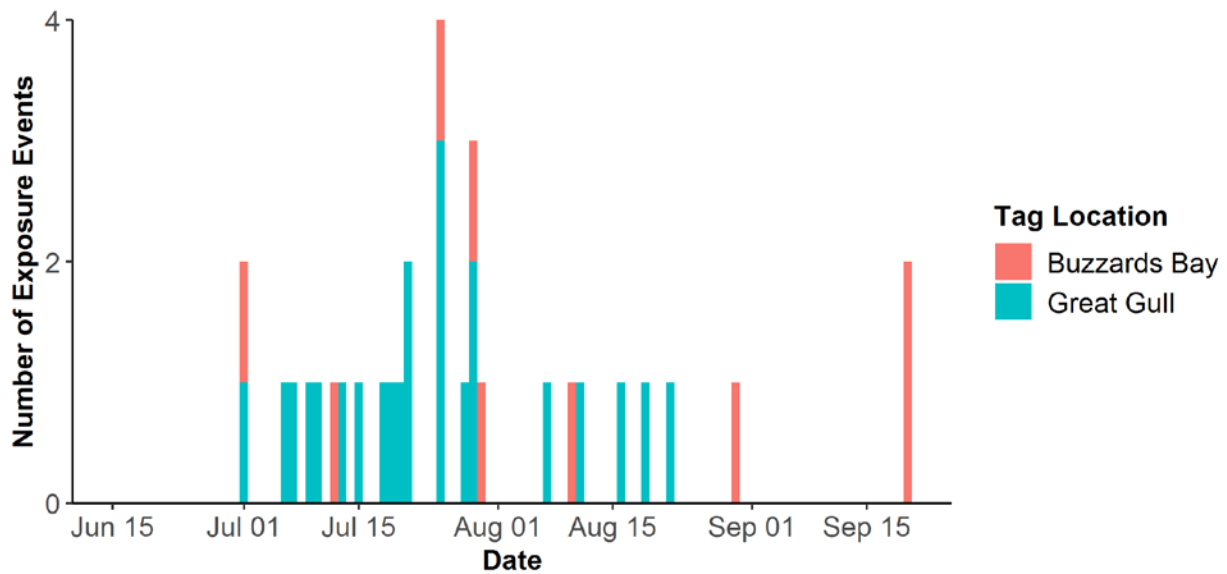


Figure 35. Frequency distribution of WEA exposure events (n=30) by date for Common Terns from 2015 to 2017 (pooled) by location of tag deployment.

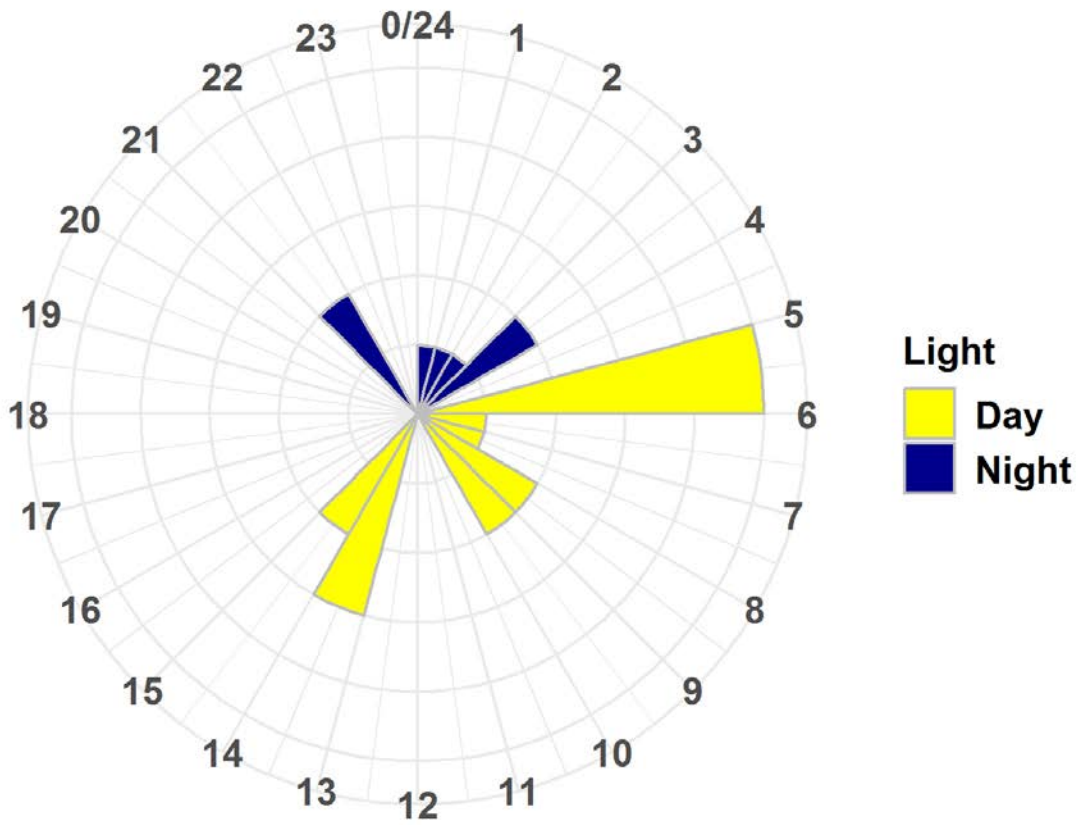


Figure 36. Diel variation (hrs, in EST) in timing of WEA exposure events (n=22) of Common Terns tagged on Great Gull Island, NY, categorized by daylight using timing of local sunrise and sunset.

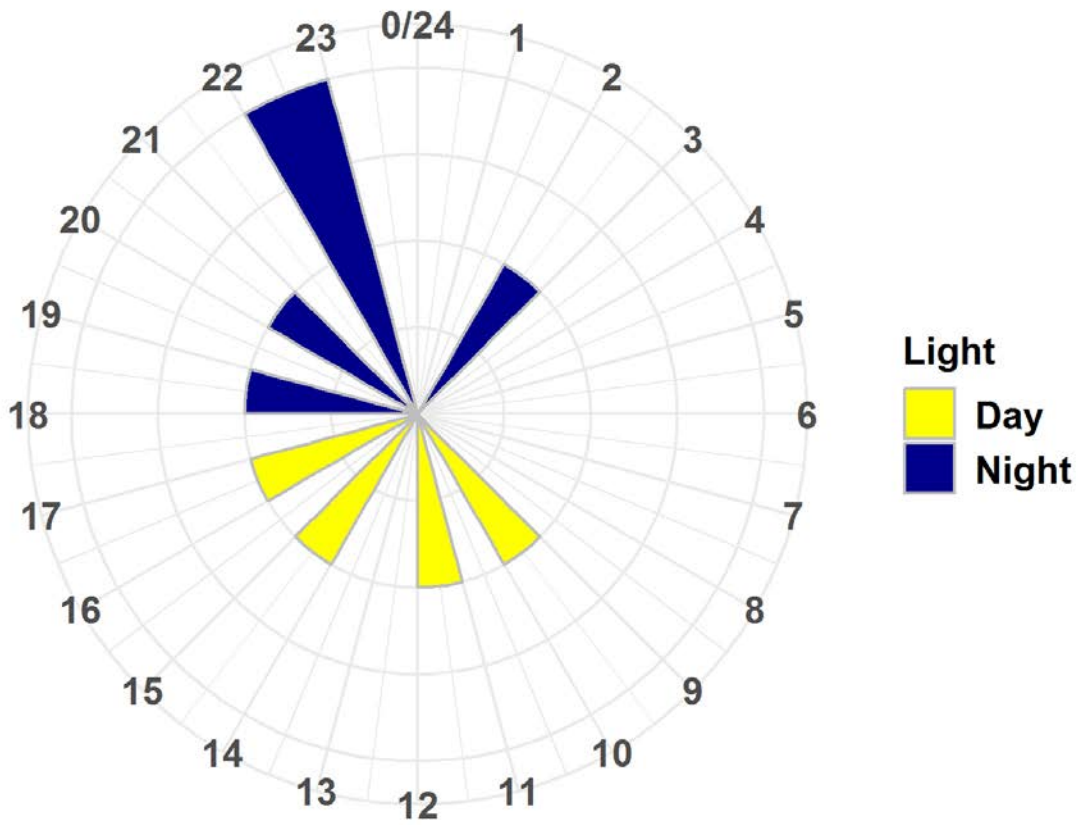


Figure 37. Diel variation (hrs, in EST) in timing of WEA exposure events (n=8) of Common Terns tagged in Buzzards Bay, MA, categorized by daylight using timing of local sunrise and sunset.

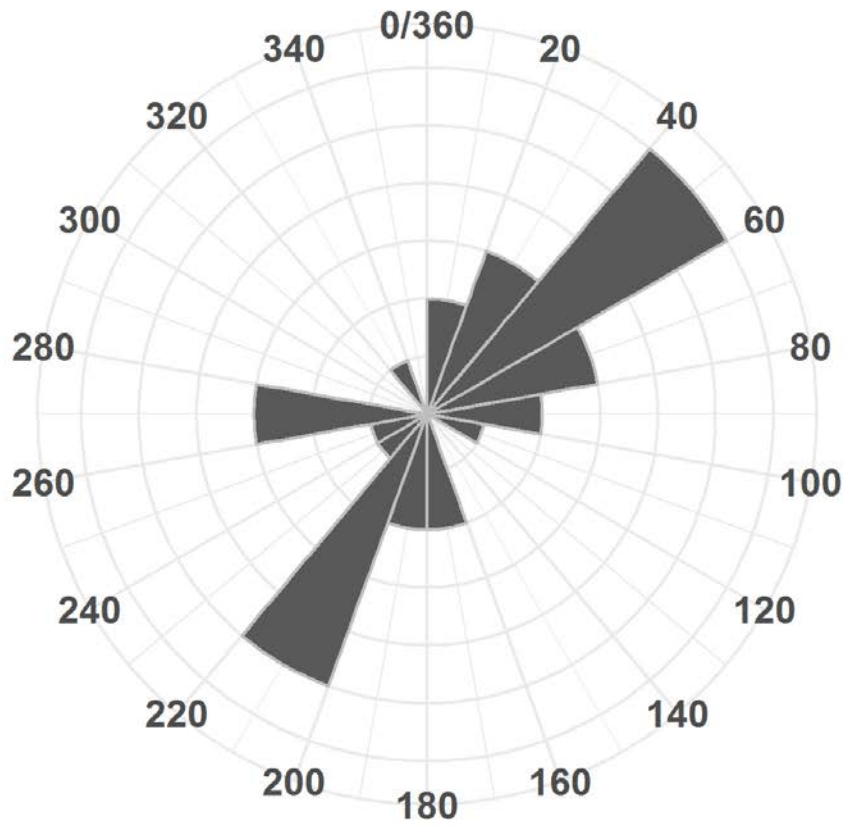


Figure 38. Circular histogram of wind direction (degrees clockwise from N) during WEA exposure events (n=30) of Common Terns from 2015 to 2017.

Table 12. Summary statistics of meteorological conditions during WEA exposure events (n=30) of Common Terns from 2015 to 2017.

	Mean	SD	Min	Max
Wind speed	5.27	3.64	0.63	14.43
Wind support (m/s)	1.99	5.18	-4.95	14.14
Visibility (m)	17,810	4550	285	20,843
Precipitation (kg/m ²)	0.06	0.20	0.00	1.03
Air temperature (C)	21.70	1.98	16.81	25.28
Pressure (Pa)	101,450	528	100,303	102,504

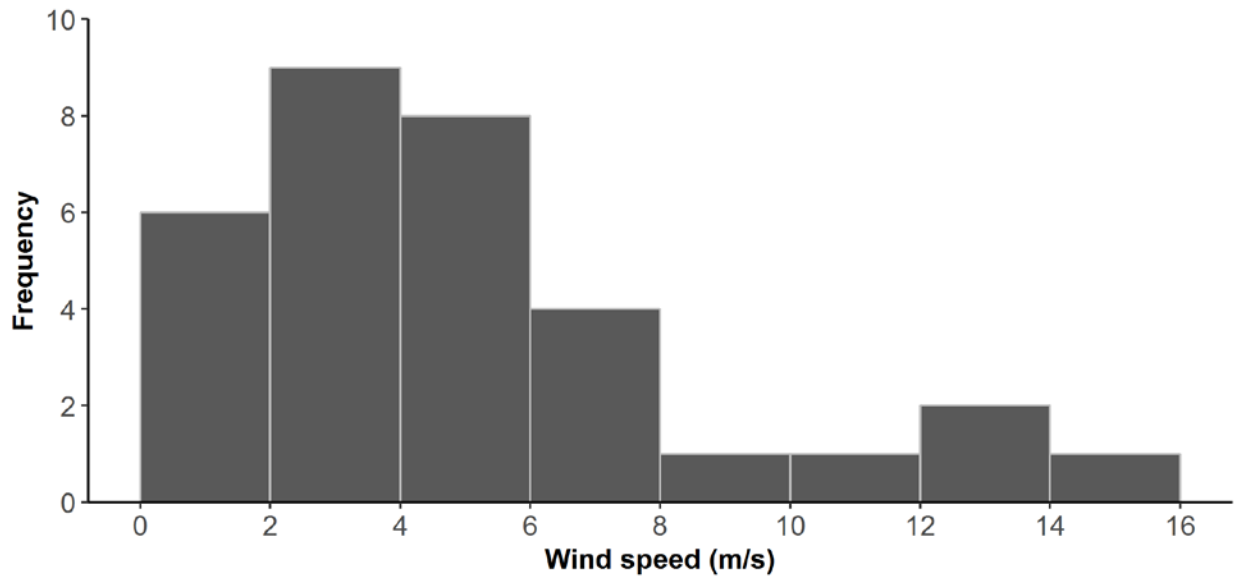


Figure 39. Frequency distribution of wind speed (m/s) during WEA exposure events (n=30) of Common Terns from 2015 to 2017.

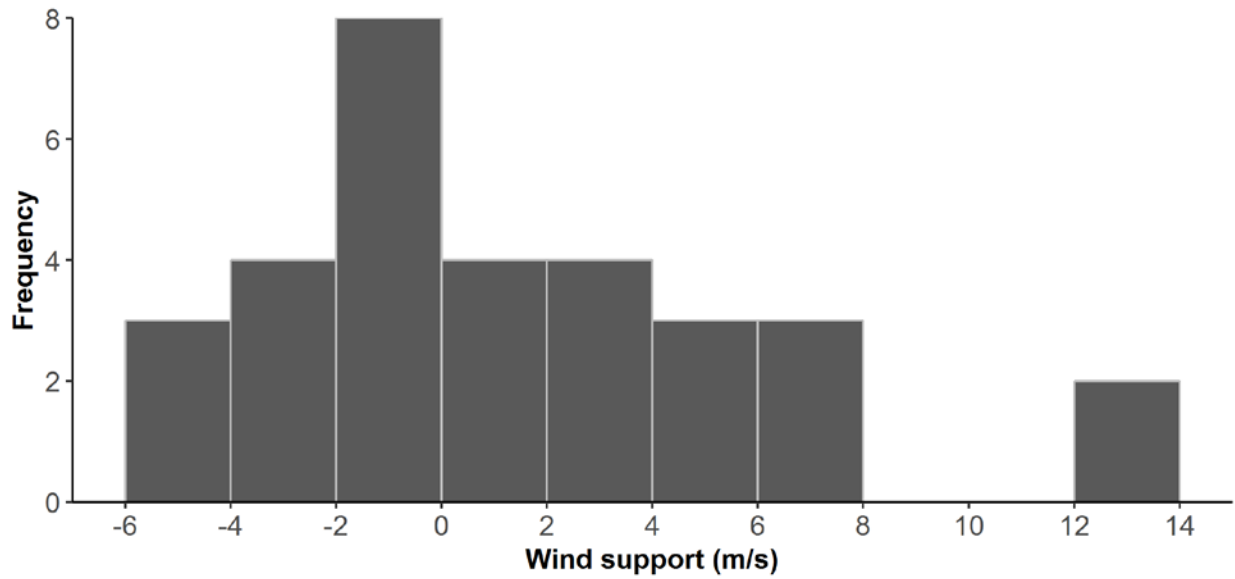


Figure 40. Frequency distribution of wind support (m/s) during WEA exposure events (n=30) of Common Terns from 2015 to 2017.

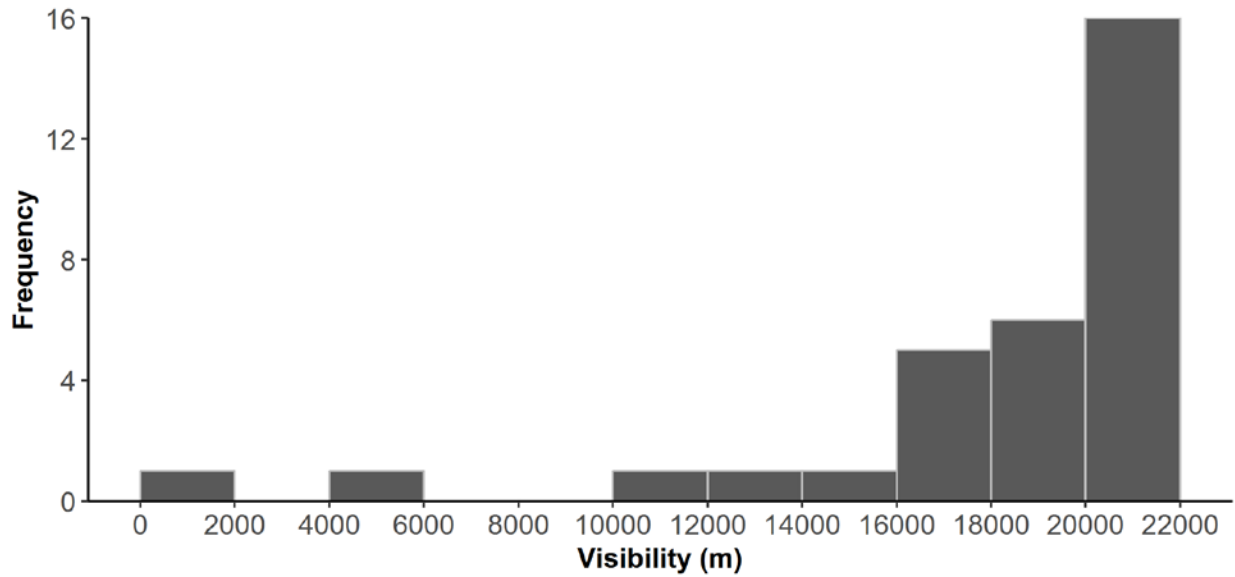


Figure 41. Frequency distribution of visibility (m) during WEA exposure events (n=30) of Common Terns from 2015 to 2017.

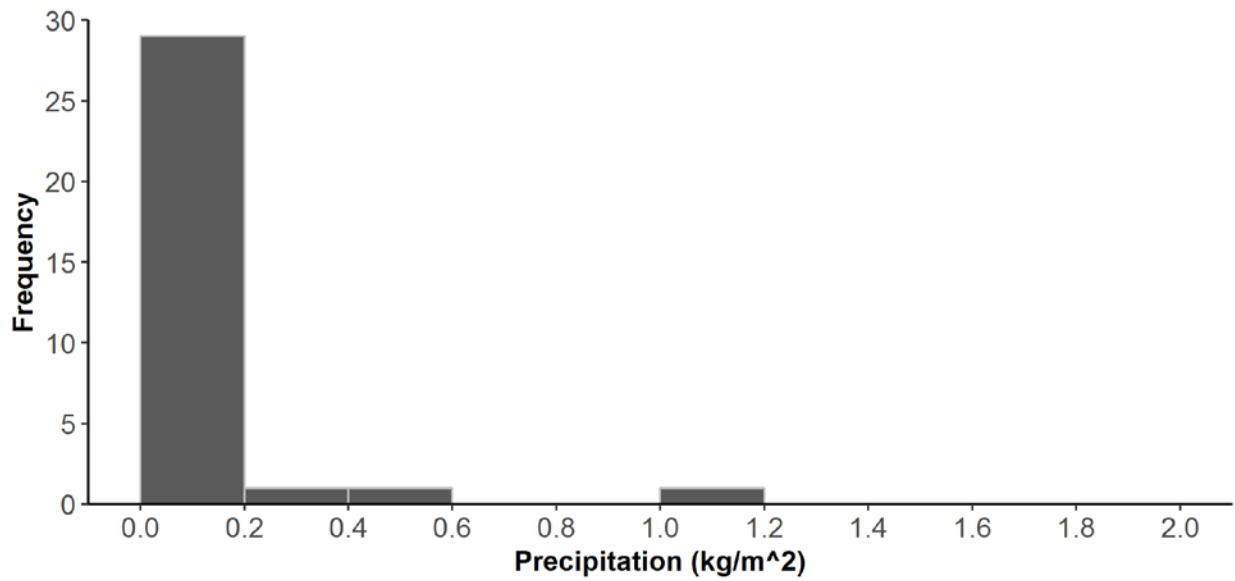


Figure 42. Frequency distribution of precipitation accumulation (kg/m²) during of WEA exposure events (n=30) of Common Terns from 2015 to 2017.

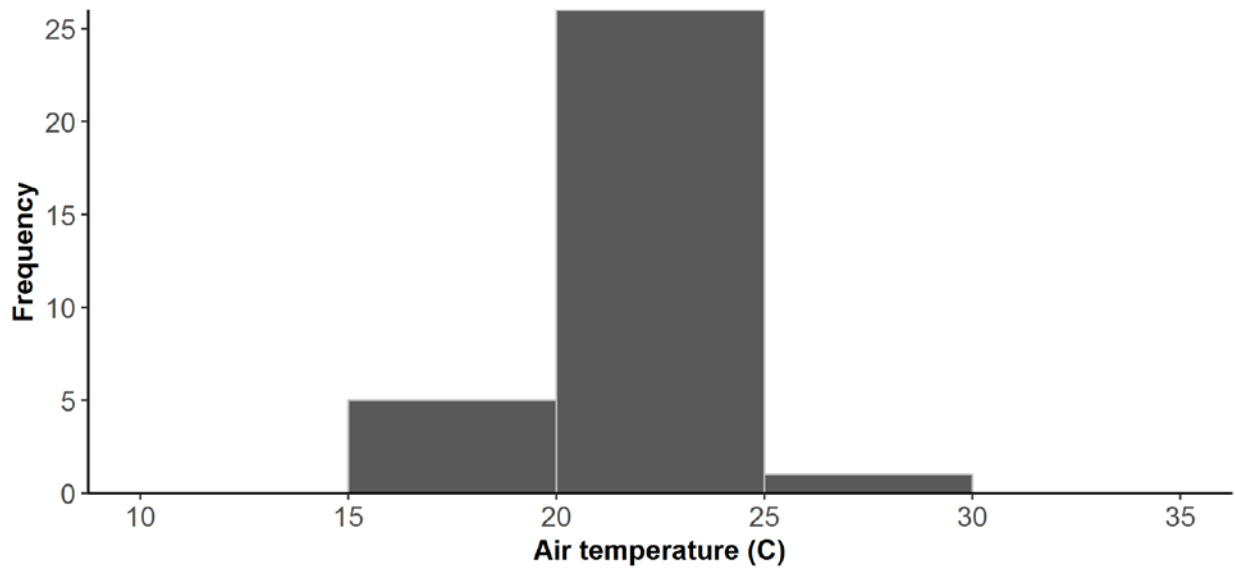


Figure 43. Frequency distribution of precipitation air temperature (°C) during of WEA exposure events (n=30) of Common Terns from 2015 to 2017.

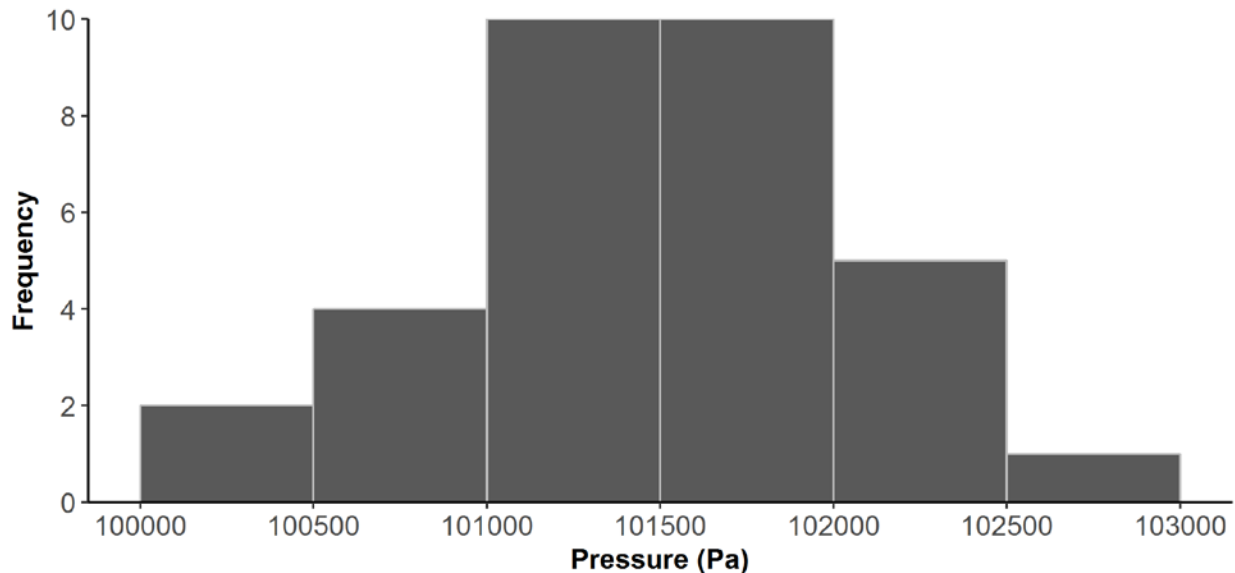


Figure 44. Frequency distribution of barometric pressure (Pa) during of WEA exposure events (n=30) of Common Terns from 2015 to 2017.

3.1.5.2 Roseate Terns

Of the 145 Roseate Terns detected by the array from 2015 to 2017, 6% (n=8) had estimated exposure to BOEM WEAs within the Study Area (Table 13, Fig. 45). The highest number of estimated exposure events at BOEM WEAs for Roseate Terns occurred in 2016 by individuals from Great Gull Island (75%, n=6 of 8). Similar to Common Terns, the estimated number of exposure events were higher for females (75%, n=6 of 8) versus males (25%, n=2 of 8). All estimated exposure events by Roseate Terns (n=8), occurred at OCS-A 0486 in Rhode Island Sound (Table 14), which also had the highest number of estimated exposure events by Common Terns. There were no estimated exposure events of Roseate Terns within BOEM Planning Areas (Table 15).

Table 13. Number of adult Roseate Terns tagged at nesting colonies in MA (Buzzards Bay) and NY (Great Gull Island) with estimated exposure to Wind Energy Areas, 2015-2017. Sample size (N) of individuals tracked per year appears in top row.

	2015 (N=30)	2016 (N=60)	2017 (N=55)	Total (N=145)
Buzzards Bay, MA	---	1	1	2
Great Gull Island, NY	0	6	0	6
Total	0	7	1	8

Table 14. The number of estimated exposure events by Roseate Terns at BOEM Lease Areas within the Study Area during breeding and post-breeding dispersal 2015-2017. Sample size (N) of individuals tracked from each tagging location appears in top row.

BOEM Lease Number	BOEM Lease Area Name	GGI (N=55)	Buzz Bay (N=90)	Total (N=145)
OCS-A 0486	Rhode Island/Massachusetts Lease Area – North	6	2	8
OCS-A 0487	Rhode Island/Massachusetts Lease Area - South	0	0	0
OCS-A 0500	Massachusetts Lease Area	0	0	0
OCS-A 0501	Massachusetts Lease Area	0	0	0
OCS-A 0512	New York Lease Area	0	0	0
OCS-A 0499	New Jersey Lease Area - North	0	0	0
OCS-A 0498	New Jersey Lease Area - South	0	0	0
OCS-A 0482	Delaware Lease Area - GSOE	0	0	0
OCS-A 0519	Delaware Lease Area - Skipjack	0	0	0
OCS-A 0490	Maryland Lease Area	0	0	0
OCS-A 0483	Virginia Lease Area	0	0	0
OCS-A 0497	Virginia Research Lease	0	0	0
	Total	6	2	8

Table 15. The number of estimated exposure events by Roseate Terns at BOEM Planning Areas within the Study Area during breeding and post-breeding dispersal 2015-2017. Sample size (N) of individuals tracked from each tagging location appears in top row.

BOEM Planning Area Name	GGI (N=55)	Buzz Bay (N=90)	Total (N=145)
Massachusetts PSN	0	0	0
New York Bight Call Area	0	0	0
New York Proposed Commercial Lease	0	0	0
Total	0	0	0

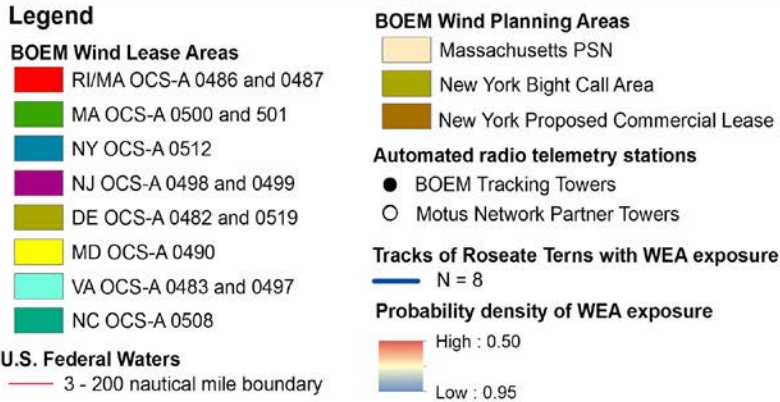
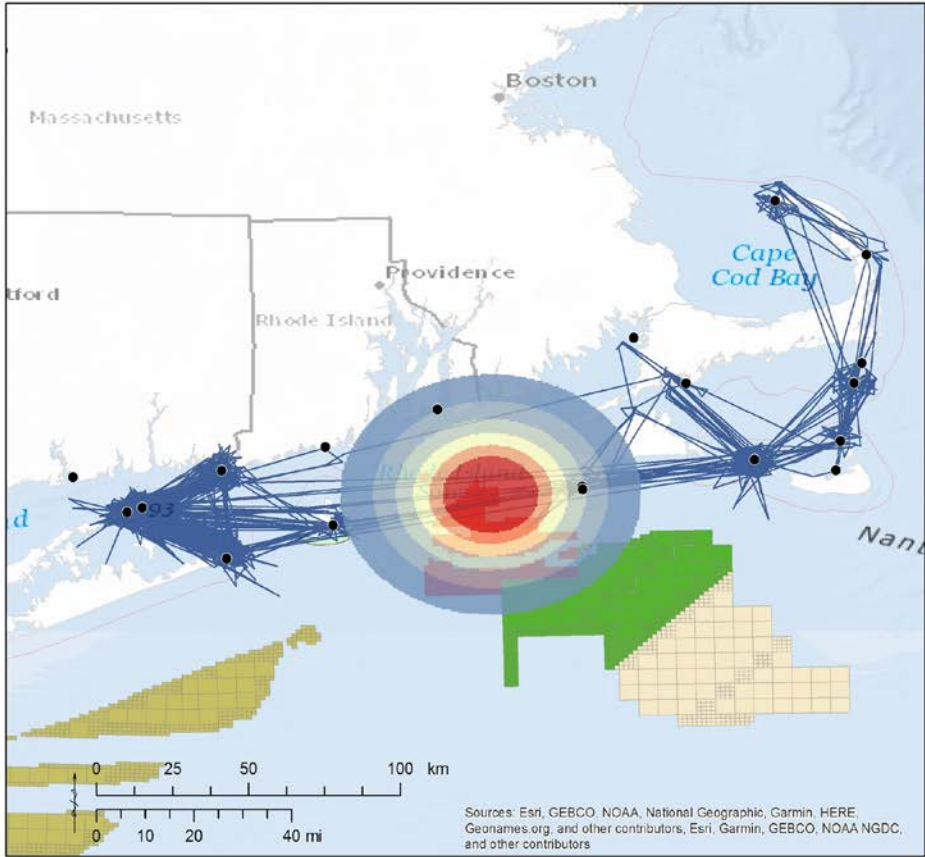


Figure 45. Movement tracks and composite probability density across WEAs of Roseate Terns (n=8), with estimated exposure to WEAs, 2016 and 2017.

Estimated exposure of Roseate Terns to WEAs occurred from June 27 through August 13, with peak exposure during late July and early August (Fig. 46). Most (88%, n=7) of the estimated WEA exposure events by Roseate Terns were diurnal (Fig. 47).

Estimated WEA exposure occurred during northeast winds (Fig. 48) with a mean speed of 5.28 m/s (Fig. 49) and slightly positive wind-support (mean 0.25 m/s, Fig. 50). As with Common Terns, flights across WEAs generally occurred during favorable weather conditions, with high visibility (mean 15,608 m; Fig. 51), no precipitation (mean <0.01 kg/m²; Fig. 52), mild air temperatures (mean 22.81° C; Fig. 53), and high atmospheric pressure (mean 101,629 Pa, Fig. 54). However, there was some evidence of estimated WEA exposure during low visibility conditions (< 500 m; Fig. 51 and Table 16).

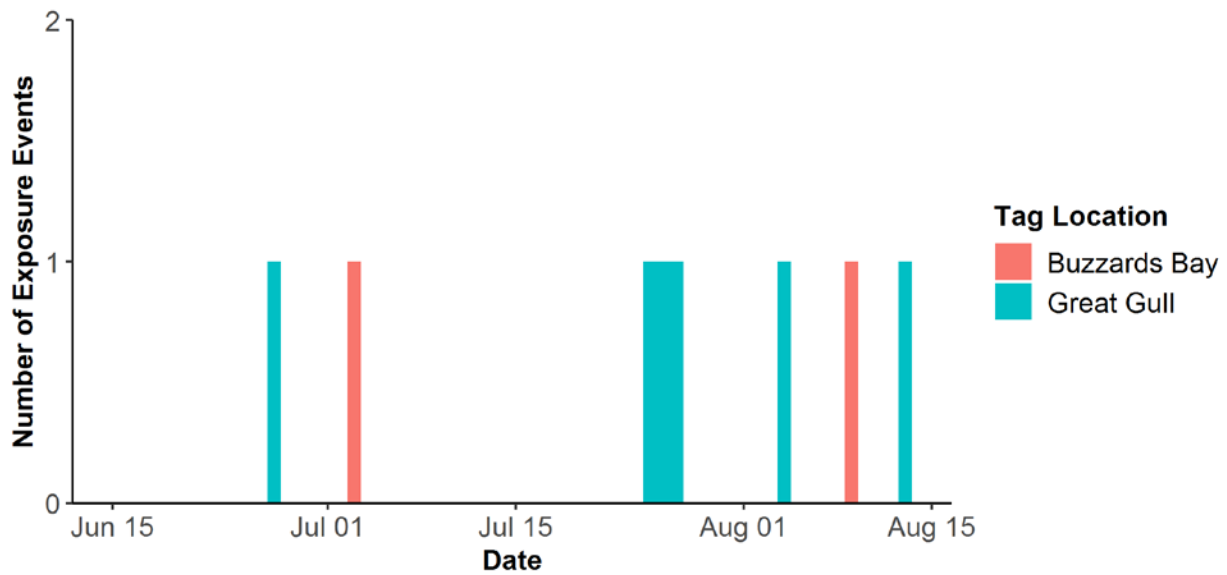


Figure 46. Frequency distribution in calendar date of WEA exposure events (n=8) of Roseate Terns in 2016 and 2017 (pooled) by location of tag deployment.

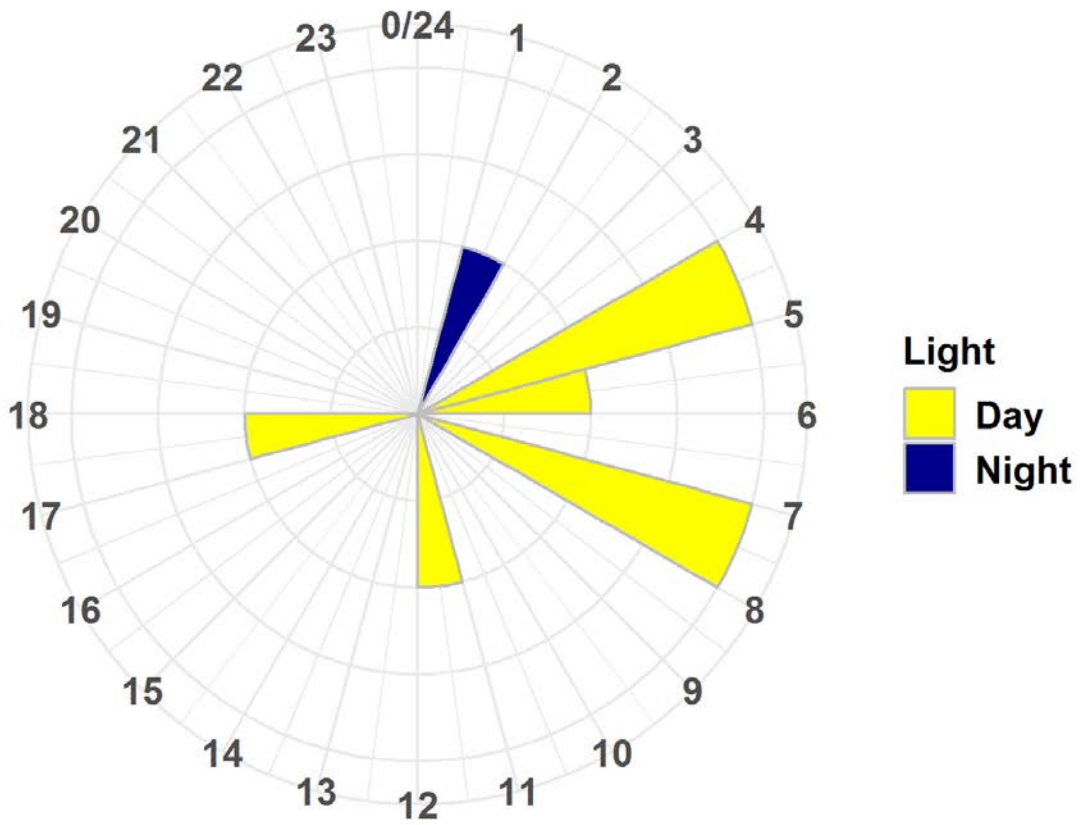


Figure 47. Diel variation (hrs, in EST) in timing of WEA exposure events (n=8) of Roseate Terns, categorized by daylight using timing of local sunrise and sunset.

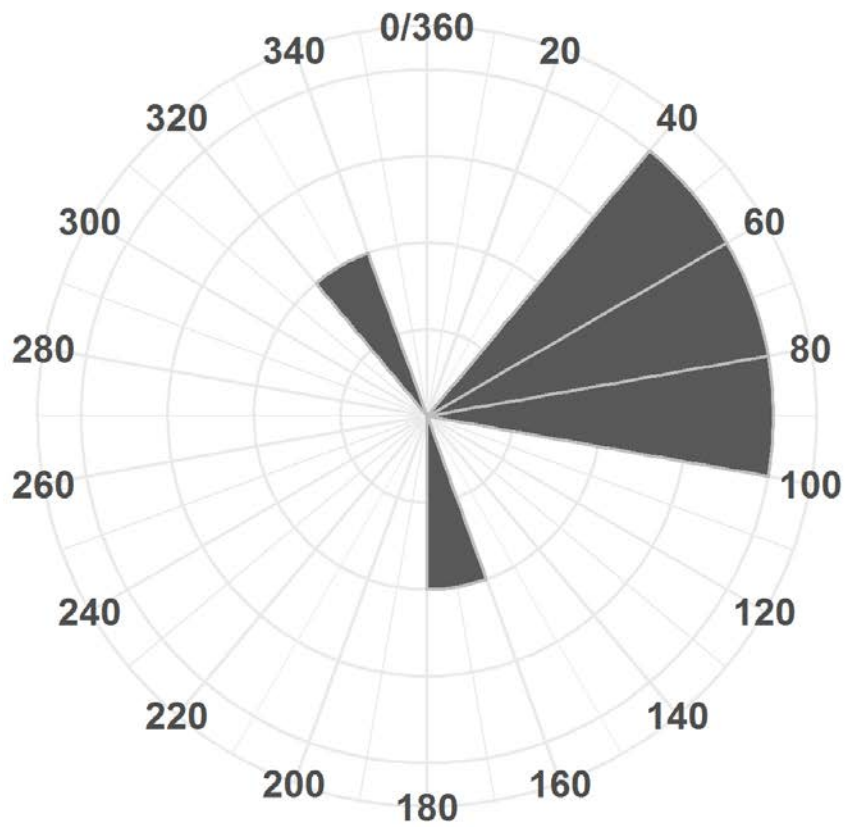


Figure 48. Circular histogram of wind direction (degrees clockwise from N) during WEA exposure events (n=8) of Roseate Terns in 2016 and 2017.

Table 16. Summary statistics of meteorological conditions during WEA exposure events (n=8) of Roseate Terns from 2016 to 2017.

	Mean	SD	Min	Max
Wind speed	5.28	2.03	2.65	8.03
Wind support (m/s)	0.25	5.03	-7.03	6.18
Visibility (m)	15,608	7,186	441	20,016
Precipitation (kg/m ²)	<0.01	<0.01	0.00	<0.01
Air temperature (C)	22.81	1.82	20.10	25.37
Pressure (Pa)	101,629	417	100,986	102,211

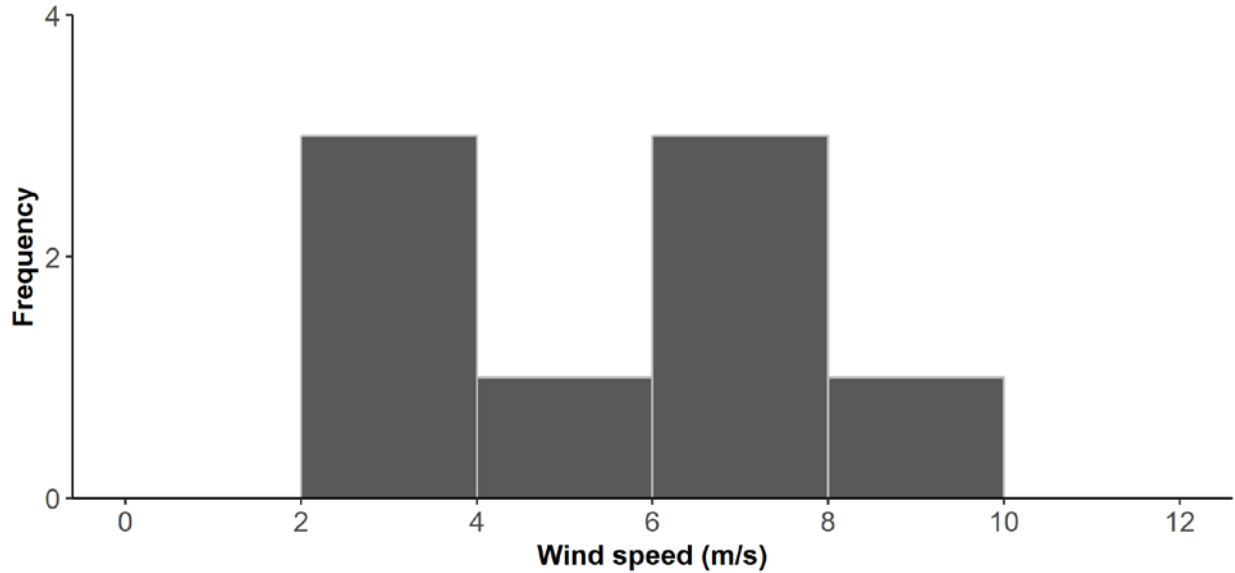


Figure 49. Frequency distribution of wind speed (m/s) during WEA exposure events (n=8) of Roseate Terns in 2016 and 2017.

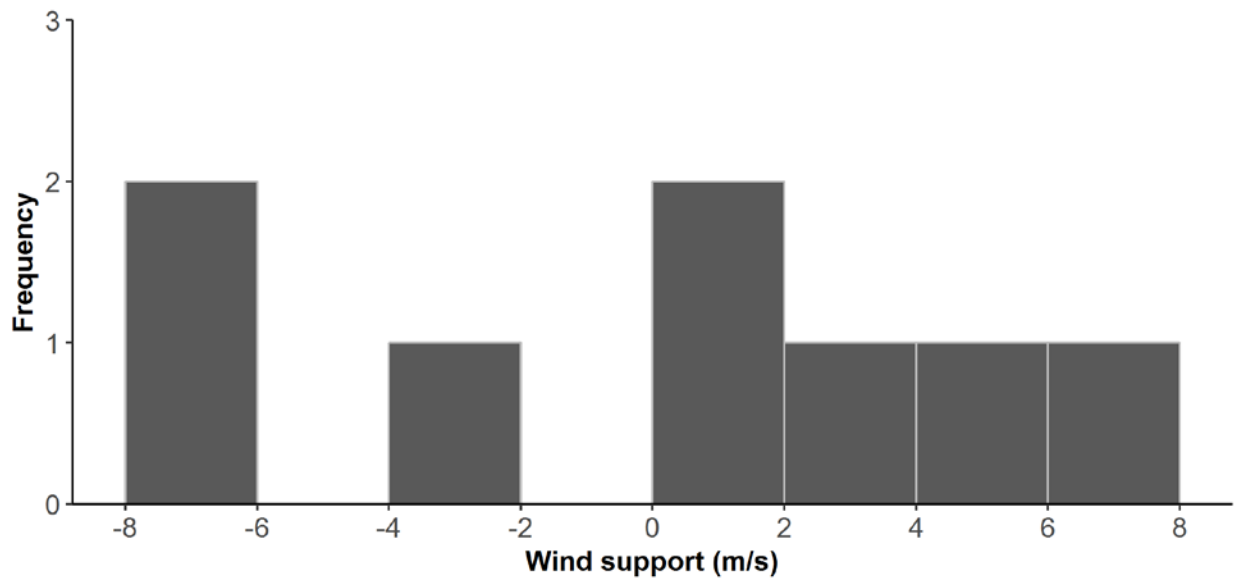


Figure 50. Frequency distribution of wind support (m/s) during WEA exposure events (n=8) of Roseate Terns in 2016 and 2017.

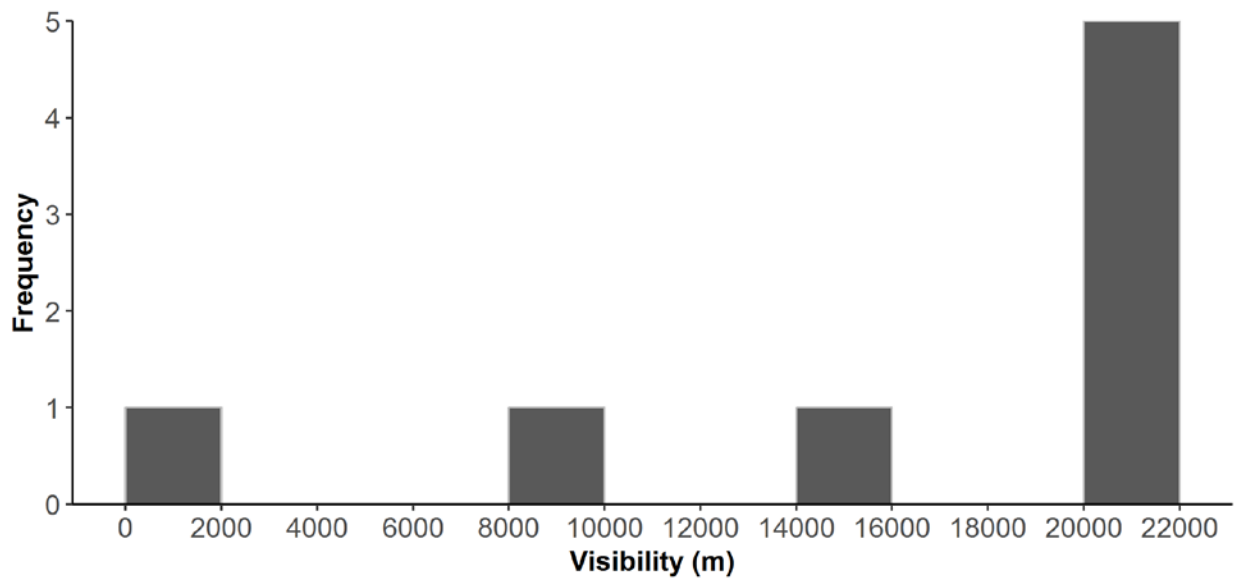


Figure 51. Frequency distribution of visibility (m) during WEA exposure events (n=8) of Roseate Terns in 2016 and 2017.

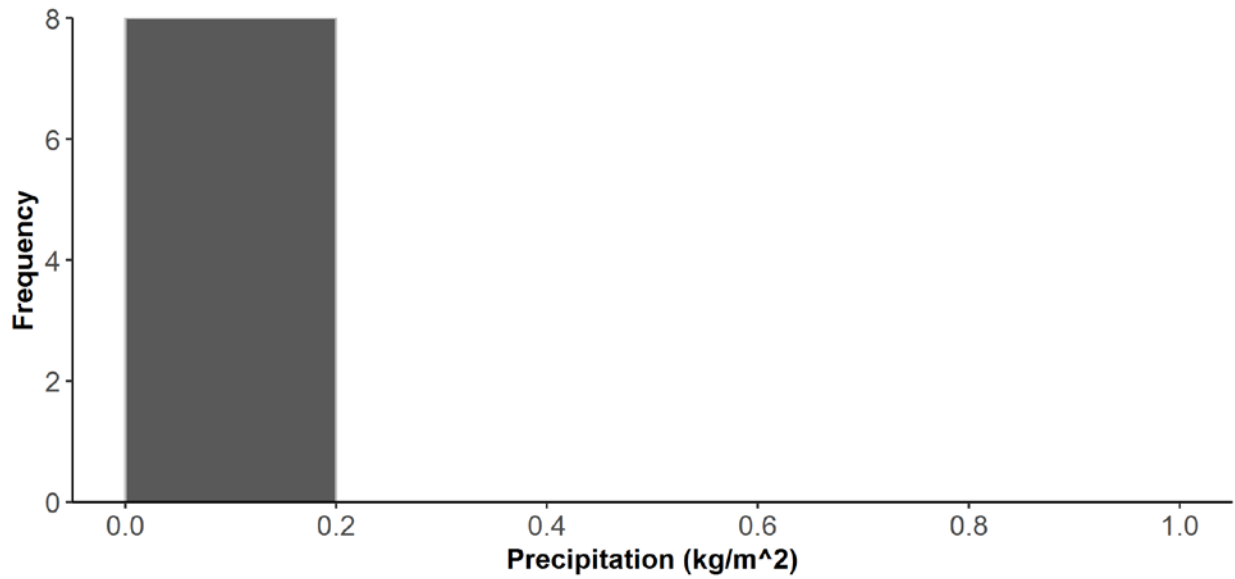


Figure 52. Frequency distribution of precipitation accumulation (kg/m²) during of WEA exposure events (n=8) of Roseate Terns in 2016 and 2017.

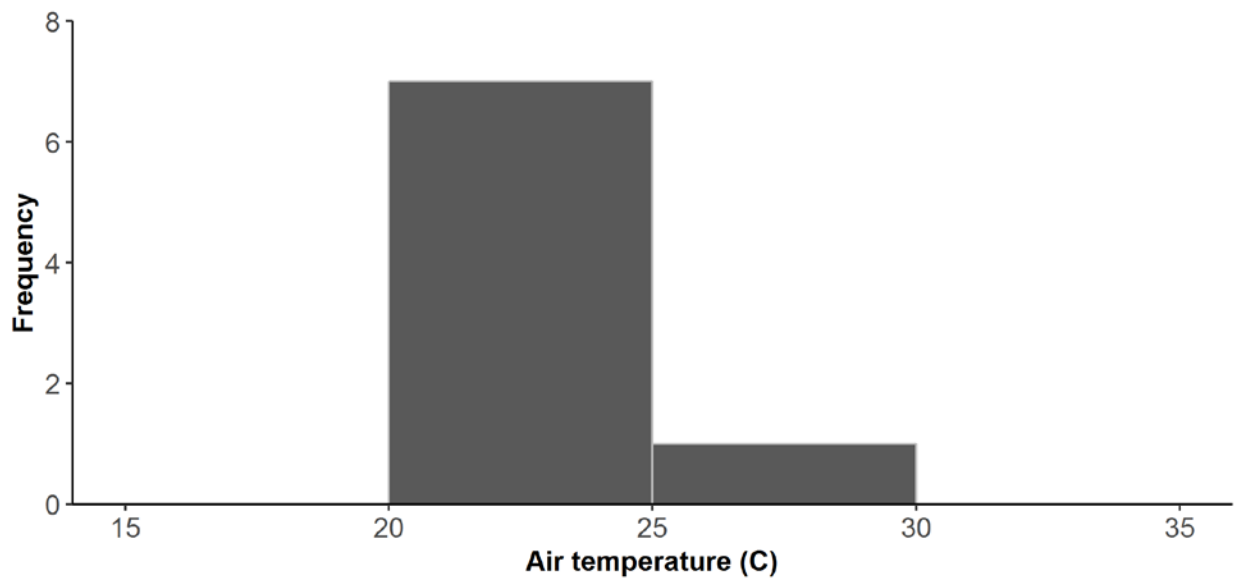


Figure 53. Frequency distribution of air temperature (C) during of WEA exposure events (n=8) of Roseate Terns in 2016 and 2017.

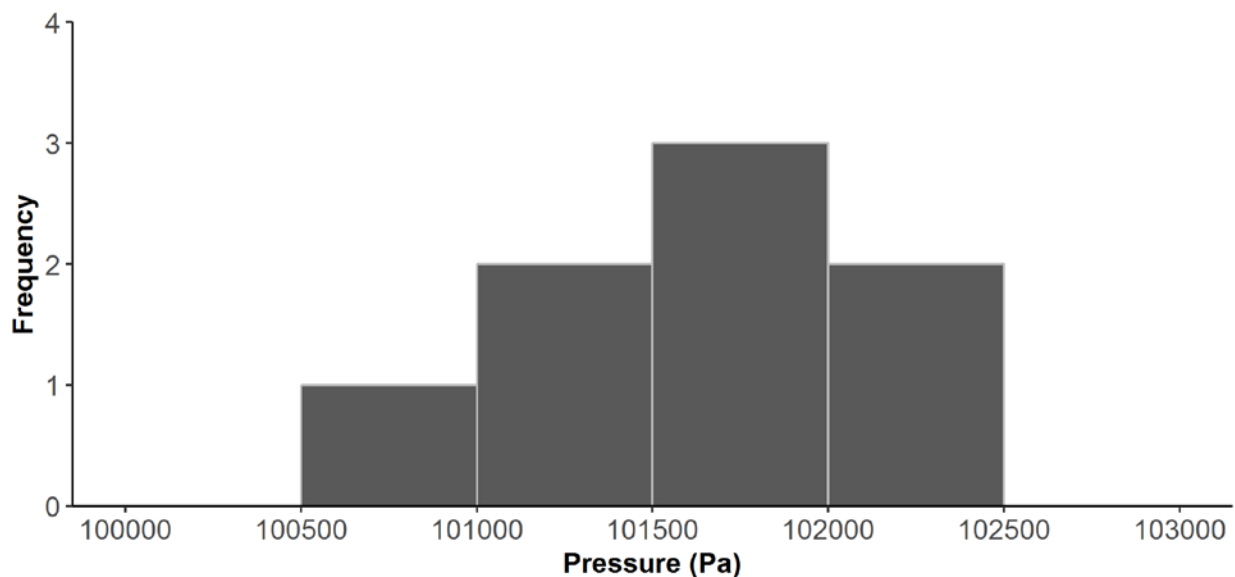


Figure 54. Frequency distribution of barometric pressure (Pa) during of WEA exposure events (n=8) of Roseate Terns in 2016 and 2017.

3.1.6 Altitude Distribution of Terns During Exposure to Federal Waters and WEAs

When in Federal waters, estimated flight altitudes of Common and Roseate terns were similar and predominantly occurred below the RSZ (25 to 250 m). Overall mean estimated altitudes were 15 m among Common Terns (Table 17, with 4.3% exposure to RSZ) and among Roseate Terns (Table 18, with 6.4% exposure to RSZ), and were similar between day and night (Figs. 55 and 56).

When exposed to WEAs, Common and Roseate terns were estimated to fly at similar altitudes as during exposure to Federal Waters generally (with typical mean differences of ~1 m in altitude), and exhibited little variability between day and night (Tables 17 and 18). Exposure to RSZ was generally less in WEAs in comparison with in Federal waters (4% among Common Terns and 0% among Roseate Terns). This may reflect the smaller sample size of exposure to WEAs, in conjunction with the infrequent exposure to RSZ overall (essentially in the tail of the altitude distribution). Estimates of exposure to the RSZ should be interpreted in the context of the model range (uncertainty) in plausible altitudes, which generally exceeded the range in estimated altitudes (Figs. 55 and 56).

Table 17. Model-estimated flight altitudes (m) of Common Terns during exposure to Federal waters and WEAs during the day and night, with sample size (number of 10-min time intervals) and frequency of estimated occurrence within the rotor-swept zone (25-250 m).

Exposure Zone	Time of Day	Mean Altitude (5-95% Range)	N (10-min intervals)	RSZ Frequency (%)
Federal waters	All	15 (11-24)	12,692	4.3
	Day	15 (11-24)	7859	3.7
	Night	15 (11-25)	4833	5.2
WEAs	All	16 (11-25)	173	4.0
	Day	15 (10-24)	112	0.9
	Night	18 (12-26)	18	9.8

Table 18. Model-estimated flight altitudes (m) of Roseate Terns during exposure to Federal waters and WEAs during the day and night, with sample size (number of 10-min time intervals) and frequency of estimated occurrence within the rotor-swept zone (25-250 m).

Exposure Zone	Time of Day	Mean Altitude (5-95% Range)	N (10-min intervals)	RSZ Frequency (%)
Federal waters	All	15 (11-26)	4272	6.4
	Day	16 (11-26)	2671	6.4
	Night	15 (11-26)	1601	6.4
WEAs	All	14 (11-20)	73	0.0
	Day	16 (11-21)	59	0.0
	Night	12 (11-13)	14	0.0

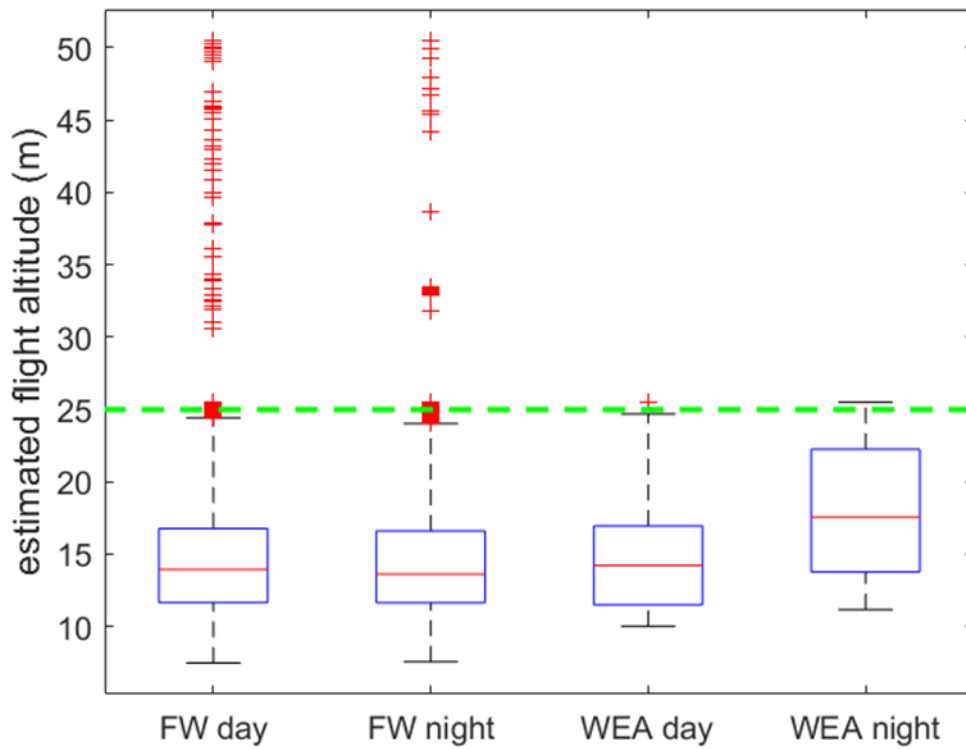


Figure 55. Model-estimated flight altitude ranges (m) of Common Terns

During exposure to Federal waters (FW) and WEAs during day and night. The green-dashed line represents the lower limit of the RSZ (25 m).

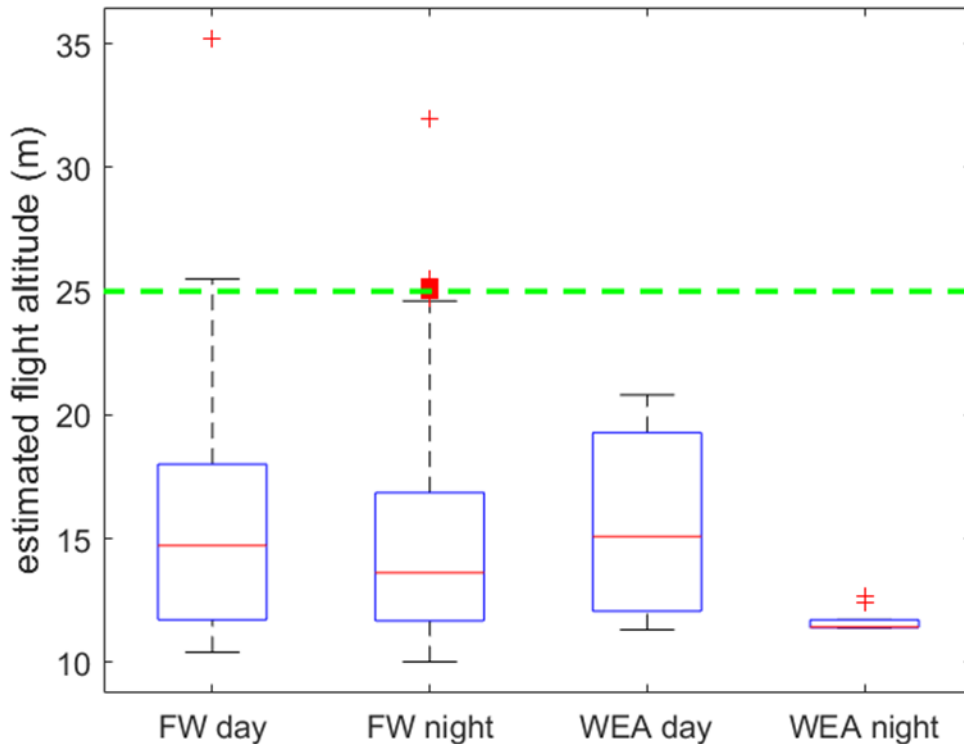


Figure 56. Model-estimated flight altitude ranges (m) of Roseate Terns

During exposure to Federal waters (FW) and WEAs during day and night. The green-dashed line represents the lower limit of the RSZ (25 m).

3.2 Piping Plovers

3.2.1 Tagging and Detection Summaries

From 2015 to 2017, we tagged 50 adult Piping Plovers each year at nesting areas in Massachusetts (n=25 per year) and Rhode Island (n=25 per year). In total, 52% (n=78 of 150) were female, 45% (n=68 of 150) were male, and the remaining 3% (n=4 of 150) were of unknown sex.

Of the 150 individuals tagged, 82% were detected by the telemetry array (range 70-88% detected per year; Table 19). Field staff observed that 25% of tagged plovers dropped their transmitters on the breeding grounds (range 16-32% of individuals with dropped tags per year; Table 19). Number of dropped transmitters was lowest in 2017, coinciding with use of the lighter (0.67 g) model of transmitter in 2017 relative to 2015 and 2016, where 1.0-g transmitters were used.

Tagged Piping Plovers were detected by the tracking array for an average of 46 days (sd 27 days, range 0-102 days; Appendix D). Due to incomplete detection probability, 47% (n=70 of 150) individuals had sufficient detection data to model migratory departure from the breeding grounds. Migratory departure events were identified by southbound departures from breeding areas tracked by two or more towers within the telemetry array.

Table 19. Tag deployment and detection summaries of adult Piping Plovers tagged at nesting areas in Massachusetts and Rhode Island, 2015-2017

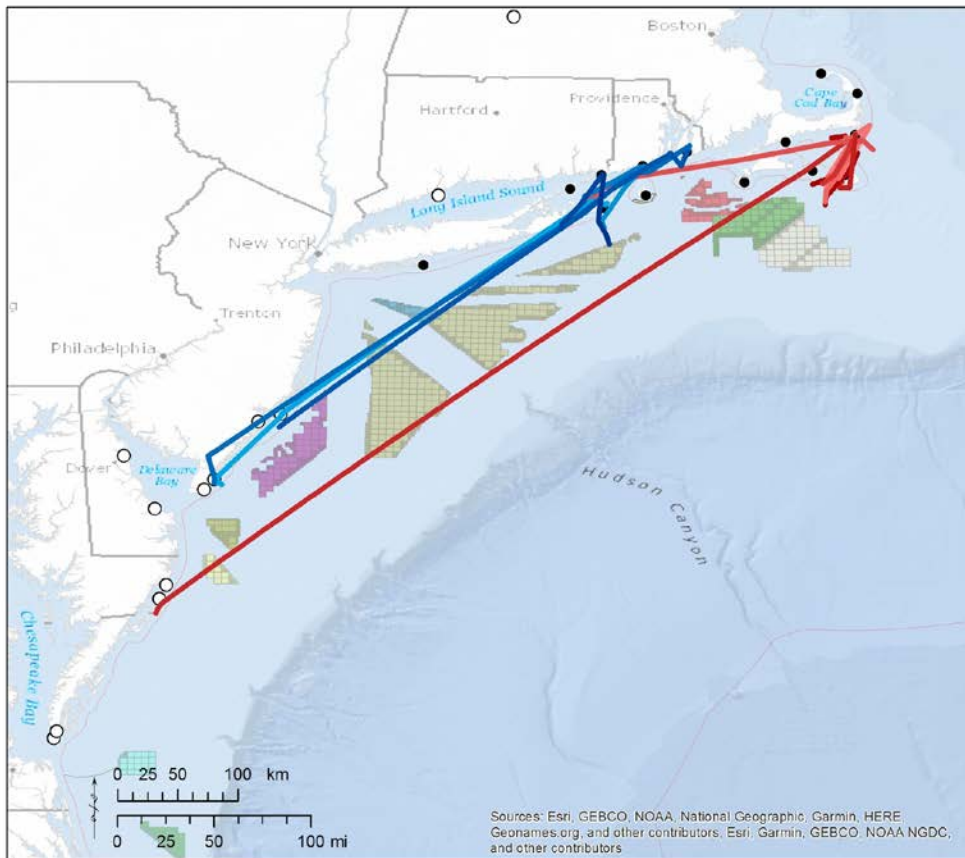
	2015	2016	2017	Total
Number of individuals tagged	50	50	50	150
Number of individuals detected	44	35	44	123
Number of dropped tags at nesting areas	16	13	8	37
Number of individuals detected during migratory departure	21	22	27	70

3.2.2 Migratory Movements in Study Area

The majority (93%) of Piping Plovers tracked during migratory departure from nesting areas in MA (n=37) departed on a south-southwest trajectory across Nantucket Sound, and the remaining 7% (n=3) departed to the west across Nantucket Sound (Fig. 57). Of the Piping Plovers that departed on a south-southwest trajectory, 68% (n=25) were last detected traveling into Federal waters south of Nantucket, due in part to limited numbers of towers in the mid-Atlantic region during 2015 (Fig. 57A). The remaining 32% were tracked along offshore routes across the mid-Atlantic Bight to coastal areas ranging from Long Island, NY to North Carolina.

All of the Piping Plovers tracked during migratory departure from nesting areas in RI (n=30) departed on a south-southwest trajectory between Block Island Sound and eastern Long Island Sound and 50% were last detected within this region. Thirty seven percent (n=11) were tracked using offshore routes across the mid-Atlantic Bight to coastal areas ranging from New Jersey to North Carolina. The remaining 13% (n=4) were tracked along a more coastal route; three were last detected in southwestern Long Island and one was tracked from southwestern Long Island, across New York Bight, and south along the coast of New Jersey to Maryland.

A.



Sources: Esri, GEBCO, NOAA, National Geographic, Garmin, HERE Geonames.org, and other contributors; Esri, Garmin, GEBCO, NOAA NGDC, and other contributors

Legend

BOEM Wind Lease Areas

- RI/MA OCS-A 0486 and 0487
- MA OCS-A 0500 and 501
- NY OCS-A 0512
- NJ OCS-A 0498 and 0499
- DE OCS-A 0482 and 0519
- MD OCS-A 0490
- VA OCS-A 0483 and 0497
- NC OCS-A 0508

U.S. Federal Waters

- 3 - 200 nautical mile boundary

BOEM Wind Planning Areas

- Massachusetts PSN
- New York Bight Call Area
- New York Proposed Commercial Lease

Block Island Wind Farm

-

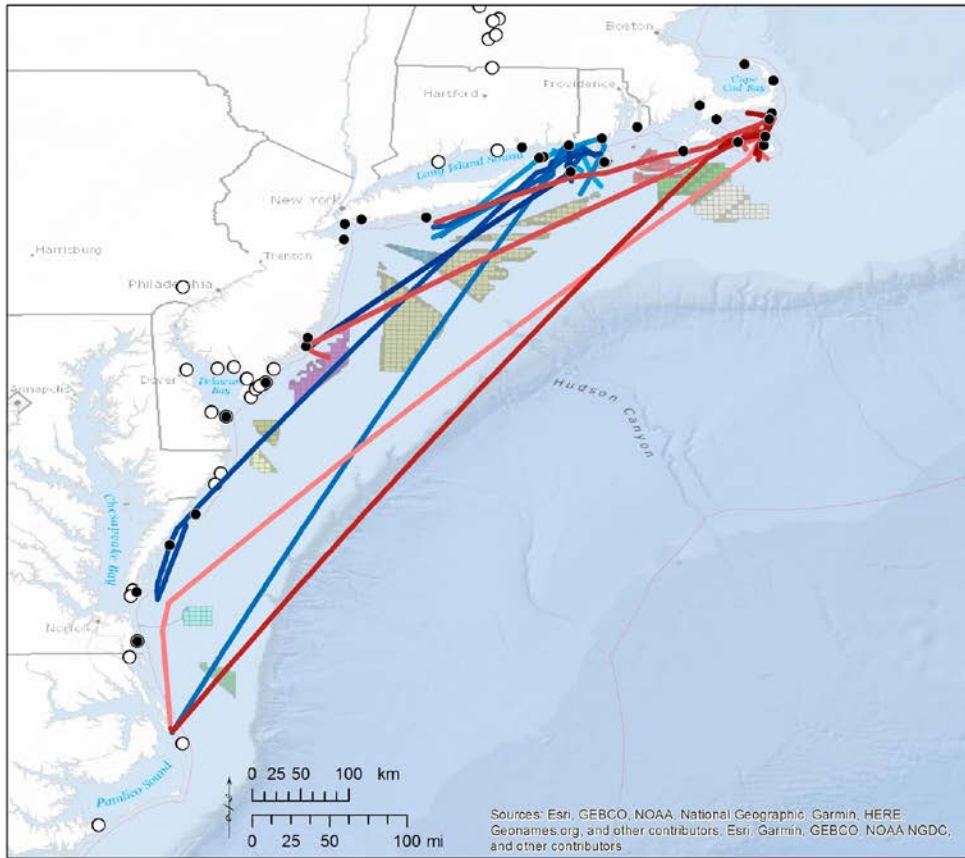
Automated radio telemetry stations

- BOEM Tracking Towers
- Motus Network Partner Towers

Migratory tracks of Piping Plovers by tagging location

- Massachusetts (n=14)
- Rhode Island (n=7)

B.



Legend

BOEM Wind Lease Areas

- RI/MA OCS-A 0486 and 0487
- MA OCS-A 0500 and 501
- NY OCS-A 0512
- NJ OCS-A 0498 and 0499
- DE OCS-A 0482 and 0519
- MD OCS-A 0490
- VA OCS-A 0483 and 0497
- NC OCS-A 0508

U.S. Federal Waters

- 3 - 200 nautical mile boundary

BOEM Wind Planning Areas

- Massachusetts PSN
- New York Bight Call Area
- New York Proposed Commercial Lease

Block Island Wind Farm

-

Automated radio telemetry stations

- BOEM Tracking Towers
- Motus Network Partner Towers

Migratory tracks of Piping Plovers by tagging location

- Massachusetts (n=10)
- Rhode Island (n=12)

C.

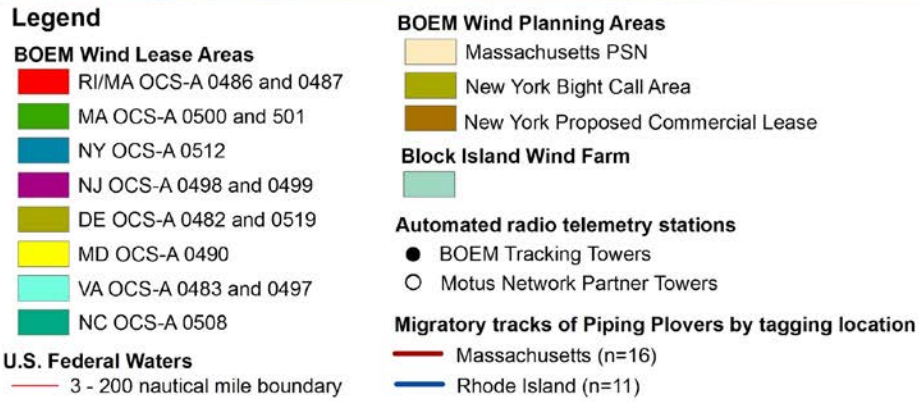
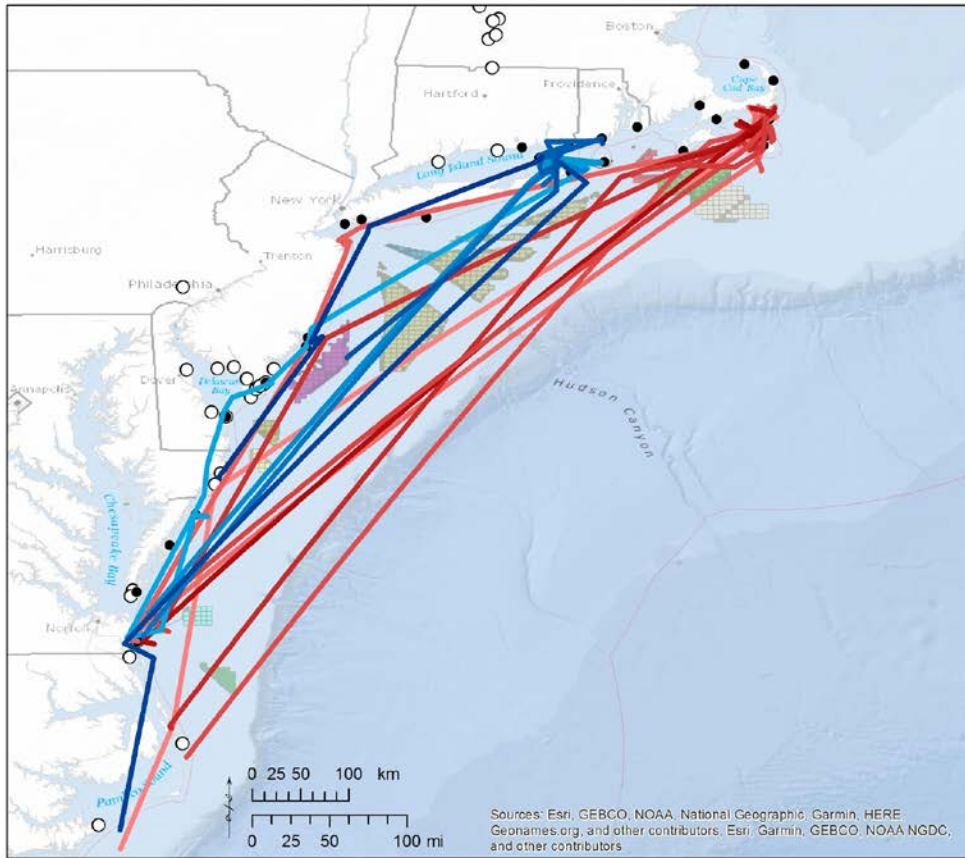


Figure 57. Model estimated migratory tracks of Piping Plovers tagged in Massachusetts (red) and Rhode Island (blue) in 2015 (A), 2016 (B), and 2017 (C).

3.2.3 Exposure to Federal Waters

Across all years, the array tracked movements of 66 Piping Plovers into Federal waters (Table 20). One individual was tracked in flight across Federal waters of Nantucket Sound during the post-breeding period, prior to migratory departure from the breeding grounds. The remaining 65 individuals were exposed to Federal waters during their migratory departure from breeding areas. Migratory departure of Piping Plovers was primarily offshore. Of the 70 individuals tracked during migratory departure, 93% (n=65) had tracks that intersected Federal waters. All (n=40 of 40) of the Piping Plovers tracked during migratory departure from Massachusetts had tracks that intersected Federal waters. Of the Piping Plovers tracked departing from Rhode Island during migration, 83% (n=25 of 30) intersected with Federal waters and the remaining 17% (n=5 of 30) were last detected by the array within state waters of Block Island Sound or eastern Long Island Sound, traveling towards Federal waters to the south. Estimated exposure to Federal waters was highest in 2017 (n=25 individuals), likely due in part to increased transmitter retention and increased tower coverage during 2017. Of the 66 Piping Plovers with estimated exposure to Federal waters, 53% (n=35) were female and 47% (n=31) were male.

Table 20. Number of adult Piping Plovers tagged from nesting areas in Massachusetts and Rhode Island that were exposed to Federal waters, 2015-2017

	2015	2016	2017	Total
Massachusetts	16	9	16	41
Rhode Island	5	11	9	25
Total	21	20	25	66

3.2.4 Covariate Analysis of Estimated Exposure to Federal Waters

The covariate analysis for Piping Plovers with boosted GAMs revealed that day of year, wind direction, and time of day were the strongest predictors of exposure to Federal Waters (Table 21), with peak exposure occurring from late July through early August, when winds were blowing to the southwest at sunset (20:00 hrs EST; Figs. 58-60). Exposure of Piping Plovers to Federal waters was also associated with higher air temperatures (Fig. 61), and increased wind-support (tailwinds; Fig. 62). Significance of the year covariate, with lower exposure in 2015 relative to 2016 and 2017 (Fig. 63), was likely due to the more limited geographic coverage of towers in 2015 to detect offshore flights to staging areas in the mid-Atlantic (Appendix G).

Table 21. Description and selection frequencies of covariates in binomial Boosted GAM analysis of exposure of Piping Plover to Federal waters, 2015-2017.

Covariate (units)	Fitting function	Selection Frequency
Date (Julian)	p-spline	0.29
Wind direction (° true N)	cyclical p-spline	0.24
Hour (EST)	cyclical p-spline	0.15
Air temperature (°C)	p-spline	0.10
Year	categorical (2015, 2016, 2017)	0.09
Wind support (m/s)	p-spline	0.08
Bird ID	Random intercept	0.06
Wind speed (m/s)	p-spline	0.00
Pressure (Pa)	p-spline	0.00
Precipitation (kg/m ²)	p-spline	0.00
Visibility (m)	p-spline	0.00
Sex	categorical (M, F, unknown)	0.00
Fledge success	categorical (0/1)	0.00
Location of Tagging	categorical (MA, RI)	0.00
Date * Fledge Success	categorical	0.00

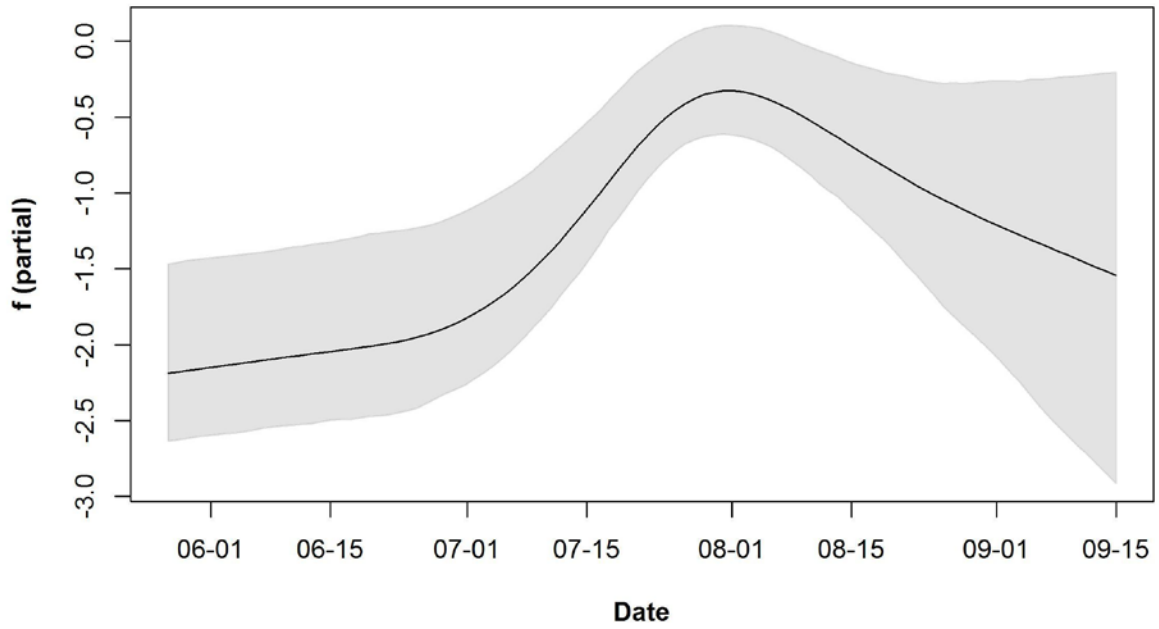


Figure 58. Boosted GAM prediction for the partial contribution of the date of year covariate (x-axis) to the likelihood (log-transformed odds ratio) of exposure to Federal waters among Piping Plovers (y-axis).
The gray-shaded area represents the 95% confidence interval for the response based on 1000 bootstrapped models.

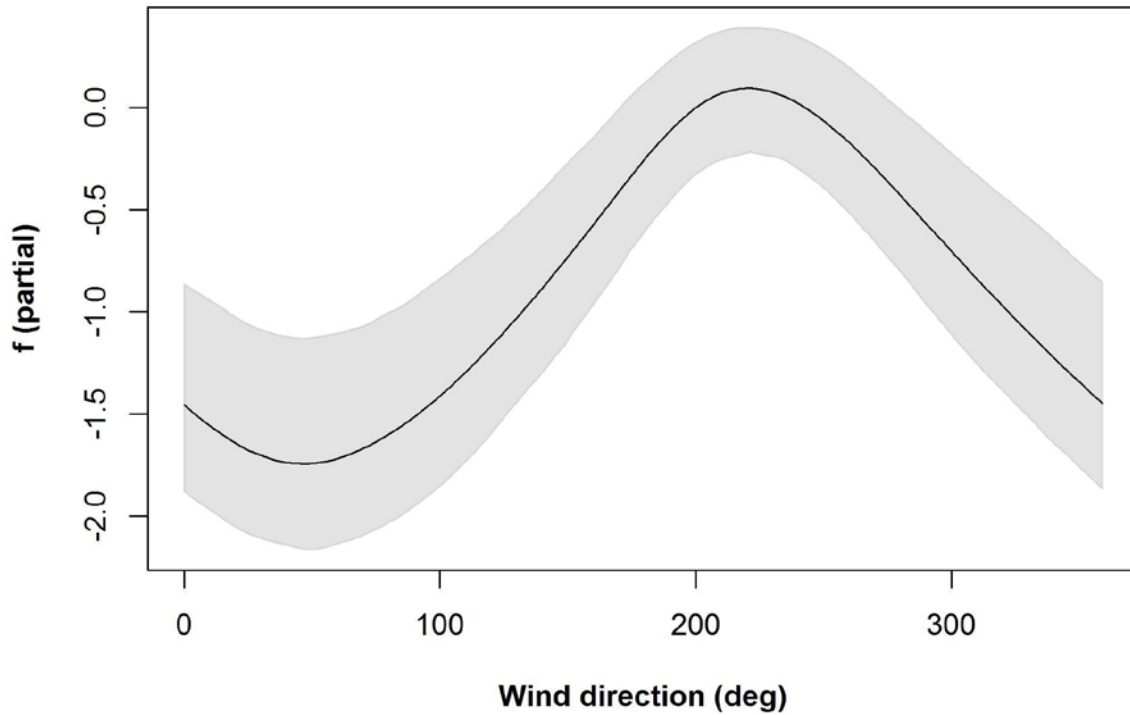


Figure 59. Boosted GAM prediction for the partial contribution of the wind direction covariate (x-axis, in degrees clockwise from Geographic North that the wind is blowing towards) to the likelihood (log-transformed odds ratio) of exposure to Federal waters among Piping Plovers (y-axis).

The gray-shaded area represents the 95% confidence interval for the response based on 1000 bootstrapped models.

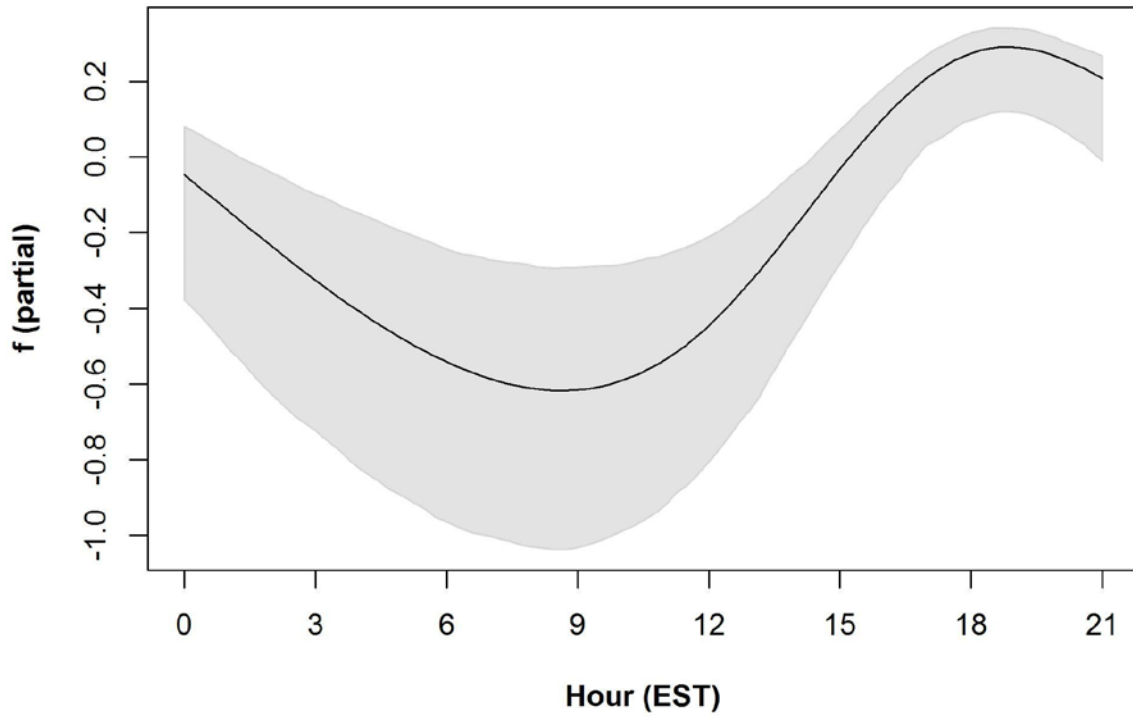


Figure 60. Boosted GAM prediction for the partial contribution of the hour of day covariate (x-axis, in EST) to the likelihood (log-transformed odds ratio) of exposure to Federal waters among Piping Plovers (y-axis).

The gray-shaded area represents the 95% confidence interval for the response based on 1000 bootstrapped models.

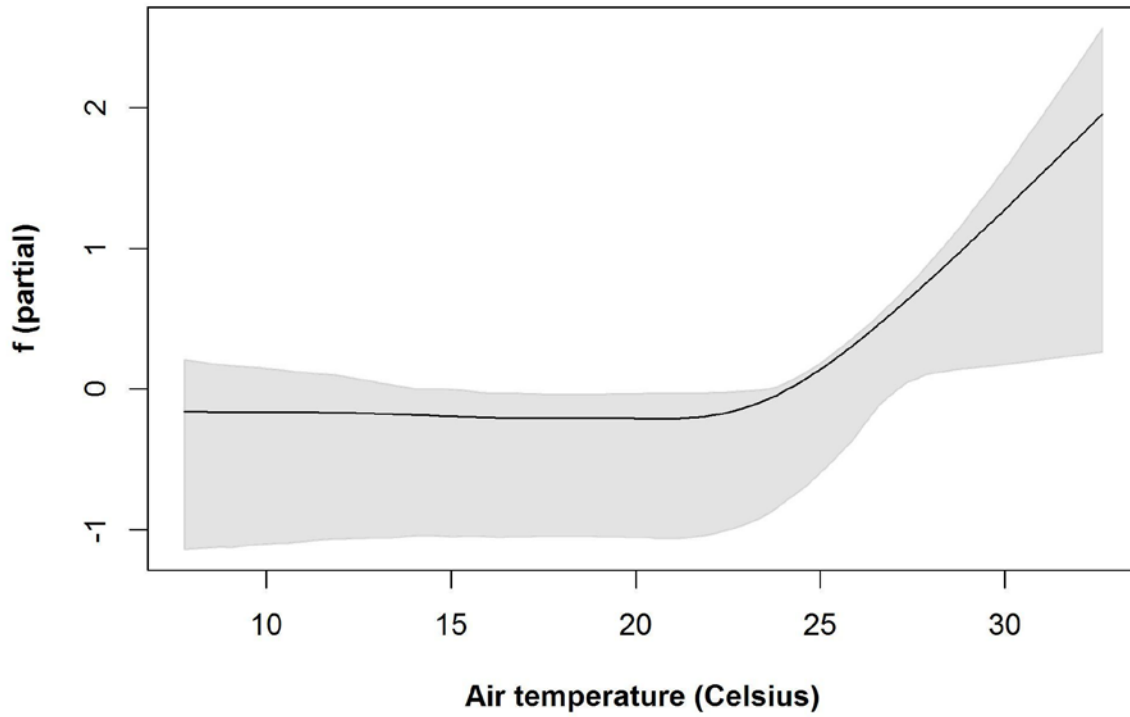


Figure 61. Boosted GAM prediction for the partial contribution of surface air temperature (x-axis, in degrees Celsius) to the likelihood (log-transformed odds ratio) of exposure to Federal waters among Piping Plovers (y-axis).

The gray-shaded area represents the 95% confidence interval for the response based on 1000 bootstrapped models.

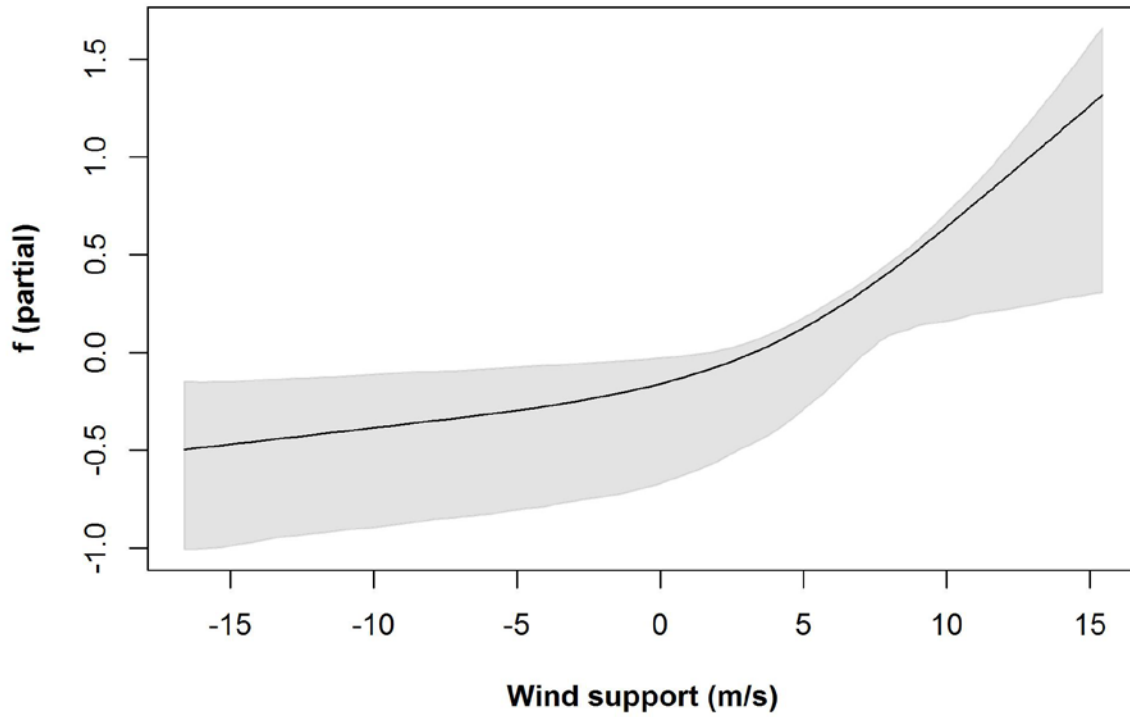


Figure 62. Boosted GAM prediction for the partial contribution of wind support (x-axis, representing tailwind component in m/s) to the likelihood (log-transformed odds ratio) of exposure to Federal waters among Piping Plovers (y-axis).
The gray-shaded area represents the 95% confidence interval for the response based on 1000 bootstrapped models.

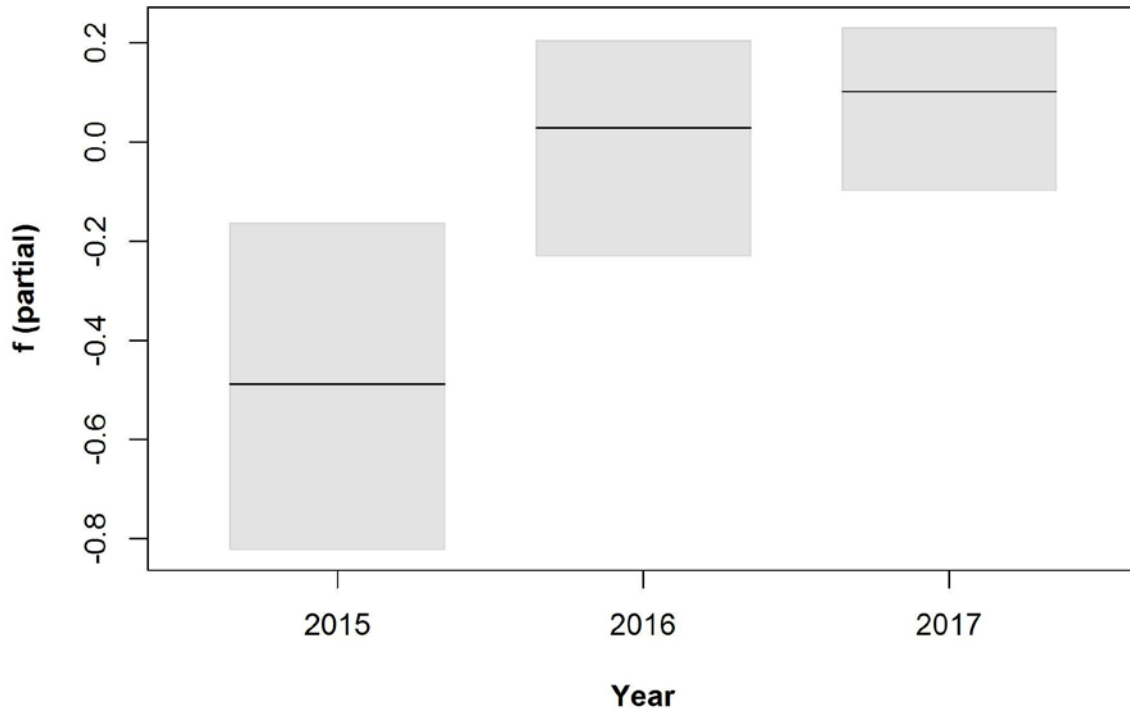


Figure 63. Boosted GAM prediction for the partial contribution of year (x-axis) to the likelihood (log-transformed odds ratio) of exposure to Federal waters among Piping Plovers (y-axis).

The gray-shaded area represents the 95% confidence interval for the response based on 1000 bootstrapped models.

3.2.5 Estimated Exposure to Wind Energy Areas

Of the 70 individuals that were tracked during fall migration, 27% (n=19) had estimated exposure to WEAs within the Study Area (Table 22). Estimated exposure to WEAs was higher for plovers tagged in Massachusetts (19%, n=13) versus those tagged in Rhode Island (8%, n=6), and slightly higher for males (58%, n=11) versus females (42%, n=8). Estimated exposure to WEAs was highest in 2017 (n=12 individuals), likely due in part to increased transmitter retention and increased tower coverage during 2017.

Individual Piping Plovers had estimated exposure to up to 4 WEAs given year (mean 1.58, sd 0.9, range 1-4 WEAs; Appendix D). There was a total of 25 estimated exposure events at BOEM Lease Areas, and 10 estimated exposure events at BOEM Planning Areas (Tables 23 and 24; Fig. 64). Among BOEM

Lease Areas, the highest estimated exposure occurred among Massachusetts-tagged plovers migrating offshore of Massachusetts and Rhode Island, at OCS-A 0500/501 (9 events) and OCS 486/487 (8 events; Table 23). Among BOEM Planning Areas, the highest estimated exposure occurred at NY Bight Call Area among plovers migrating from nesting areas in Rhode Island (n=7) and Massachusetts (n=1; Table 24).

Table 22. Number of adult Piping Plovers tagged from nesting areas in Massachusetts and Rhode Island with estimated exposure to BOEM Wind Energy Areas, 2015-2017

	2015	2016	2017	Total
Massachusetts	1	3	9	13
Rhode Island	2	1	3	6
Total	3	4	12	19

Table 23. The number of estimated exposure events by Piping Plovers at BOEM Lease Areas within the Study Area during fall migration, 2015-2017. Sample size (N) of individuals tracked from each tagging location appears in top row.

BOEM Lease Number	BOEM Lease Area Name	MA (N=58)	RI (N=44)	Total (N=102)
OCS-A 0486	Rhode Island/Massachusetts Lease Area – North	5	0	5
OCS-A 0487	Rhode Island/Massachusetts Lease Area - South	3	0	3
OCS-A 0500	Massachusetts Lease Area	6	0	6
OCS-A 0501	Massachusetts Lease Area	3	0	3
OCS-A 0512	New York Lease Area	0	1	1
OCS-A 0499	New Jersey Lease Area - North	1	1	2
OCS-A 0498	New Jersey Lease Area - South	0	0	0
OCS-A 0482	Delaware Lease Area - GSOE	1	0	1
OCS-A 0519	Delaware Lease Area - Skipjack	0	0	0
OCS-A 0490	Maryland Lease Area	2	2	4
OCS-A 0483	Virginia Lease Area	0	0	0
OCS-A 0497	Virginia Research Lease	0	0	0
	Total	21	4	25

Table 24. The number of estimated exposure events by Piping Plovers at BOEM Planning Areas within the Study Area during fall migration, 2015-2017. Sample size (N) of individuals tracked from each tagging location appears in top row.

BOEM Planning Area Name	MA (N=58)	RI (N=44)	Total (N=102)
Massachusetts PSN	0	0	0
New York Bight Call Area	1	6	7
New York Proposed Commercial Lease	0	3	3
Total	1	9	10

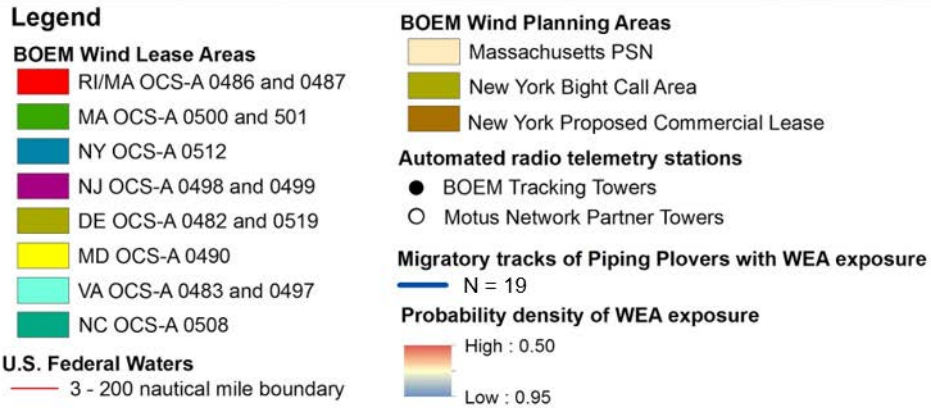
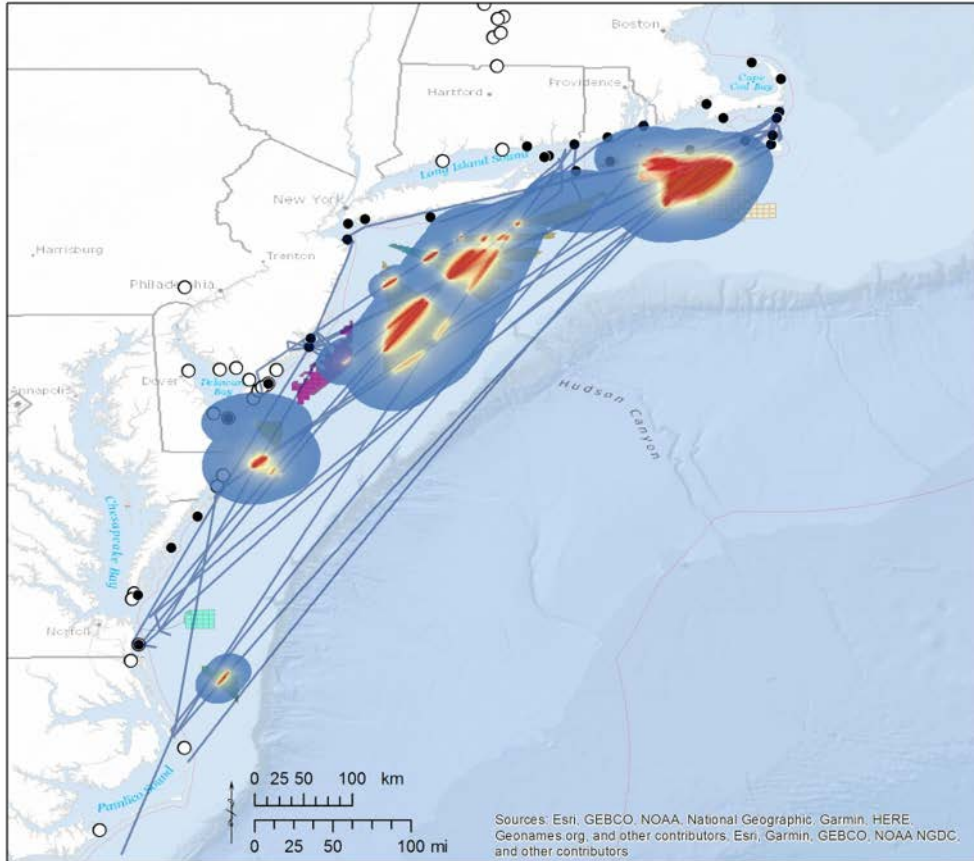


Figure 64. Migratory tracks and composite probability density across WEAs of Piping Plovers (n=19) with estimated exposure to WEAs, 2015 to 2017.

3.2.6 Temporal and Meteorological Variation in WEA Exposure

Estimated exposure of Piping Plovers to WEAs occurred between July 5 and August 14, with a peak in late July (Fig. 65). For Piping Plovers tagged in Massachusetts, peak estimated WEA exposure occurred within four hours of local sunset (19:00 hrs), with 36% (n=8) events occurring at night and 64% (n=14) during daylight (Fig. 66). All estimated WEA exposure events of Piping Plovers tagged in Rhode Island occurred at night, between 19:00 and 01:00 hrs EST (Fig. 67).

Piping Plovers had estimated exposure to WEAs during southwest winds (median 213°; Fig. 68) with a mean wind speed of 7.30 m/s (Fig. 69), providing a tail-wind (mean wind support 4.77 m/s; Fig. 70 and Table 25). Weather conditions during estimated WEA exposure events were generally fair, with high visibility (Fig. 71), little precipitation (Fig. 72), and mild temperatures (Fig. 73), and high atmospheric pressure (Fig. 74).

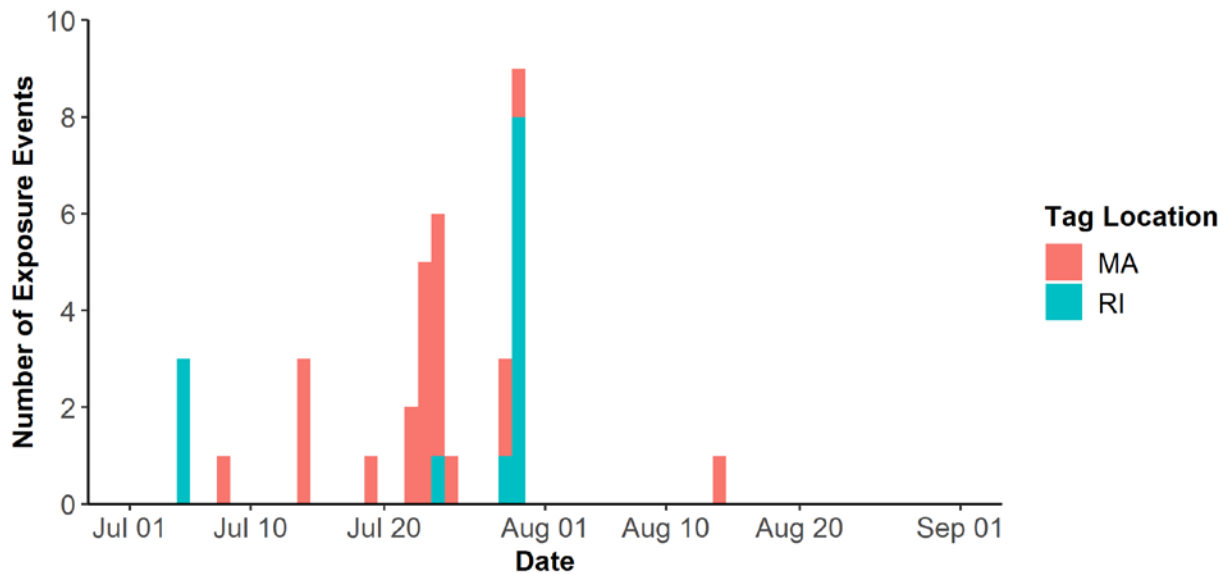


Figure 65. Frequency distribution in calendar date of WEA exposure events (n=35) of Piping Plovers from 2015 to 2017 (pooled) by location of tag deployment.

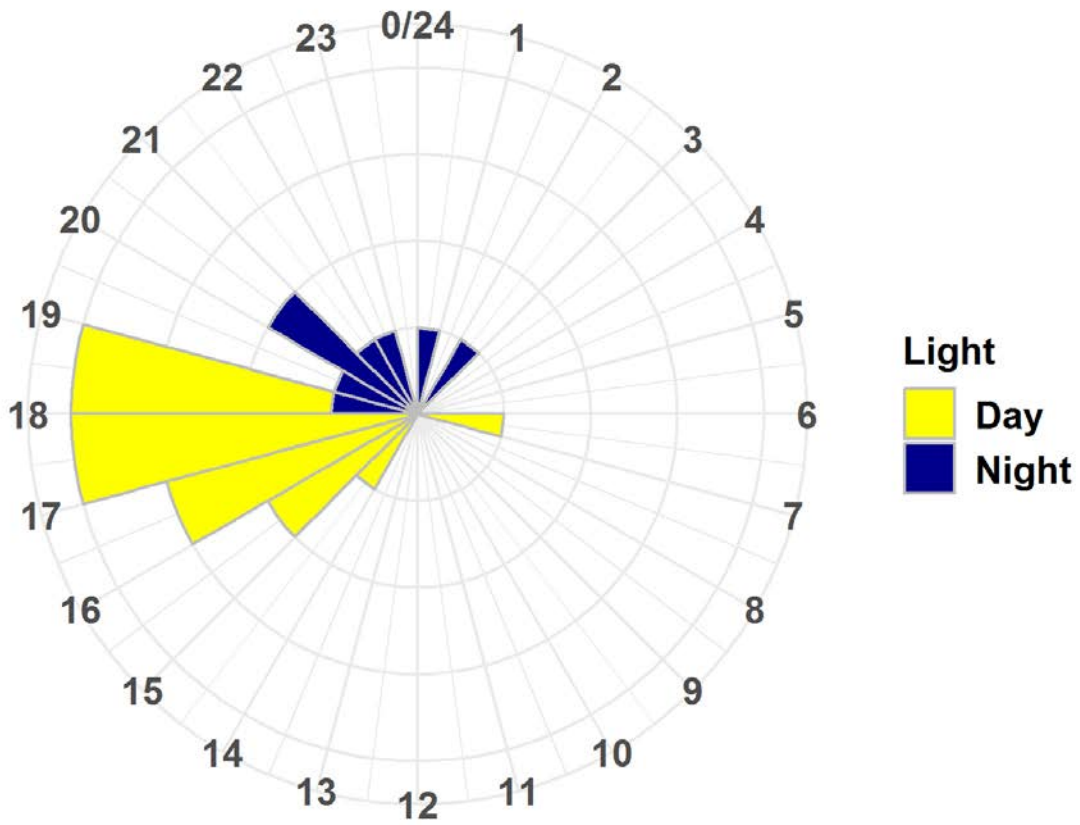


Figure 66. Diel variation (hrs, in EST) in timing of WEA exposure events (n=22) of Piping Plovers tagged in Massachusetts, categorized by daylight using timing of local sunrise and sunset.

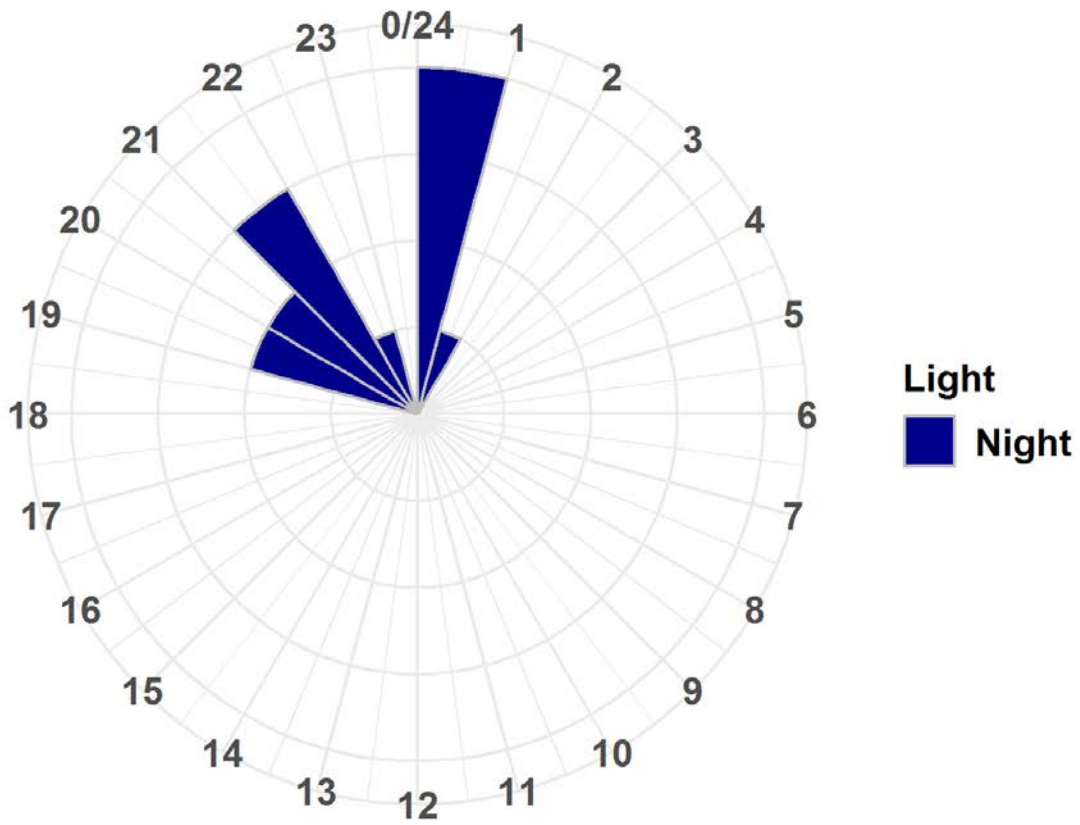


Figure 67. Diel variation (hrs, in EST) in timing of WEA exposure events (n=13) of Piping Plovers tagged in Rhode Island, categorized by daylight using timing of local sunrise and sunset.

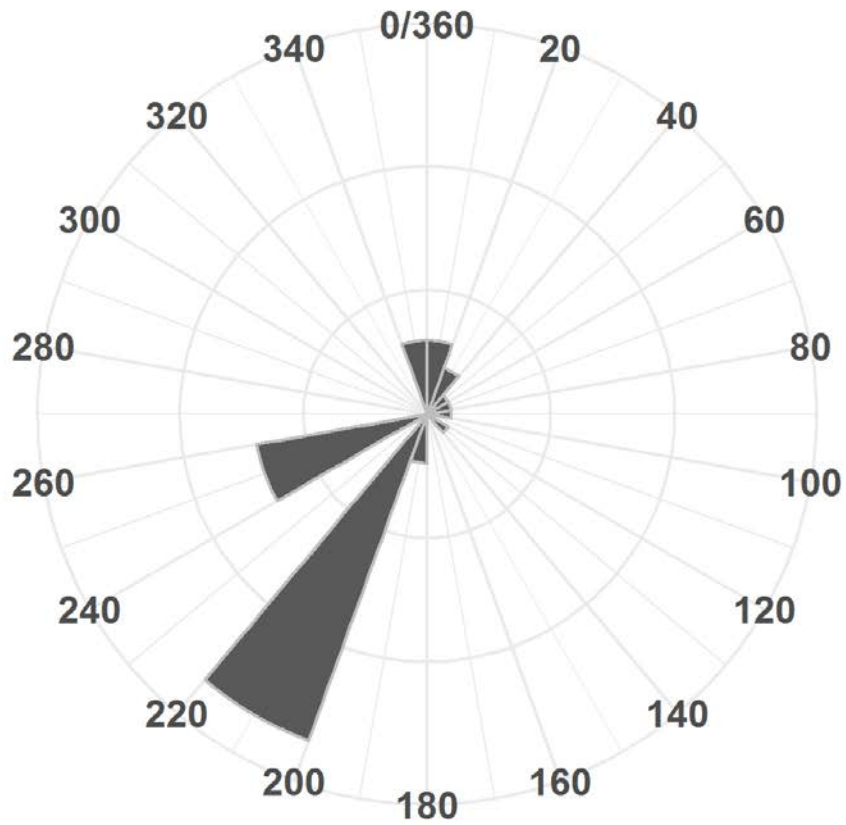


Figure 68. Circular histogram of wind direction (degrees clockwise from N) during WEA exposure events (n=35) of Piping Plovers from 2015 to 2017.

Table 25. Summary statistics of meteorological conditions during WEA exposure events (n=35) of Piping Plovers from 2015 to 2017.

	Mean	SD	Min	Max
Wind speed	7.30	3.77	1.94	13.06
Wind support (m/s)	4.77	5.80	-8.52	12.58
Visibility (m)	19,138	2103	11,073	20,022
Precipitation (kg/m ²)	0.22	0.55	0.00	2.76
Air temperature (°C)	21.96	3.10	16.83	32.10
Pressure (Pa)	101,175	320	100,330	102,194

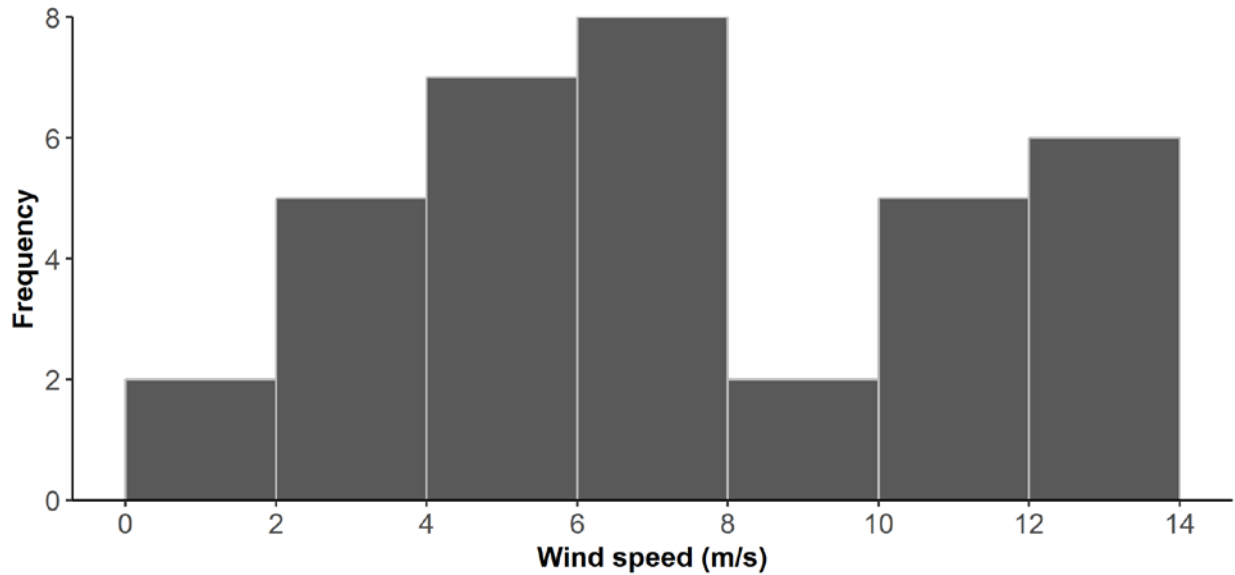


Figure 69. Frequency distribution of wind speed (m/s) during WEA exposure events (n=35) of Piping Plovers from 2015 to 2017.

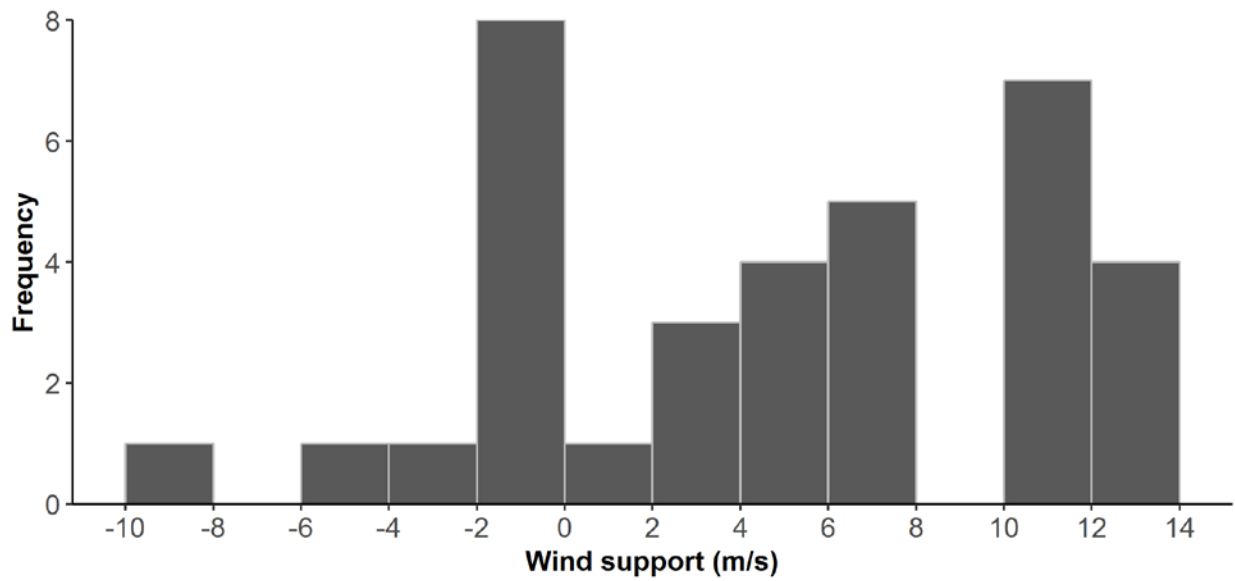


Figure 70. Frequency distribution of wind support (m/s) during WEA exposure events (n=35) of Piping Plovers from 2015 to 2017.

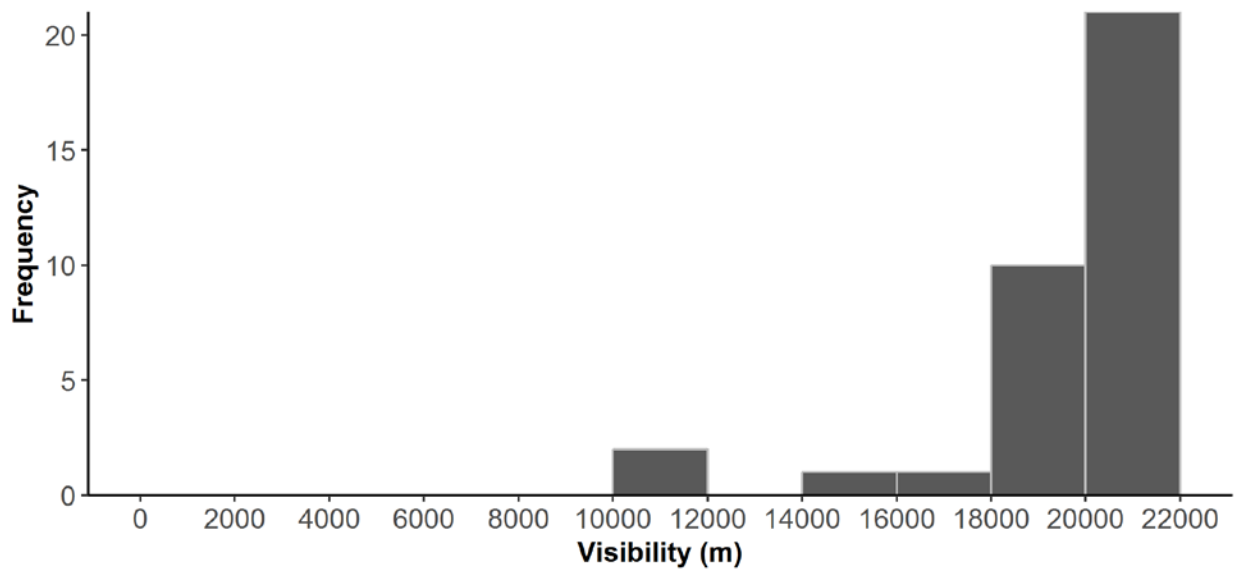


Figure 71. Frequency distribution of visibility (m) during WEA exposure events (n=35) of Piping Plovers from 2015 to 2017.

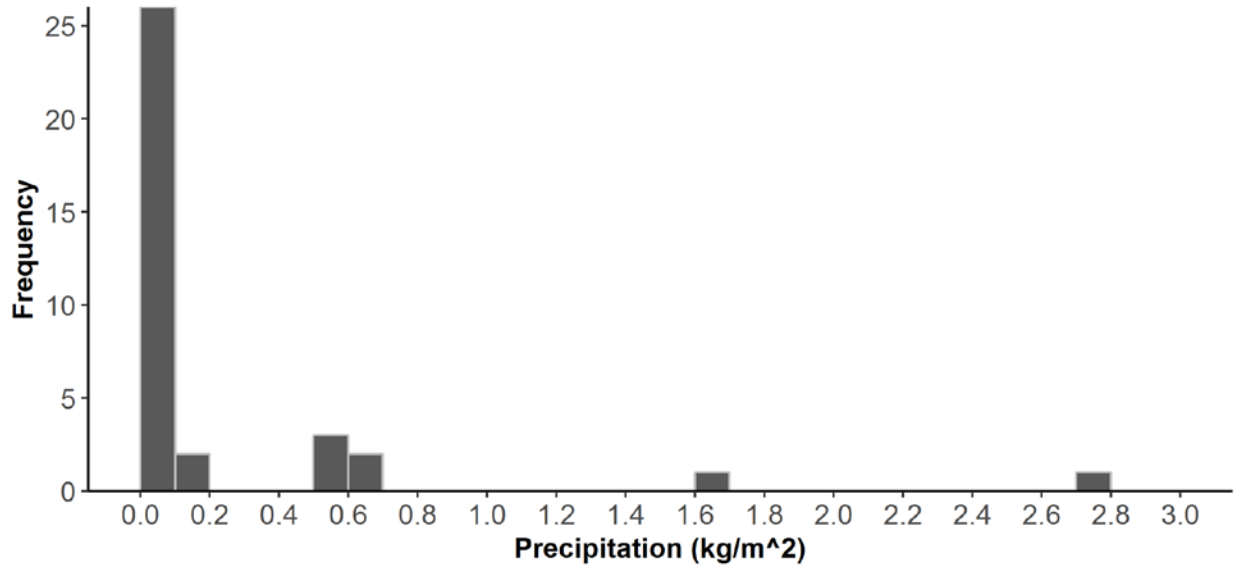


Figure 72. Frequency distribution of precipitation accumulation (kg/m²) during of WEA exposure events (n=35) of Piping Plovers from 2015 to 2017.

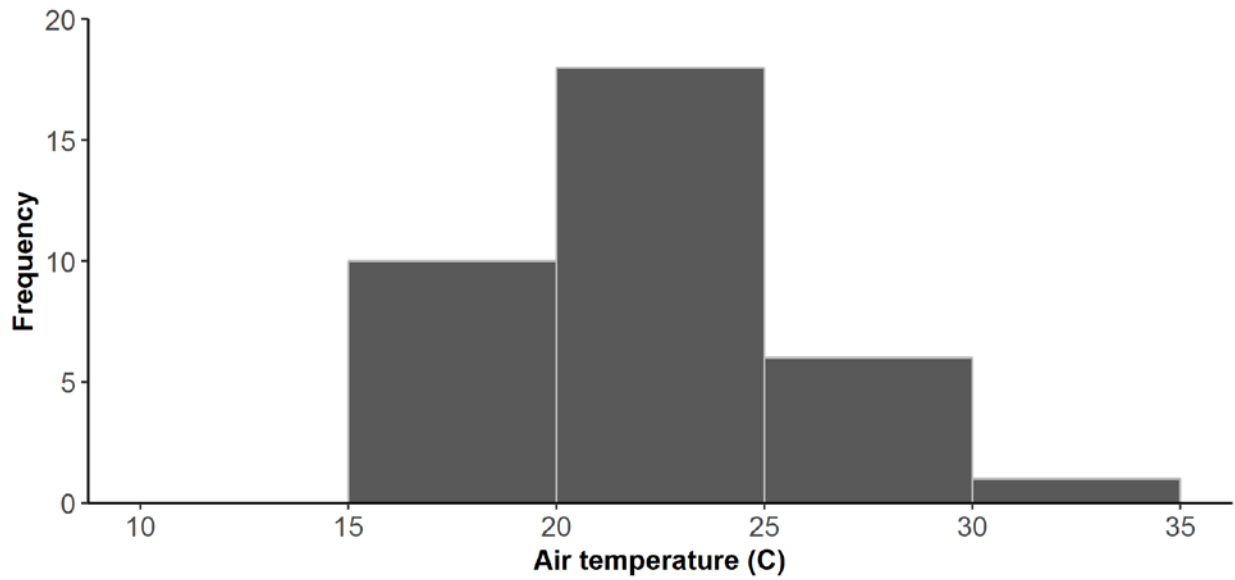


Figure 73. Frequency distribution of precipitation air temperature (°C) during of WEA exposure events (n=35) of Piping Plovers from 2015 to 2017.

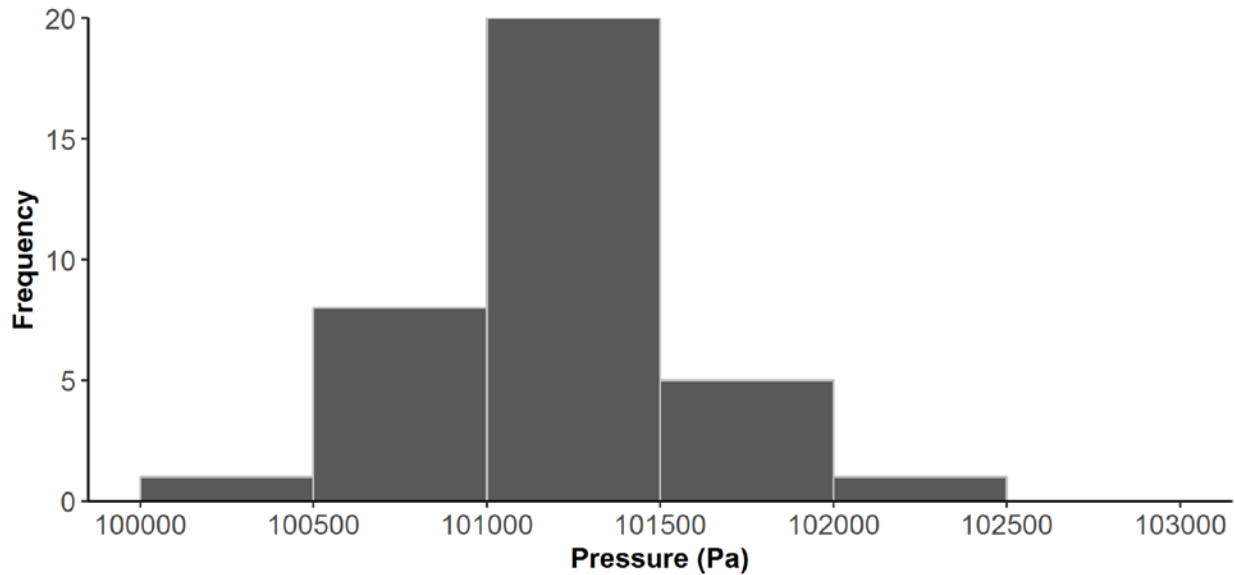


Figure 74. Frequency distribution of barometric pressure (Pa) during of WEA exposure events (n=35) of Piping Plovers from 2015 to 2017.

3.2.7 Altitude Distribution of Piping Plovers During Exposure to Federal Waters and WEAs

Model-estimated flight altitudes of Piping Plovers typically occurred above the RSZ (25 to 250 m) both over Federal Waters (mean 287 m, 5-95% range 48-377, n = 10,359; Fig. 75) and WEAs (mean 317 m, 5-95% range 235-391 m, n = 1,200; Fig. 75). Exposure to the RSZ was higher during flights over Federal waters (21.3%) versus WEAs specifically (15.2%), where flights tended to occur above the RSZ. Exposure to the RSZ was higher at night versus during the day, over Federal waters (Fig. 75) and WEAs (Table 26).

Table 26. Model-estimated flight altitudes (m) of Piping Plovers during exposure to Federal waters and WEAs during the day and night, with sample size (number of 10-min time intervals) and frequency of estimated occurrence within the rotor sept zone (25-250 m).

Exposure Zone	Time of Day	Mean Altitude (5-95% Range)	Sample Size	RSZ Frequency (%)
Federal waters	All	287 (48-377)	10,359	21.3
	Day	289 (26-397)	3,966	19.1
	Night	286 (61-355)	6,393	22.7
WEAs	All	317 (235-391)	1,200	15.2
	Day	338 (327-396)	428	0.7
	Night	306 (231-343)	772	23.2

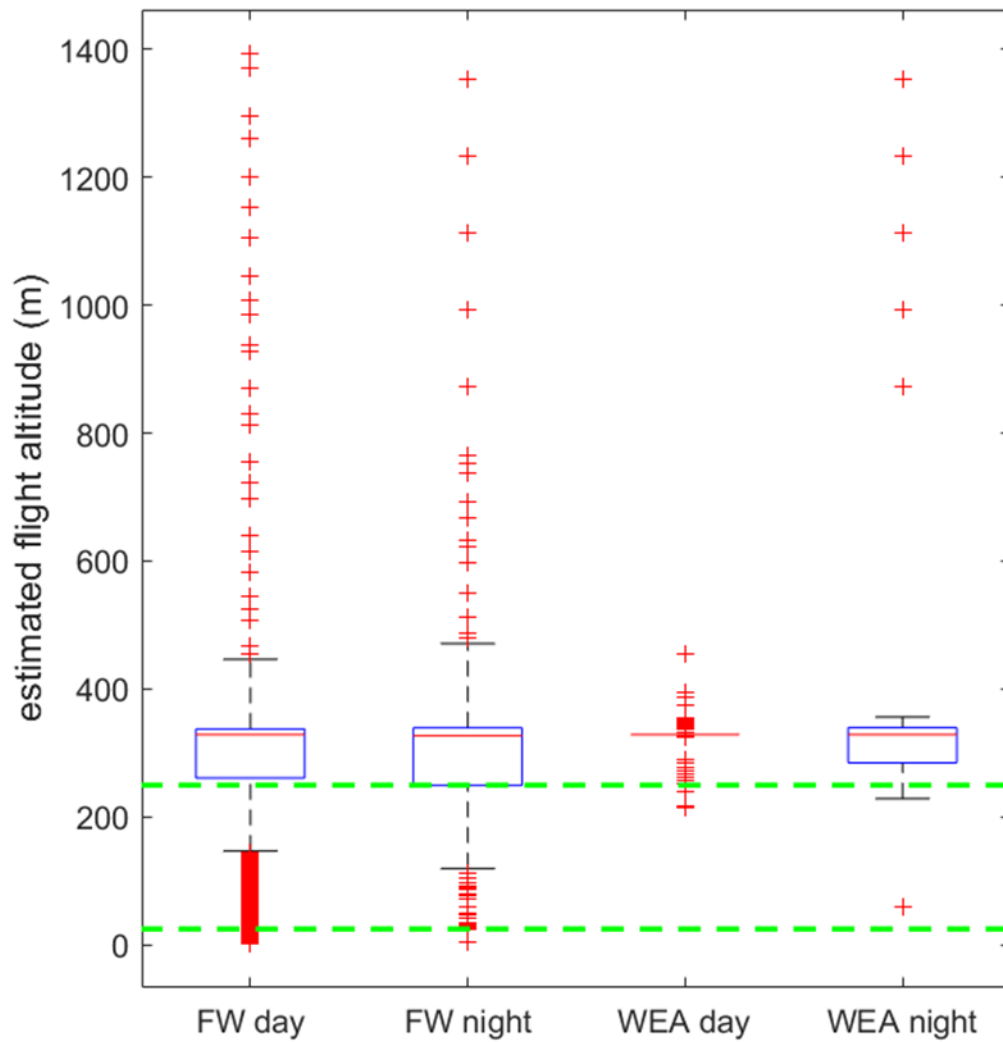


Figure 75. Model-estimates flight altitude ranges (m) of Piping Plovers

During exposure to Federal waters (FW) and WEAs during day and night. The green-dashed lines represent the lower and upper limits of the RSZ (25-250 m).

4 Discussion

4.1 VHF Tracking Technology

Through this work, we demonstrate the utility of digital VHF telemetry and automated radio telemetry stations for monitoring the flights of individually-marked birds within Federal waters and across offshore WEAs. The primary benefit of digital VHF technology is that it facilitates continuous monitoring of focal areas when tagged birds are within detection range of an active station, typically within 5-20 km. This around-the-clock monitoring makes it possible to track movements and exposure of birds to focal areas during periods of darkness and inclement weather, addressing a key information gap in risk analyses of offshore WEAs (Allison et al. 2006). Through the use of coded VHF technology, it is possible to track the movements of thousands of uniquely tagged individuals, with known demographic characteristics (e.g. age, sex, reproductive status, breeding population), continuously and simultaneously on a shared frequency. Participation in Motus Wildlife Tracking Network expands opportunities to collect tracking data on additional tagged species across extended geographic areas (Taylor et al. 2017).

Challenges of utilizing digital VHF tracking technology over large spatial scales, such as the Atlantic OCS, are primarily due to limited ranges of land-based tracking equipment to detect birds flying far offshore and resultant irregularly-spaced time gaps between detections. We attempted to increase offshore coverage by deploying automated radio telemetry stations on boats that regularly occur offshore (passenger ferry, whale watching boat, NOAA research vessel) and through aerial telemetry surveys. However, due to space limitations on survey platforms, each of the boat-based stations used a single, omni-directional antenna, which were subject to high-levels of electromagnetic interference and had very limited detection range (approximately 500 m). We are currently field-testing 5-element Yagi antennas on a passenger ferry in Long Island Sound that appear to have higher detection range (> 1 km) and lower levels of electromagnetic interference relative to the omni-directional antennas used in the present study. The 4-element Yagi antennas used for aerial surveys were also subject to high-levels of electromagnetic noise from the aircraft. In addition, the burst rate of nanotag transmitters (5 seconds) made it challenging to track signals from the aircraft traveling at speeds of ~110 knots due to limited detection range (<6 km) and high directionality of the aircraft-mounted Yagi antennas.

Additional limitations with digital VHF technology resulted from issues with detection probability due to offline receiving stations and tag loss from birds prior to their departure from the Study Area. In 2014, due to logistical delays, several receiving stations within the network were not installed until mid to late July, which likely caused key movements during the earlier portion of the study window to go undetected. Throughout all years of the study, several stations were occasionally offline for periods of several days to several weeks (usually due to power or other maintenance issues), resulting in gaps in detection coverage within certain time periods and geographic areas. Birds were closely monitored near their breeding areas, but after they departed, detection probability decreased through incomplete or unknown retention of transmitters fitted with temporary attachment methods (e.g. glue, sutures). Our approach explicitly estimated error around exposure probability to provide estimates of uncertainty due to factors such as low detection probability, and we removed estimates with high uncertainty from our exposure analysis. Additionally, since the tracking array likely missed flights that occurred within our Atlantic OCS Study Area (due to offline stations or limited detection ranges), and since we do not know if the final detections

of birds corresponded with departure from the Study Area or were a result of tag loss, the estimates of exposure to Federal waters and WEAs reported here should be considered a minimum.

4.2 Movement Models

The movement model represents, to our knowledge, the first application of radio propagation theory based on measured signal strength applied to bird migration. It represents part of ongoing multidisciplinary research aiming to refine and improve analysis of Motus Wildlife Tracking Network data and thereby understanding of the movement ecology of many small-bodied species (Taylor et al. 2017). The incorporation of multipath (ground-reflected) signal propagation and development of information regarding altitudinal movements are particularly novel, and our classification of non-stop versus stopover movements supports recent work advocating identification of distinct modes of movement when quantifying remote sensing data (Jonsen 2016).

Our study highlights the importance of accounting for the inherent uncertainty in received signal strength, here through combining information from sequences of near-simultaneous detections and single-beam detections. The relatively small discrepancy in the kite calibration between predicted and actual (GPS) locations and altitude (on the order of 1 km and 10 m, respectively) attests to the potential for future work to verify that model accuracy, resulting in more confident assessment of flight behavior to support exposure assessments with a higher degree of spatial resolution. However, the validation data also revealed that the model's predicted uncertainty was much greater than its accuracy. This estimated uncertainty originated from the range of plausible locations around the median location, given measured signal strength alone, rather than from error in the median location. In other words, our models probably exhibited higher precision than their global uncertainty estimates would indicate.

Nonetheless, substantial uncertainty remains regarding (1) distinguishing between plausible and probable locations; (2) the resolution of flight altitude, which can create large uncertainty in the horizontal range; and (3) temporal gaps in the data, causing large uncertainty in interim flight trajectories. Another issue relating to flight altitude is that, since detections beyond 50 km offshore were sparse, many high-altitude flights remain unresolved, and best estimate (median) flight altitudes over exposure areas may well be underestimated. The first issue (large range uncertainty) deflates exposure estimates, whereas the latter issue may lead to an overestimate of direct exposure to the RSZ. For this reason, we removed estimates with large spatial uncertainty (>30 km) from our exposure analysis, and provide a conservative interpretation of our results.

Burger et al. (2011) identified three general levels of exposure for avian risk assessments: macro-scale exposure (occurrence within geographical area of interest), meso-scale exposure (occurrence within rotor-swept altitudes), and micro-scale exposure (occurrence within the rotor-swept area, where risk decreases as avoidance behavior increases). In this study, we applied the three-dimensional movement model to digital VHF telemetry data to assess macro-scale exposure of focal species within the following geographical areas of interest: 1) U.S. Federal waters of the Study Area, and 2) individual WEAs contained within Federal waters of the Study Area. When individual birds were detected simultaneously by multiple receiving stations, we estimated meso-scale exposure of flying birds to rotor-swept altitudes (25 to 250 m ASL). However, due to variability in detection probability from irregularly spaced towers,

uncertainty of exposure estimates varied throughout the Study Area (Appendix G). The coastline of the southern New England and Long Island region contains offshore islands and peninsulas that provided several vantage points for triangulation across WEAs, particularly in Rhode Island Sound. Triangulation from land-based towers in the mid-Atlantic region was more limited due to the relatively linear coastline, resulting in reduced coverage for estimating offshore movements in the southern portion of the Study Area.

4.3 Common and Roseate Terns

Overall, the telemetry array detected movements of nearly all (98%) tagged Common and Roseate Terns. However, not all terns had complete data through the post-breeding period, so modeled movements were not representative of the entire breeding and post-breeding period for many individuals. The glue and suture method used to attach transmitters to terns was temporary, and we were unable to monitor the tag retention of individual terns in the present study. During a pilot study in 2013, we monitored tag retention of adult terns nesting in productivity plots from tag attachment (mid-incubation) through the fledge dates of their chicks (25 days following hatch; Appendix C). Most tagged terns (81%, $n = 48$) retained their tags until their chicks had fledged, but the remainder dropped their tags within an average of 30 days following attachment (Appendix D). Thus, in the present study, detection probability was likely highest during the breeding period and decreased through the post-breeding period due to tag loss.

In addition, the land-based tower array had limited range to detect flights far from shore, particularly for species flying at low altitudes, further reducing the probability of detection in offshore areas. Altitude estimates of most Common and Roseate terns flights were <25 m asl, to which land-based stations typically have a horizontal detection range of <20 km (Appendix G). During aerial telemetry surveys in August, we detected Common Terns in Federal waters off the coast of Cape Cod, MA, up to 35 km offshore. These detections occurred in an area predicted to have long-term average relative abundance of Common and Roseate Terns during summer, based on spatial predictive modeling applied to over two decades of boat and aerial survey data (Winship et al. 2018). Thus, terns may have frequented offshore areas beyond the detection array of our land-based towers throughout the duration of the study. Due to incomplete detection probability from tag loss and limitations of land-based towers to track individuals into Federal waters, estimates of the numbers of individuals exposed to Federal waters and WEAs reported in this study should be considered a minimum. In particular, estimates of exposure in Federal waters and WEAs within the Study Area should be interpreted in the context of detection probability, (Appendix G), which is limited to within 20-km of a tracking station for terns flying at altitudes <25 m asl.

Despite these limitations, the majority of terns tagged in this study had estimated exposure to Federal waters. Flights of terns in Federal waters occurred from the time of tag attachment in June (during late incubation-early chick hatching period) through the post-breeding dispersal period in mid-July to late September. During the pre-fledging period, (June through mid-July), Common and Roseate Terns were exposed to Federal waters during chick provisioning flights to feeding areas located up to 50 km from their nesting colonies. These results were up to three times farther than previously published estimates of foraging flight distances for either species. For example, boat based surveys have estimated that Common and Roseate Terns forage up to 30 km from their colonies in Buzzards Bay and Great Gull Island,

however, these are limited in their ability to identify the colony of origination (Duffy 1986, Heinemann 1992). Only recently has tracking technology become available to accurately assess actual foraging ranges of smaller marine birds such as Common and Roseate terns. For example, Fijn et al. (2017) recently used GPS-transmitters to estimate foraging ranges of the slightly larger Sandwich Terns (*Thalasseus sandvicensis*) and found that most trips ranged between 20 to 80 km in length. In the German North Sea, Becker et al. (1993) tracked Common Terns with conventional VHF transmitters and estimated cumulative flight distances of 30 km, with terns typically foraging within a 6-km radius of their nesting colony. A meta-analysis conducted by Thaxter et al. (2012) estimated a mean maximum foraging range of 15.2 km (maximum = 30 km) for Common Tern and 16.6 km (maximum = 30 km) for Roseate Terns. Perrow et al. (2011) tracked foraging flights of Common Terns off England by following them in a rigid-hulled boat and estimated cumulative flight distance of 29 km that were up to <9 km from the nesting colony. Rock and Leonard (2007) radio-tracked Roseate Terns from a plane and found birds foraging up to 7 km from their nesting colony in Nova Scotia. Differences between the flight distances and durations between our study and previous research are probably due in part to methodological differences, although the spatial distribution of prey near other colonies presumably also affects foraging movements (Duffy 1986; Nisbet et al. 2014). Terns may be at higher risk of colliding with turbines and other structures during provisioning flights (Henderson 1996; Stienen et al. 2008), due to frequency of flights and increased focus on searching for and delivering prey (Masden and Cook 2016).

We did not monitor the nesting productivity of most Common and Roseate Terns tagged in the present study, and thus were unable to assess movements relative to reproductive success. However, results from previous studies indicated that unsuccessful breeders may range more widely offshore following nest loss. In a radio-telemetry study of Little Terns (*Sterna albifrons*), Perrow et al. (2006) found that the ranges of successful breeders were less than 6 km², whereas the foraging ranges of failed breeders exceeded 50 km². During 2014, tagged terns from the Great Gull Island colony dispersed across Federal waters to Monomoy NWR in early July, coinciding with low food availability around Great Gull Island, and a series of storms that caused widespread nest loss throughout the colony (Loring 2016). Color-banded Roseate Terns have also been observed moving between colony sites following nest-loss (Spendelov et al. 2018).

In the present study, exposure to Federal waters and WEAs was highest from mid-July to late September, when tagged Common and Roseate terns made extensive movements throughout the eastern Long Island Sound to Cape Cod region. Common and Roseate terns disperse from their nesting areas within 10 to 20 days of the fledge dates of their chicks (Nisbet et al. 2014; Nisbet et al. 2017); therefore, it is likely that this peak corresponded with post-breeding dispersal movements. Large numbers of post-breeding Roseate Terns from colonies ranging from western Long Island to the Gulf of Maine have been shown to disperse distances of over 300 km to stage by the thousands at sites within the Cape Cod and Islands region of Massachusetts (Trull et al. 1999; Jedrey et al. 2010). Common and Roseate Terns have also been directly observed over 200 km East of Cape Cod, within the Atlantic OCS (over George's Bank) during the post-breeding season (Goyert et al. 2014). In the present study, although there was some variation in site use among years, the Cape Cod and Islands region of southeastern MA supported the highest densities of staging Common and Roseate terns from all colonies. Exposure to WEAs was highest among Common Terns (and to a lesser extent Roseate Terns) from Great Gull Island dispersing across BOEM lease areas in Rhode Island Sound to reach staging areas in southeastern MA. The array detected a few longer

distance (>850 km) movements of tagged Common Terns from Great Gull Island and Buzzards Bay colonies to sites in the mid-Atlantic, which resulted in WEA exposure events to the New York Lease Area, the New York Bight Call Area, and the Virginia Lease Area.

Exposure to Federal waters and WEAs was higher for Common Terns relative to Roseate Terns, which may be due in part to differences in their foraging ecology during the breeding season. Previous studies from the breeding season have shown that Roseate Terns primarily foraged for sandlance (*Ammodytes* spp.) in shallow, warmer waters near shoals, inlets, and rip currents close to shore (Safina 1990; Safina et al. 1990; Heinemann 1992; Rock et al. 2007). In contrast, Common Terns fed on a broader array of fish species in deeper, colder waters, often for forage fish driven to the surface by bluefish (*Pomatomus saltatrix*; Safina 1990; Safina et al. 1990). Post-breeding studies have shown direct associations among the distribution and abundance of Common and Roseate Terns, with sandlance in nearshore waters, as well as predatory fish and marine mammals in offshore waters (Goyert 2014, Goyert et al. 2014). Thus, in Federal waters, terns are likely to associate with good sandlance habitat, as well as with other marine birds and subsurface predators that help to increase the detectability and accessibility of sandlance.

For both tern species, peak exposure to Federal waters occurred during the morning hours (spanning sunrise). This timing could relate to both foraging flights into Federal waters or longer distance dispersal flights crossing Federal waters. Peak foraging activity is known to occur largely during morning hours (Burger and Gochfeld 1991; Galbraith et al. 1999). In a pilot study of post-breeding regional tern movements conducted in 2013, Common Terns initiated post-breeding movements from nesting colonies in the Gulf of Maine to staging areas on Cape Cod, MA typically within two hours prior to sunrise (Appendix B). In the present study, exposure to Federal waters was associated with cooler air temperatures during morning hours and high atmospheric pressure (fair weather).

Predicted flight altitudes during exposure events indicated that in both Federal waters and WEAs, terns occasionally fly in the lower part of the RSZ (4 % to 6% flights in Federal waters and 0% to 4% of flights in WEAs). Based on observations of over 19,000 Common Terns primarily from boat-based surveys, Johnston et al. (2014) estimated that 2.5% of birds were flying at altitudes within the RSZ. Previous studies have shown that when feeding, Roseate and Common terns typically fly less than 12 m (Hatch and Kerlinger 2004) and at heights <30 m while in transit (Perkins et al. 2003). The higher altitude during directed flight is consistent with both theory and evidence that seabirds take advantage of vertical structure to maximize wind support (Alerstam 1979, McLaren et al 2016), indicating that exposure risk offshore may increase in stronger tailwinds (Ainley et al 2015).

In one of the most detailed comparisons conducted to date of seabird flight altitudes, Johnston and Cook (2016) contrasted estimates between boat-based and aerial surveys for seven species. They found that during boat-based surveys, ca. 8% of Sandwich Terns were estimated to occur in the RSZ, whereas aerial surveys suggested that ca. 57% of Sandwich Terns were flying at altitudes within the RSZ. Thus, ocular estimates may underestimate flight altitude and a higher proportion of Common and Roseate Terns may be flying in the RSZ than estimated from boat-based survey data (see also Borkenhagen et al. 2018). This underestimation of flight heights in boat surveys has been additionally validated with the use of drones (Harwood et al. 2018).

Migrating terns may fly at much higher altitudes, although we did not observe evidence of tern flights >50 m in the present study. Using radar, Alerstam (1985) found evidence that Common Terns initiated high altitude (1,000 to 3,000 m) migratory flights during evening hours. These findings are consistent with observations described by Veit and Petersen (1993) of large flocks of terns departing from fall staging sites in Massachusetts at high altitudes. Common and Roseate Terns depart on migration from the southern New England region during mid-July through early October (Nisbet et al 2014, Nisbet et al 2017). That we tracked terns in the region through late September, but did not observe high-range simultaneous detections from multiple towers indicating ascents to migratory altitudes, suggests that terns departed from Study Area at low altitudes.

4.4 Piping Plovers

Overall, 82% of tagged Piping Plovers were detected by the telemetry array and 25% lost their transmitters on the breeding grounds, where field staff monitored the retention of Piping Plover tags from tag attachment through chick fledge (or nest loss). Tag retention was highest in 2017 (16% tag loss), compared to 2015 and 2014 (26% to 32% tag loss). Higher retention in 2017 was likely due to use of a lighter (0.67 g) transmitter model with a flatter attachment surface relative to the 1.0 g model used in previous years. Despite being able to account for some tag loss, estimates of the numbers of individuals exposed to Federal waters and WEAs reported here still should be considered a minimum due to potential for additional unobserved tag loss and due to incomplete coverage to offshore waters of the Study Area by the land-based telemetry array. The offshore range of land-based telemetry stations to detect Piping Plovers at altitudes >200 m asl is approximately 40 km, although individuals departing from the Study Area at lower altitudes may only be detected at distances of up to 10-20 km offshore (Appendix G).

Despite these limitations, our study provides the first empirical evidence that Piping Plovers migrate across AOCS, rather than taking a more circuitous route along the coast, addressing a key information gap for this species (Burger et al 2011). Piping Plovers departing from their breeding grounds primarily used offshore routes to sites in mid-Atlantic. The majority of Piping Plovers from Massachusetts departed on a south-southwest trajectory across the eastern end of Nantucket Sound into Federal waters south of Nantucket. The majority of Piping Plovers from coastal Rhode Island departed to the southwest, through Block Island Sound and eastern Long Island Sound into Federal waters of New York Bight. During 2015, the array was limited to the region between Cape Cod, MA and eastern Long Island, NY so only departure trajectories were tracked. The expanded array of towers operated during 2016 and 2017 tracked offshore movements of Piping Plovers across the mid-Atlantic Bight to coastal areas ranging from New Jersey to North Carolina.

The covariate analysis of Piping Plovers strongly indicated that these birds make directed movements into Federal waters during specific meteorological conditions favoring the shorter direct ocean crossing to the mid-Atlantic rather than a longer route following the coast. Specifically, plovers tended to depart in the early evening during early August, when winds were blowing to the south-southwest, which coincided with their general flight direction and thus provided positive wind support. Although migratory timing and flight conditions have not previously been described for Piping Plovers, these results are consistent with previous results from radar studies conducted on shorebirds during fall migration, showing departure

prior to sunset and selection of tail-wind conditions favorable to long-distance flights across the Atlantic Ocean (Richardson 1979).

In this study, individual Piping Plovers had estimated exposure to up to four WEAs on offshore flights across the Study Area. For plovers tagged in Massachusetts, highest exposure occurred within Lease Areas in Rhode Island Sound and south of Nantucket. Piping Plovers departing from Rhode Island had highest exposure to the NY Bight Call Area. However, to date (April 2019), the size of the NY Bight Call Area has been significantly reduced (<https://www.boem.gov/NY-Bight-WEA-BW-Base/>) relative to the boundary used in the exposure analysis (v. 25 Jul 2018, BOEM 2018), likely reducing overall risk of exposure. As with exposure to Federal waters in general, positive wind support, wind direction (SW), date (early August) were the highest predictors of exposure to WEAs. Estimated exposure to WEAs was highest during 2017, likely due to increased transmitter retention and increased tower coverage. Across all years, many Piping Plovers were last detected departing from their nesting areas along trajectories that intersected Federal waters and headed towards WEAs just beyond the range of land-based towers to detect exposure, such as WEAs offshore of Nantucket, MA. Therefore, estimates of exposure to Federal waters and WEAs in this report should be interpreted in the context of detection probability of the telemetry array (Appendix G). This is particularly for the 2015 results, when the distribution of towers was limited to the northern portion of the Study Area. In 2015, there was minimal coverage for tracking flights across offshore WEAs south of Nantucket, MA and no coverage in the mid-Atlantic region from NJ to VA (Appendix G, Fig. G-4).

During migration, offshore flight altitudes of Piping Plovers were generally in the upper range of the RSZ and above, although Piping Plovers spent more time within the RSZ when over Federal waters generally (21.3%) versus within WEAs specifically (15.2%), when they tended to fly at higher altitudes. Offshore radar studies have recorded shorebirds migrating at altitudes exceeding 1 to 2 km (Richardson 1976; Williams and Williams 1990), whereas nearshore studies documented local and migratory flights of shorebirds occurring at altitudes <100 m (Dirksen et al. 2000). However, during migration, flight altitudes might vary with weather as shorebirds search to find suitable tailwinds (Shamoun-Baranes et al. 2010; Senner et al 2018). Migratory birds may also descend into the RSZ during periods of limited visibility, low cloud ceiling, and/or inclement weather, increasing their risk of collision with offshore wind turbines (Langston et al. 2004; Hüppop et al. 2006; Senner et al 2018).

5 Future Directions

In the present study, we quantified macro-scale exposure of focal species to Federal waters and WEAs throughout a portion of the U.S. Atlantic OCS, and provided some insights into meso-scale exposure to the RSZ (Burger et al 2011). However, this information is limited to adults tagged during the breeding period and tracked through post-breeding dispersal (terns) or fall migratory departure (plovers). Additional research is needed to understand the movements and possible exposure of additional demographic cohorts, such as the hatch year age class. Hatch year Roseate Terns are known to disperse in large numbers to Cape Cod, Massachusetts during staging (Trull et al. 1999; Jedrey et al. 2010; Althouse et al. 2016), and thus may be subjected to exposure to offshore WEAs during flights from breeding colonies to staging grounds. Relative to adults, hatch year terns are less agile in flight (Watson and Hatch

1999), and thus may be at higher risk of collision with offshore wind turbines. There is presently no information on the migratory routes and offshore exposure of hatch year Piping Plovers.

In addition, we suggest that future efforts track movements of focal species during spring (northbound) migration. Evidence from geolocator studies indicate that Common and Roseate Terns migrate offshore during spring, but this information is limited by a small sample size and coarse spatial resolution (>100 km accuracy) of the geolocator tracks. Pilot efforts conducted within the present study provide some indication that Common Terns and Piping Plovers migrate across the Atlantic OCS during spring (Appendix I and Appendix J), although more information is needed to quantify routes and conditions associated with offshore migratory flights. Shorebirds may be more likely to migrate during inclement weather in spring due to less stable atmospheric conditions and time constraints to reach breeding areas (O'Reilly and Wingfield 1995). These conditions may lead to increased collision risk with offshore wind turbines during spring relative to fall (Richardson 2000). In addition, tagging studies conducted during spring may offer an opportunity to track courtship flights of terns and plovers, when they may spend a higher proportion of time flying in the RSZ (Burger et al. 2011). Ultimately, information on the demographic variation in movement patterns of focal species throughout the full annual cycle is needed to estimate additive mortality of offshore WEAs to migratory bird populations (Burger et al 2011).

Recent advances in satellite-based tracking technologies are providing increasing opportunities to collect data on full-annual cycle movements of wide-ranging migratory species. As part of this study, we piloted 2-g solar powered satellite transmitters for tracking the movements of Common Terns. These transmitters collected daily, relatively high accuracy (optimally 250 m) two-dimensional locations with an operating life of >2 years. The pilot study revealed new information on the specific timing, routes, and meteorological conditions associated with migratory flights of terns across the entire Atlantic OCS, during both spring and fall migration (Appendix J). Unlike nanotag technology, which is limited by geographic range of tracking towers (generally <20 km for terns), satellite tracking technology is global in scale. The satellite data in the pilot study provided the first robust estimates of cumulative exposure of terns to multiple WEAs in the Atlantic OCS throughout the annual cycle, particularly during offshore migratory flights that occur far beyond range of the land-based nanotag tracking array.

Lightweight (1 to 3 g) GPS loggers are becoming more widely available and are currently capable of acquiring hundreds of high accuracy (<10 m) locations, including altitude, programmed to a customized schedule. Although these units are archival and need to be recovered to access the data that is stored on board, these new GPS tags have enormous potential for collecting high-accuracy, 3-dimensional tracking data from species with high site fidelity to breeding areas, including the focal species in the present study.

In the present study, we estimated exposure birds to offshore areas in relation to meteorological conditions associated with collision risk. However, marine birds may also be affected by habitat displacement resulting from the development of offshore wind energy facilities within foraging areas (Drewitt and Langston 2006). We did not specifically address habitat displacement in the present study, as the land-based telemetry array is more suitable for tracking flights through offshore areas versus estimating specific locations and habitat use within offshore areas, particularly for areas that are beyond detection range. Satellite telemetry technologies are an effective alternative for monitoring habitat use and associations of seabirds offshore to address potential effects of habitat displacement (Spiegel et al. 2017).

Additional studies on possible displacement of Common and Roseate terns from WEAs in the Atlantic OCS may be warranted, although there is some evidence Europe that Common Terns exhibited little avoidance of offshore wind facilities (Dierschke et al. 2016).

Although new satellite-based technologies offer unprecedented opportunities to track full-annual cycle movements of birds throughout their migratory range, digital VHF telemetry remains a viable option for continuously monitoring movements of birds and bats through high-priority areas, such as within the spatial scale of individual WEAs. In the present study, a land-based telemetry station located 5.5 km from the RI Renewable Energy Zone provided continuous monitoring of nano-tagged birds in the vicinity of Block Island Wind Farm (Appendix K). Using a localized array of digital VHF telemetry stations on offshore infrastructure to monitor specific WEAs could further address questions related to collision risk of birds through WEAs, as well as habitat displacement of birds from WEAs given suitable detection range and coverage. During fall of 2017, an automated radio telemetry station was installed on an offshore wind turbine platform at the Block Island Wind Farm for a BOEM-funded study to assess detection rates and accuracy of movement models, based on simultaneous detections from two land-based tracking towers on Block Island (Fig. 76). These techniques could be expanded as additional wind energy facilities are developed throughout the AOCs given additional opportunities to integrate equipment with developing infrastructure.

We suggest that future efforts within the scale of individual WEAs focus on collecting high-resolution (meso-scale to micro-scale) tracking data on flight paths, flight altitudes and behavioral avoidance responses of focal species across a range of environmental conditions (e.g. daylight versus night, fair versus inclement weather) to further address information needs for avian risk assessments (Garthe and Hüppop 2004; Burger et al 2011). These efforts could be improved by combining digital VHF telemetry fine-scale exposure estimates through WEAs. For example, development of digital VHF transmitters with altitude sensors, such as those that have been developed for conventional VHF systems (Bowlin et al. 2015), would increase the accuracy of estimating occurrence in the RSZ and would be useful for calibrating altitude estimates produced by movement models. Other opportunities may exist to integrate digital VHF tracking systems with current technologies for monitoring bird flight paths through offshore WEAs, including radar (three-dimensional tracking of unknown or targeted individuals) and infrared based imagery (used to assess collision). Strategic deployment of digital VHF tracking technologies on additional offshore wind turbines, as facilities are developed throughout the Atlantic OCS, offers a promising opportunity to estimate the exposure of many different species of birds and bats to multiple facilities throughout their migratory range. This is critical to addressing information needs to support conservation efforts and to assess cumulative effects as required by the NEPA process (Goodale and Milman 2016).



Figure 76. Block Island offshore wind turbines

As seen from top of the telemetry tower located at the Southeast Lighthouse, Block Island, Rhode Island (photo: Brett Still).

6 References

- Agostinelli C, Lund U. 2017. R package 'Circular': Circular Statistics (version 0.4-93); [accessed 2017 July 1]. <https://cran.r-project.org/web/packages/circular/>.
- Ainley DG, Porzig E, Zajanc D, Spear LB. 2015. Seabird flight behavior and height in response to altered wind strength and direction. *Marine Ornithology* 43:25-36.
- Alerstam T. 1979. Optimal use of wind by migrating birds: Combined drift and overcompensation. *J Theor Biol.* 79:341-353.
- Alerstam T. 1985. Strategies of migratory flight, illustrated by Arctic and Common Terns, *Sterna paradisaea* and *Sterna hirundo*. *Contributions in Marine Science Supplement* 27:580-603
- Allison TD, Jedrey E, Perkins S. 2008. Avian issues for offshore wind development. *Marine Technology Society Journal* 42:28-38.
- Althouse MA, Cohen JB, Spendelow JA, Karpanty SM, Davis KL, Parsons KC, Luttazi CF. 2016. Quantifying the effects of research band resighting activities on staging terns in comparison to other disturbances. *Waterbirds* 39:415-419.
- Baddeley A, Rubak E, Turner R. 2015. *Spatial Point Patterns: Methodology and Applications with R*. London: Chapman and Hall/CRC Press.
- Bai H. 2016. Estimation of Parameters in Avian Movement Models [Dissertation proposal], University of Massachusetts Amherst, Department of Electrical and Computer Engineering.
- Becker PH, Frank D, Sudmann SR. 1993. Temporal and spatial patterns of Common Tern (*Sterna hirundo*) foraging in the Wadden Sea. *Oecologia* 93:389-393.
- Bivand RS, Pebesma S, Gomez-Rubio V. 2013. *Applied spatial data analysis with R*, Second edition. Springer, NY.
- Bivand R, Lewin-Koh N. 2016. R package 'Mapprools' (version 0.9-2); [accessed 2017 July 1]. <https://cran.r-project.org/web/packages/mapprools/>.
- BOEM. 2017. Environmental Studies Program Studies Development Plan, 2018-2020; [accessed 2017 November 20]. <https://www.boem.gov/FY-2018-2020-SDP/>.
- BOEM. 2018. Renewable Energy GIS Data (version 25 Jul 2018); [accessed 2018 August 20]. <https://www.boem.gov/Renewable-Energy-GIS-Data/>.
- Borkenhagen K, Corman A-M, Garthe S. 2018. Estimating flight height of seabirds using optical rangefinders and GPS data loggers: a methodological data comparison. *Marine Biology* 165:17.

- Bowlin MS, Enstrom DA, Murphy BJ, Plaza E, Jurich P, Cochran J. 2015. Unexplained altitude changes in a migrating thrush: long-flight altitude data from radio-telemetry. *Auk* 132:808-816.
- Breton AR, Nisbet ICT, Mostello CS, Hatch JJ. 2014. Age-dependent breeding dispersal and adult survival within a metapopulation of Common Terns *Sterna hirundo*. *Ibis* 156(3):534-547.
- Brown JM, Taylor PD. 2017. Migratory Blackpoll Warblers (*Setophaga striata*) make regional-scale movements that are not oriented toward their migratory goal during fall. *Mov. Ecol.* 5(15).
- Brzustowski J. 2015. R package 'SensorGnome' (version 1.0.16); [accessed 2017 August 20].
<https://www.sensorgnome.org/>.
- Bühlmann P, Hothorn T. 2007. Boosting Algorithms: Regularization, Prediction and Model Fitting. *Statist. Sci.* 22(4):477-505.
- Burger J, Gochfeld M. 1991. *The Common Tern: Its Breeding Biology and Social Behavior*. Columbia University Press, New York, New York, USA, 413 pp.
- Burger AE, Shaffer SA. 2008. Perspectives in ornithology application of tracking and data-logging technology in research and conservation of seabirds. *Auk* 125:253-264.
- Burger J, Gordon C, Niles L, Newman J, Forcey G, Vlietstra L. 2011. Risk evaluation for Federally listed (Roseate Tern, Piping Plover) or candidate (Red Knot) bird species in offshore waters: A first step for managing the potential impacts of wind facility development on the Atlantic Outer Continental Shelf. *Renewable Energy* 36:338-351.
- Cairns WE. 1977. Breeding biology and behaviour of the Piping Plover (*Charadrius melodus*) in southern Nova Scotia. M.S. Thesis. Dalhousie University, Halifax, Nova Scotia.
- Cochran WW, Warner DW, Tester JR, Kuechle VB. 1965. Automatic radio-tracking system for monitoring animal movements. *BioScience* 15:98-100.
- Cochran WW. 1980. Wildlife telemetry. Pages 507-520 in *Wildlife Management Techniques* (S. P. Schemnitz, Ed.), 4th ed. The Wildlife Society, Inc., Washington, D.C.
- Dierschke V, Furness RW, Garthe S. 2016. Seabirds and offshore wind farms in European waters: Avoidance and attraction. *Biological Conservation* 202:59-68.
- Dirksen S, Spaans AL, van der Winden J. 2000. Studies on Nocturnal Flight Paths and Altitudes of Waterbirds in Relation to Wind Turbines: A Review of Current Research in the Netherlands. In *Proceedings of the National Avian-Wind Power Planning Meeting III*, San Diego, California, May 2000. Prepared for the National Wind Coordinating Committee. Ontario: LGL Ltd.
- Drewitt AL, Langston RH. 2006. Assessing the impacts of wind farms on birds. *Ibis* 148:29-42

- Drewitt AL, Langston RH. 2008. Collision effects of wind-power generators and other obstacles on birds. *Annals of the New York Academy of Sciences* 1134(1):233-266.
- Duffy DC. 1986. Foraging at patches: interactions between Common and Roseate Terns. *Ornis Scandinavica* 17:47-52.
- Duijns S, Niles LJ, Dey A, Aubry Y, Friis C, Koch S, Anderson AM, Smith PA. 2017. Body condition explains migratory performance of a long-distance migrant. *Proc. R. Soc. B* 284:20171374.
- Elliott-Smith E, Haig SM. 2004. Piping Plover (*Charadrius melodus*), *The Birds of North America Online* (A. Poole, Ed.). [accessed 2017 August 20]; <https://doi.org/10.2173/bna.2>
- Everaert J, Stienen EM. 2008. Impact of wind turbines on birds in Zeebrugge (Belgium). Pages 103-117 in D. Hawksworth, and A. Bull, editors. *Biodiversity and Conservation in Europe*. Springer, Netherlands.
- Exo KM, Huppopp O, Garthe S. 2003. Birds and offshore wind farms: a hot topic in marine ecology. *Wader Study Group Bulletin* 100:50-53.
- Fijn RC, de Jong J, Courten W, Verstraete H, Stienen EWM, Poot MJM. 2017. GPS-tracking and colony observations reveal variation in offshore habitat use and foraging ecology of breeding Sandwich Terns. *Journal of Sea Research* 127:203-211.
- Fox AD, Desholm M, Kahlert J, Christensen TK, Petersen IBK. 2006. Information needs to support environmental impact assessment of the effects of European marine offshore wind farms on birds. *Ibis* 148:129-144.
- Friis H. 1946. A note on a simple transmission formula. *Proc. I.R.E Waves Electrons*, 254-256.
- Furness RW, Wade HM, Masden EA. 2013. Assessing vulnerability of marine bird populations to offshore wind farms. *Journal of Environmental Management* 110:56-66.
- Galbraith, H, Hatch JJ, Nisbet ICT, Kunz TH. 1999. Age-specific reproductive efficiency among breeding Common Terns *Sterna hirundo*: measurement of energy expenditure using doubly-labelled water. *Journal of Avian Biology* 30:85-96.
- Gehring J, Kerlinger P, Manville AM. 2009. Communication towers, lights, and birds: successful methods of reducing the frequency of avian collisions. *Ecological Applications*, 19(2):505-514.
- Goodale MW, Milman A. 2016. Cumulative adverse effects of offshore wind energy development on wildlife, *Journal of Environmental Planning and Management* 59(1):1-21.
- Goyert HF. 2014. Relationship among prey availability, habitat, and the foraging behavior, distribution, and abundance of common terns *Sterna hirundo* and roseate terns *S. dougallii*. *Marine Ecology Progress Series* 506:291-302.

- Goyert HF, Manne LL, Veit RR. 2014. Facilitative interactions among the pelagic community of temperate migratory terns, tunas and dolphins. *Oikos* 123(11):1400-1408.
- Goyert HF. 2015. Foraging specificity and prey utilization: evaluating social and memory-based strategies in seabirds. *Behaviour* 152:861-895.
- Goyert HF, Gardner B, Sollmann R, Veit RR, Gilbert AT, Connelly EE, Williams KA. 2016. Predicting the offshore distribution and abundance of marine birds with a hierarchical community distance sampling model. *Ecological Applications* 26:1797-1815.
- Gratto-Trevor C, Haig SM, Miller MP, Mullins TD, Maddock S, Roche E, Moore P. 2016. Breeding sites and winter site fidelity of piping plovers wintering in The Bahamas, a previously unknown major wintering area. *Journal of Field Ornithology* 87(1):29-41
- Grolemund G, Wickham H. 2011. Dates and Times Made Easy with lubridate. *Journal of Statistical Software* 40(3):1-25.
- Gulf of Maine Seabird Working Group (GOMSWG). 2014. 2014 Gulf of Maine Seabird Working Group Census Results. [accessed 2017 August 20].
http://gomswg.org/pdf_files/GOMSWG%20Census%20Data%202014.pdf
- Haig SM, Plissner JH. 1993. Distribution and abundance of Piping Plovers: Results and implications of the 1991 International census. *Condor* 95:145-156.
- Harwood AJP, Perrow MR, Berridge BJ, Tomlinson ML, Skeate ER. 2017. Unforeseen responses of a breeding seabird to the construction of an offshore wind farm. Pages 19-21 *in* Wind energy and wildlife interactions (J. Köppel, ed). Springer, Switzerland.
- Harwood AJ, Perrow MR, Berridge RJ. 2018. Use of an optical rangefinder to assess the reliability of seabird flight heights from boat-based surveyors: implications for collision risk at offshore wind farms. *Journal of Field Ornithology*. 89(4):372-383
- Hastie T, Tibshirani R, Friedman J. 2009. Boosting and additive trees. Pages 337-387 *in* The Elements of Statistical Learning. Springer, NY.
- Hatch JJ, Kerlinger P. 2004. Evaluation of the Roseate Tern and Piping Plover for the Cape Wind Project, Nantucket Sound. ESS Group, Inc. Appendix 5.7-H
- Hays H, DiCostanzo J, Cormons G, Antas PDTZ, do Nascimento JLX, do Nascimento IDLS, Bremer RE. 1997. Recoveries of Roseate and Common Terns in South America (Recobro de Individuos de *Sterna dougallii* y *S. hirundo* en Sur América). *Journal of Field Ornithology* 79-90.
- Henderson IG, Langston RWH, Clark NA. 1996. The response of common terns *Sterna hirundo* to power lines: An assessment of risk in relation to breeding commitment, age and wind speed. *Biol. Conserv.* 77:185-192.

- Hedenstrom A, Klaassen RHG, Akesson S. 2013 Migration of the Little Ringed Plover *Charadrius dubius* breeding in South Sweden tracked by geolocators Bird Study 60:466-474.
- Heinemann, D. 1992. Foraging Ecology of Roseate Terns on Bird Island, Buzzards Bay, Massachusetts. Unpublished Report to U.S. Fish and Wildlife Service, Newton Corner, MA.
- Horne JS, Garton EO, Krone SM, Lewis JS. 2007. Analyzing animal movements using Brownian bridges. Ecology 88:2354-2363
- Hüppop O, Dierschke J, Exo KM, Fredrich E, Hill R. 2006. Bird Migration Studies and Potential Collision Risk with Offshore Wind Turbines. Ibis 148:90-109
- Janaswamy, R. 2001. Radiowave Propagation and Smart Antennas for Wireless Communication, Springer Science and Business Media, 312 p.
- Janaswamy R, Loring PH, McLaren JD. 2018. A State Space Technique for Wildlife Position Estimation Using Non-Simultaneous Signal Strength Measurements. arXiv.org: Electric Engineering & Systems Science. arXiv:1805.11171v1 [eess.SP].
- Jedrey EL, Harris RJ, Ray EA. 2010. Roseate Terns – citizens of the world: the Canada to Cape Cod connection. Bird Observer 38:146-150.
- Johnston A, Cook ASCP, Wright LJ, Humphreys EM, Burton NHK. 2013. Modelling flight heights of marine birds to more accurately assess collision risk with offshore wind turbines. Journal of Applied Ecology 51:31-41.
- Johnston A, Cook ASCP. 2016. How high do birds fly? Development and methods and analysis of digital aerial data on seabird flight heights. British Trust for Ornithology Research Report 676. Norfolk, UK.
- Jonsen I. 2016. Joint estimation over multiple individuals improves behavioural state inference from animal movement data. Sci. Rep. 6(1):20625.
- Kemp MU, Shamoun-Baranes J, van Loon EE, McLaren JD, Dokter AM, Bouten W. 2012. Quantifying flow-assistance and implications for movement research. J Theor Biol 308:56-67
- Kenward R. 1987. Wildlife radio tagging. Academic Press, San Diego, California.
- Kranstauber B, Kays R, LaPoint SD, Wikelski M, Safi K. 2012. A dynamic Brownian bridge movement model to estimate utilization distributions for heterogeneous animal movement. Journal of Animal Ecology, 81:738-746.
- Kushlan, JA, Steinkamp MJ, Parsons KC, Capp J, Acosta Cruz M, Coulter M, Davidson I, Dickson L, Edelson N, Elliot R, Erwin RM, Hatch S, Kress S, Milko R, Miller S, Mills K, Paul R, Phillips R, Saliva JE, Sydeman B, Trapp J, Wheeler J, Wohl K. 2002 . Waterbird Conservation for the Americas: The North

- American Waterbird Conservation Plan, Version 1. Waterbird Conservation for the Americas, Washington, DC, USA, 78 pp.
- Langston RH, Pullan JD. 2003. Wind farms and birds: an analysis of the effects of wind farms on birds, and guidance on environmental assessment criteria and site selection issues. Council of Europe.
- Langston RH. 2013. Birds and wind projects across the pond: a UK perspective. *Wildlife Society Bulletin* 37:5-18.
- Lavesseur P, Veinotte A, Longsdorf J, Mostello C, Regosin J. 2017. Summary of the 2017 Massachusetts Piping Plover census. Annual Report, Massachusetts Division of Fish and Wildlife, Westborough, MA.
- Loring PH. 2016. Evaluating digital VHF technology to monitor shorebird and seabird use of offshore wind energy areas in the Western North Atlantic. [Doctoral dissertation], University of Massachusetts, Amherst, MA.
- Loring PH, Griffin CR, Sievert PR, Spiegel CS. 2017a. Comparing satellite and digital radio telemetry to estimate space and habitat use of American Oystercatchers (*Haematopus palliatus*) in Massachusetts, USA. *Waterbirds*, 40(1):19-31.
- Loring, PH, Ronconi RA, Welch LJ, Taylor PD, Mallory ML. 2017b. Post-breeding dispersal and staging of Common and Arctic Terns throughout the western North Atlantic. *Avian Conservation and Ecology* 12(2):20.
- Loring PH, McLaren JD, Smith PA, Niles LJ, Koch SL, Goyert HF, Bai H. 2018. Tracking movements of threatened migratory *rufa* Red Knots in U.S. Atlantic Outer Continental Shelf Waters. Sterling (VA): US Department of the Interior, Bureau of Ocean Energy Management. OCS Study BOEM 2018-046. 145 p.
- Maloney KO, Schmid M, Weller DE. 2012. Applying additive modelling and gradient boosting to assess the effects of watershed and reach characteristics on riverine assemblages. *Methods Ecol. Evol.* 3:116-128.
- Masden EA, Cook ASCP. 2016. Avian collision risk models for wind energy impact assessments. *Environ. Impact Asses.* 56:43-49.
- McLaren JD, Shamoun-Baranes J, Bouten W. 2012. Wind selectivity and partial compensation for wind drift among nocturnally migrating passerines. *Behav. Ecol.* 23:1089-1101.
- McLaren JD, Shamoun-Baranes J, Camphuysen CJ, Bouten W. 2016. Directed flight and optimal airspeeds: homeward-bound gulls react flexibly to wind yet fly slower than predicted. *J Avian Biol* 47:476-490.
- Mostello CS, Nisbet ICT, Oswald SA, Fox JW. 2014. Non-breeding season movements of six North American Roseate Terns *Sterna dougallii* tracked with geolocators. *Seabirds* 27:1-21.
- Mostello CS, Longsdorf J, Veinotte A. 2018. Inventory of terns, Laughing Gulls, and skimmers nesting in Massachusetts in 2016. Annual Report., Massachusetts Division of Fish and Wildlife. Westborough, MA.

- Motus Wildlife Tracking System. 2016. Motus Wildlife Tracking System Collaboration Policy. January 2016; [accessed 2017 August 20]. <https://motus.org/wp-content/uploads/2016/01/MotusCollaborationPolicy.January2016.pdf>.
- Musial W, Beiter P, Schwabe P, Tian T, Stehly T, Spitsen P, Robertson A, Gevorgian V. 2017. 2016 Offshore Wind Technologies Market Report; [accessed 2017 November 20]. <https://energy.gov/sites/prod/files/2017/08/f35/2016%20Offshore%20Wind%20Technologies%20Market%20Report.pdf>
- Nisbet ICT, Mostello CS, Veit RR, Fox JW, Afanasyev V. 2011a. Migrations and winter quarters of five Common Terns tracked using geolocators. *Waterbirds* 34:32-39.
- Nisbet ICT, Szczys P, Mostello CS, Fox JW. 2011b. Female Common Terns *Sterna hirundo* start autumn migration earlier than males. *Seabird* 24:103-106.
- Nisbet ICT, Gochfeld M, Burger J. 2014. Roseate Tern (*Sterna dougallii*), *The Birds of North America Online* (A. Poole, Ed.). [accessed 2017 August 20]. <http://bna.birds.cornell.edu/bna/species/370> doi:10.2173/bna.370
- Nisbet ICT, Arnold JM, Oswald SA, Pyle P, Patten MA. 2017. Common Tern (*Sterna hirundo*) *The Birds of North America* (P. G. Rodewald, Ed.). [accessed 2017 August 20]. <https://doi.org/10.2173/bna.comter.03>
- National Oceanic and Atmospheric Administration. 2017. National Centers for Environmental Prediction North American Regional Reanalysis; [accessed 2017 May 20]. <http://www.esrl.noaa.gov/psd/data/gridded/data.narr.html>.
- Normandeau Associates. 2011. New insights and new tools regarding risk to Roseate Terns, Piping Plovers, and Red Knots from wind facility operations on the Atlantic Outer Continental Shelf. A Final Report for the U.S. Department of the Interior, Bureau of Ocean Energy Management, Regulation and Enforcement, Report No. BOEMRE 048-2011. Contract No. M08PC20060.
- Northeast Regional Ocean Council. 2017. Northeast Ocean Data Portal; [accessed 2017 May 20]. <https://www.northeastoceandata.org/data-explorer/>.
- O'Connell A, Spiegel CS, Johnston S. 2011. Compendium of Avian Occurrence Information for the Continental Shelf Waters along the Atlantic Coast of the United States, Final Report (Database Section - Shorebirds). Prepared by the U.S. Fish and Wildlife Service, Hadley, MD for the USGS Patuxent Wildlife Research Center, Beltsville, MD. U.S. Department of the Interior, Geological Survey, and Bureau of Ocean Energy Management Headquarters, OCS Study BOEM 2012-076.
- O'Reilly KM, Wingfield JC. 1995. Spring and Autumn Migration in Arctic Shorebirds: Same Distance, Different Strategies, *Integrative and Comparative Biology* 35(3):222-233.

- Perkins S, Jones A, Allison T. 2003. Survey of tern activity within Nantucket Sound, Massachusetts, during pre-migratory fall staging. Final Report for Massachusetts Technology Collaborative. Massachusetts Audubon Society, Lincoln, MA, USA.
- Perrow MR, Skeate ER, Lines P, Brown D, Tomlinson ML. 2006. Radio telemetry as a tool for impact assessment of wind farms: the case of Little Terns *Sterna albifrons* at Scroby Sands, Norfolk, UK. *Ibis* 148:57-75.
- Perrow MR, Skeate ER, Gilroy JJ. 2011. Visual tracking from a rigid-hulled inflatable boat to determine foraging movements of breeding terns. *Journal of Field Ornithology* 82:68-79.
- Poessel SA, Duerr AE, Hall JC, Braham MA, Katzner TE. Improving estimation of flight altitude in wildlife telemetry studies. *Journal of Applied Ecology*. 2018.
- R Development Core Team. 2017. R: a language and environment for statistical computing v. 3.3.2. R Foundation for Statistical Computing, Vienna, Austria. [accessed 2017 December 20]. <http://www.R-project.org/>.
- Richardson WJ. 1976. Autumn migration over Puerto Rico and the Western Atlantic: a radar study. *Ibis* 118(3):309-332
- Richardson WJ. 1978. Timing and amount of bird migration in relation to weather: a review. *Oikos*. 224-72.
- Richardson WJ. 1979. Southeastward shorebird migration over Nova Scotia and New Brunswick in autumn: a radar study. *Canadian Journal of Zoology* 57(1):107-124.
- Richardson WJ. 2000. Bird migration and wind turbines: migration timing, flight behavior, and collision risk. Pp. 132-140 in Proceedings of the National Avian-Wind Power Planning Meeting III, San Diego, CA, May 1998. Prepared for the Avian Subcommittee of the National Wind Coordinating Committee by LGL, Ltd., King City, ON, Canada.
- Robinson Willmott JC, Forcey G, Kent A. 2013. The Relative Vulnerability of Migratory Bird Species to Offshore Wind Energy Projects on the Atlantic Outer Continental Shelf: An Assessment Method and Database. Final Report to the U.S. Department of the Interior, BOEM Study BOEM 2013-207. 275 pp.
- Rock JC, Leonard ML, Boyne A. 2007. Foraging habitat and chick diets of Roseate Tern, *Sterna dougallii*, Breeding on Country Island, Nova Scotia. *Avian Conservation and Ecology* 2:4.
- Safina C, Burger J. 1985. Common tern foraging: seasonal trends in prey fish densities and competition with bluefish. *Ecology*, 66(5):1457-1463.
- Safina C, Burger J. 1989. Inter-annual variation in prey availability for Common Terns at different stages in their reproductive cycle. *Colonial Waterbirds* 12:37-42.

- Safina C, Wagner RH, Witting DA, Smith KJ. 1990. Prey delivered to Roseate and Common Tern chicks; Composition and temporal variability. *Journal of Field Ornithology* 61:331-338.
- Safina C. 1990. Foraging habitat partitioning in Roseate and Common Terns. *Auk* 107:351-358.
- Senner NR, Stager M, Verhoeven MA, Cheviron ZA, Piersma T, Bouten W. 2018. High-altitude shorebird migration in the absence of topographical barriers: Avoiding high air temperatures and searching for profitable winds. *Proceedings of the Royal Society of London. Series B, Biological Sciences*: 285(1881).
- Shamoun-Baranes J, Leyrer J, van Loon E, Bocher P, Robin F, Meunier F, Piersma T. 2010. Stochastic atmospheric assistance and the use of emergency staging sites by migrants. *Proc Biol Sci* 277:1505-1511
- Shealer DA, Kress SW. 1994. Post-Breeding Movements and Prey Selection of Roseate Terns at Stratton Island, Maine. *Journal of Field Ornithology*:349-362.
- Smolinsky JA, Diehl RH, Radzio TA, Delaney DK, Moore FR. 2013. Factors influencing the movement biology of migrant songbirds confronted with an ecological barrier. *Behavioral Ecology and Sociobiology*, 67(12):2041-2051.
- Spendelow JA, Nichols JD, Nisbet ICT, Hays H, Cormons GD. 1995. Estimating annual survival and movement rates of adults within a metapopulation of Roseate Terns. *Ecology* 76:2415-2428.
- Spendelow JA, Hines JE, Nichols JD, Nisbet ICT, Cormons G, Hays H, Hatch JJ, Mostello CS. 2008. Temporal variation in adult survival rates of Roseate Terns during periods of increasing and declining populations. *Waterbirds* 31(3):309-319.
- Spendelow JA, Eichenwald AJ. 2018. Rapid departure of Roseate Terns (*Sterna dougallii*) following large-scale nest failure. *The Wilson Journal of Ornithology* 30(2):485-492.
- Spiegel, CS, Berlin AM, Gilbert AT, Gray CO, Montevecchi WA, Stenhouse IJ, Ford SL, Olsen GH, Fiely JL, Savoy L, Goodale MW, Burke CM. 2017. Determining Fine-scale Use and Movement Patterns of Diving Bird Species in Federal Waters of the Mid-Atlantic United States Using Satellite Telemetry. Sterling (VA): U.S. Department of the Interior, Bureau of Ocean Energy Management. OCS Study BOEM 2017-069.
- Stantial ML, Cohen JB. 2015. Estimating flight height and flight speed of breeding Piping Plovers, *J. of Field Ornithology* 86:369-377.
- Stantial ML, Cohen JB, Darrah AJ, Iaquinto KE, Loring PH, Paton PWC. 2018. Radio transmitters did not affect daily nest and chick survival of Piping Plovers (*Charadrius melodus*). *Wilson Journal of Ornithology* 130:518-524.
- Stienen EWM, Courtens W, Everaert J, Van De Walle M. 2008. Sex-Biased Mortality of Common Terns in Wind Farm Collisions. *Condor* 110:154-157.

- Sumner, MD. 2016. trip: Spatial analysis of animal track data. R package version 1.5.0. [accessed 2018 September 20]. <https://cran.r-project.org/web/packages/trip/index.html>
- Taylor PD, Crewe TL, Mackenzie SA, Lepage D, Aubry Y, Crysler Z, Finney G, et al. 2017. The Motus Wildlife Tracking System: A Collaborative Research Network to Enhance the Understanding of Wildlife Movement. *Avian Conservation and Ecology* 12(1).
- Thaxter, CB, Lascelles B, Sugar K, Cook ASCP, Roos S, Bolton M, Langston RHW, Burton NHK. 2012. Seabird foraging ranges as a preliminary tool for identifying candidate Marine Protected Areas. *Biological Conservation* 145:53-61.
- Trull P, Hecker S, Watson MJ, Nisbet ICT. 1999. Staging of Roseate Terns *Sterna dougallii* in the post-breeding period around Cape Cod, Massachusetts, USA. *Atlantic Seabirds*, 1(4):145-158.
- USFWS. 1985. Endangered and Threatened Wildlife and Plants; Determination of Endangered and Threatened Status for the Piping Plover. Final rule. Federal Register 50:50726-50734.
- USFWS. 1987. Endangered and Threatened Wildlife and Plants; Determination of Endangered and Threatened Status for Two Populations of the Roseate Tern. Federal Register 52:42064-42068.
- USFWS 2002. Trustom Pond National Wildlife Refuge Comprehensive Conservation Plan. Northeast Region, Hadley, Massachusetts. 85 pp.
- USFWS. 2018. Northwest Atlantic Seabird Catalog, Version 2. Accessed through U.S. Department of Interior; [accessed 13 Apr. 2018].
- Veit R and Petersen W. 1993. Birds of Massachusetts. Massachusetts Audubon Society, Lincoln, MA.
- Veit, Richard, R., White, Timothy, P., S.A. Perkins, S. Curley. 2016. Abundance and Distribution of Seabirds off Southeastern Massachusetts, 2011-2015. U.S. Department of the Interior, Bureau of Ocean Energy Management, Sterling, Virginia. OCS Study BOEM 2016-067. 82 pp.
- Wakeling JM, Hodgson J. 1992. Optimisation of the flight speed of the little, common and sandwich tern. *Journal of experimental biology*, 169(1):261-266.
- Watson MJ, Hatch JJ. 1999. Differences in foraging performance between juvenile and adult Roseate Terns at a pre-migratory staging area. *Waterbirds* 22:463-465.
- Wickham H. 2011. The Split-Apply-Combine Strategy for Data Analysis. *Journal of Statistical Software* 40(1):1-29.
- Wiggins DA, Morris RD. 1987. Parental care of the Common Tern *Sterna hirundo*. *Ibis* 129:533-540.
- Williams TC, Williams JM. 1990. Open ocean bird migration. *IEEE Proceedings F - Radar and Signal Processing* 137:133-137.

Winship AJ, Kinlan BP, White TP, Leirness JB, Christensen J. 2018. Modeling At-Sea Density of Marine Birds to Support Atlantic Marine Renewable Energy Planning: Final Report. U.S. Department of the Interior, Bureau of Ocean Energy Management, Office of Renewable Energy Programs, Sterling, VA. OCS Study BOEM 2018-010. 67 pp.

Woodworth BK, Mitchell GW, Norris DR, Francis CM, Taylor PD. 2015. Patterns and correlates of songbird movements at an ecological barrier during autumn migration assessed using landscape- and regional-scale automated radiotelemetry. *Ibis* 157:326-339.



Department of the Interior (DOI)

The Department of the Interior protects and manages the Nation's natural resources and cultural heritage; provides scientific and other information about those resources; and honors the Nation's trust responsibilities or special commitments to American Indians, Alaska Natives, and affiliated island communities.



Bureau of Ocean Energy Management (BOEM)

The mission of the Bureau of Ocean Energy Management is to manage development of U.S. Outer Continental Shelf energy and mineral resources in an environmentally and economically responsible way.

BOEM Environmental Studies Program

The mission of the Environmental Studies Program is to provide the information needed to predict, assess, and manage impacts from offshore energy and marine mineral exploration, development, and production activities on human, marine, and coastal environments. The proposal, selection, research, review, collaboration, production, and dissemination of each of BOEM's Environmental Studies follows the DOI Code of Scientific and Scholarly Conduct, in support of a culture of scientific and professional integrity, as set out in the DOI Departmental Manual (305 DM 3).